1988

Structure-function Relationships In The Rna Binding Activities Of Ribosomal Protein S20 Of Escherichia Coli

Brooke Cameron Donly

NOTICE

The quality of this microform is heavily dependent upon the quality of the original thesis submitted for microfilming. Every effort has been made to ensure the highest quality of reproduction possible.

If pages are missing, contact the university which granted the degree.

Some pages may have indistinct print especially if the original pages were typed with a poor typewriter ribbon or if the university sent us an inferior photocopy.

Previously copyrighted materials (journal articles, published tests, etc.) are not filmed.

AVIS

La qualité de cette microforme dépend grandement de la qualité de la thèse soumise au microfilmage. Nous avons tout fait pour assurer une qualité supérieure de reproduction.

S'il manque des pages, veuillez communiquer avec l'université qui a conféré le grade.

La qualité d'impression de certaines pages peut laisser à désirer, surtout si les pages originales ont été dactylographiées à l'aide d'un ruban usé ou si l'université nous a fait parvenir une photocopie de qualité inférieure.

Les documents qui font déjà l'objet d'un droit d'auteur (articles de revue, tests publiés, etc.) ne sont pas microfilmés.

STRUCTURE-FUNCTION RELATIONSHIPS IN THE RNA BINDING ACTIVITIES OF RIBOSOMAL PROTEIN S20 OF *ESCHERICHIA COLI*

by

Brooke Cameron Donly

Department of Biochemistry

Submitted in partial fulfillment of
the requirements for the degree of
Doctor of Philosophy

Faculty of Graduate Studies
The University of Western Ontario
London, Ontario
June 1988

ISBN 0-315-43278-0

ABSTRACT

The ribosomal protein S20 of *Escherichia coli* is one of only six small subunit proteins capable of binding independently to 16S rRNA. It is unique among r-proteins in being alone in its transcriptional unit, while its control is autogenous like the other r-proteins. For these reasons, S20 is a good model for the study of the interactions of ribosomal proteins with both rRNA and mRNA.

To define the regions of S20 required for binding to 16S rRNA, the binding of S20 and a number of C-terminal deletion mutants to 16S rRNA were measured. Mutant S20s constructed using recombinant DNA technology were synthesized *in vitro* by coupled transcription-translation and assayed directly. The affinity of S20 produced *in vitro* for 16S rRNA was found to be $1.2 \times 10^7\ M^{-1}$ using a gel filtration assay. Removal of just 6 residues from the C-terminus of the protein resulted in a sharp drop in binding activity, suggesting the presence of critical residues in this region.

To characterize the functional basis for the ability of S20 to regulate its own production at a post-transcriptional step, the affinity of S20 for S20 mRNA was also measured. RNA transcripts of the S20 operon were generated *in vitro* and affinity for S20 was measured by three methods: gel filtration, filter binding, and gel

retardation. Only gel filtration was capable of clearly measuring binding of S20 to a positive control consisting of residues 1 to 560 of 16S rRNA transcribed in vitro. When S20 mRNA was utilized in this assay no S20 binding was detectable, indicating the K_a of S20 for its own messenger is probably no greater than about 10^5 M^{-1}. This suggests the possibility that S20 may interact with more complex intermediates involved in the initiation of its own translation, rather than with mRNA alone.

Finally, the roles of the S20 leader and UUG initiation codon in autoregulation and translation efficiency were also examined. Deletions and point mutations in these sequences were tested for efficiency of S20 translation in vitro. These values were correlated with data on the degree of autoregulation in vivo which also result from these mutations. A change in the initiation codon from UUG to AUG was found to cause a significant increase in translational efficiency as well as almost complete relief from regulation. The intrinsic translational efficiency of the S20 mRNA is apparently one of the primary determinants of the extent of autoregulation in S20 expression.

For Margaret Innes Donly

Acknowledgements

I would first like to express my appreciation to George Mackie for his genuine interest in teaching his students. Your enthusiasm has always been appreciated.

I would also like to extend my thanks to Tom Linn, Bob Cook and Stan Dunn for guidance with this project.

Thanks to my labmates, John Lott, Philip Wong, Gaylene Parsons and Andrew White my stay in the lab has been an enjoyable one.

Finally, I would specially like to thank Carol for her help with this thing and putting up with me during it.

TABLE OF CONTENTS

LIST OF FIGURES

CHAPTER 3

CHAPTER 4

LIST OF TABLES

LIST OF APPENDICES

ABBREVIATIONS

°C	degrees Celsius
bp	base pairs
BPB	bromophenol blue
DNA	deoxyribonucleic acid
dpm	disintegrations per minute
EDTA	ethylene-diaminetetra-acetate
mRNA	messenger RNA
PEG	polyethylene glycol
PEP	2-phosphoenolpyruvate
pmole	picomole
RNA	ribonucleic acid
r-protein	ribosomal protein
rRNA	ribosomal RNA
SDS	sodium dodecyl sulfate
TBE	100 mM Tris-borate, 25 mM EDTA, pH 8.3
TE	10 mM Tris (pH 7.6), 1 mM EDTA
Tris	Tris(hydroxymethyl)aminomethane
UV	ultraviolet
U	units

CHAPTER 1

GENERAL INTRODUCTION

All proteins in living organisms are ultimately derived from the activities of the ubiquitous cellular organelle known as the ribosome. This complex of proteins and stable RNAs represents one of the most intensively investigated structures in the cell due to its pivotal role in cellular metabolism: the polymerization of amino acids into proteins. The earliest observations of ribosomes date back to studies by Claude (1940) on Rous sarcoma in which "small granules" were noted in cellular extracts. Luria et al. (1943) were the first to report "granular material" in the cytoplasm of bacteria while studying phage lysis of E. coli. However, it was not until the mid 1950's that ribosomes would be firmly established as the cellular site of protein synthesis (Littlefield et al., 1955).

(a) Ribosome Structure

Ribosomes are found in all cell types, both eukaryotic and prokaryotic. In the enteric bacterium Escherichia coli, the ribosome is composed of two major subunits designated as 30S and 50S, based on their sedimentation rates in sucrose gradients. These two subunits make up a complete 70S ribosome which includes 52 unique protein components (31 in the 50S and 21 in the 30S subunit), and 3 species of RNA: 5S and 23S in the 50S

subunit and 16S in the 30S subunit (Wittmann, 1986). Each of the component proteins is present in unit stoichiometry with the exception of the 50S protein L7/L12, which is present as a tetramer (Subramanian, 1975). This is a typical, as well as the most thoroughly characterized, prokaryotic ribosome. Its structure is similar to that of ribosomes found in the chloroplasts and mitochondria of eukaryotes. In the eukaryotic cytoplasm, larger ribosomes are found (referred to as 80S), which are composed of 40S and 60S subunits (Wittmann, 1986). It appears, however, that all ribosomes regardless of their source function by similar mechanisms (excluding only their means of initiating protein synthesis).

(b) Ribosomal RNA

Two thirds of the mass of the prokaryotic ribosome is made up of RNA (Nierhaus, 1982). Ribosomal RNA (rRNA) along with the transfer RNAs comprise the bulk of the cell's stable RNA. Unlike messenger RNA, whose rate of turnover can be very rapid, rRNA is sequestered by the binding of ribosomal proteins (r-proteins) into stable ribosomal structures. Each of the three RNA species represented in the E. coli ribosome has been sequenced through its corresponding ribosomal DNA (Brosius et al.,

1981), or by direct RNA sequencing as well (Carbon et al., 1978).

Several models for potential secondary structure have been derived from primary structural information (for reviews see Brimacombe and Stiege, 1985; Noller, 1984). The principal tool utilized in deducing these models has been comparative sequence analysis using corresponding rRNA sequences from various organisms. The principle of this approach assumes that a common higher order structure is maintained between the rRNAs of related organisms. Hence any variations seen in the corresponding RNA sequences of related organisms in helical regions will be compensated for in the opposing strands.

A variety of experimental means have also been employed in deriving and refining these models. In particular, chemical modification of RNA using both single and double strand-specific probes has been widely applied. Some of the more useful single strand-specific reagents include kethoxal (Noller, 1974), diethyl pyrocarbonate (Peattie and Gilbert, 1980), bisulfite (Woese et al., 1980) and carbodiimide and dimethyl sulfate (Moazed et al., 1986) to name a few. Modification with such agents can now be combined with methods allowing for rapid detection of the modified residues, such as primer extension (Moazed et al., 1986). Double strand-specific chemical reagents consist mainly

of psoralen derivatives (Rabih and Crothers, 1979), compounds which are also often used as cross-linking reagents (discussed below).

Single and double strand specificity can also be found in the range of enzymatic probes available. Single strand specificity occurs in RNases T_2 (Vigne et al., 1973), T_1, and A (Carbon et al., 1979), as well as S_1 nuclease (Ross and Brimacombe, 1979). Cobra venom RNase is specific for double-stranded RNA (Carbon et al., 1979). Other methodologies include the use of single-stranded oligonucleotide probes for binding to regions of unpaired rRNA, direct observations of partially folded rRNA structures by electron microscopy, and nuclear magnetic resonance techniques (all reviewed in Noller, 1984).

A recent model of the secondary structure of E. coli 16S rRNA is shown in Fig. 1 as presented in Noller et al. (1986). On the basis of secondary structure, the 16S rRNA molecule is subdivided into 3 major structural domains and one minor one by 3 sets of long range interactions (Maly and Brimacombe, 1983; Noller, 1984). Clues to the existence of a three-domain structure originally came from nuclease studies on reconstituted 30S particles (Zimmermann, 1974). These showed the existence of 3 groups of 30S proteins, each capable of association with a specific 16S rRNA fragment representing one of the major domains mentioned above.

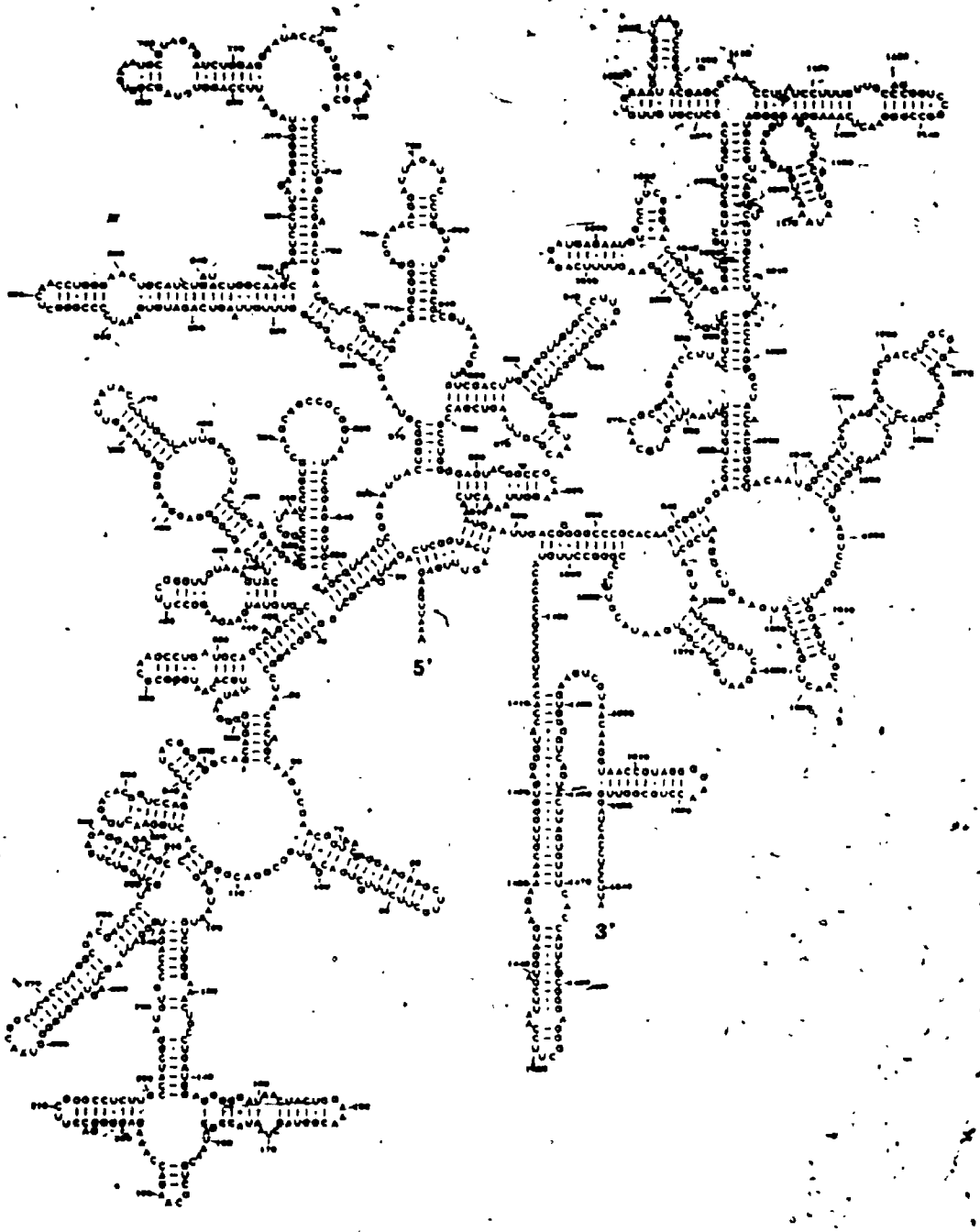

Figure 1. Secondary structure of the 16S ribosomal RNA of E. coli. Taken from Noller et al., (1986).

Identification of the specific long range pairings was predominantly based on experiments utilizing chemical agents such as nitrogen mustards (Stiege et al., 1982) psoralen compounds (Thompson and Hearst, 1983) or UV irradiation (Zwieb and Brimacombe, 1980) to cross-link RNA residues which are in close proximity. This methodology has the advantage that it further reveals interactions and/or simple proximities which result from features of tertiary structure as well. Such higher order configurations of RNA present unique problems however, in that long range associations integral to the function of the ribosome may be disrupted in isolated RNA. This is particularly relevant to the use of compounds like the psoralens which can be effective when used with intact subunits (Brimacombe and Stiege, 1985). To date, numerous significant tertiary interactions have been identified in isolated RNA by cross-linking (Thompson and Hearst, 1983; Wollenzein and Cantor, 1982) suggesting substantial interaction within, as well as between, the major secondary structure domains.

(c) Ribosomal Proteins

The complete amino acid sequences of all 52 proteins from the E. coli ribosome have now been determined (Giri-et al., 1984). As a group the r-proteins are strongly

basic, with extremely high percentages of lysine and arginine (as well as alanine, valine, and leucine). This is especially true of S20, which contains almost 30% alanine residues alone, as well as 25% arginine and lysine, and has a pK of greater than 12 (Kaltschmidt, 1971). S20 is also typical of 30S subunit proteins in having a very high predicted α helical content from its primary structure (Wittmann et al., 1980). However, experimental estimates discussed by Giri et al. (1984) using circular dichroism gave the contrary result that α helical content is low in S20. The primary data for this assertion, however, were not available for study. Secondary and tertiary structures of the r-proteins have been investigated by numerous techniques (reviewed in Giri et al., 1984) but have as yet failed to yield a common structural motif for their rRNA binding properties.

Localization of the various r-proteins in intact subunits has also been undertaken, with the most fruitful methodologies devised for this purpose including immune electron microscopy (IEM), chemical cross-linking, fluorescence energy transfer, and particularly neutron scattering (all reviewed in Wittmann, 1986). Neutron scattering provides estimates for the distances between the mass centres of gravity of pairs of proteins in intact subunits. Data for all 21 proteins of the 30S subunit has recently been compiled into a comprehensive

map of their spatial arrangement (Capel et al., 1987). S20 is found to be located in the lower region of the 30S subunit "head" structure, neighbouring proteins S1, S2, S3, S4, S10 and S16. The model correlates well with the available IEM and cross-linking data on the protein topography of the small subunit. A model for the 50S subunit is presently in a less developed stage (Nowotny et al., 1986).

(d) Ribosome Assembly

Active E. coli 30S ribosomal subunits were first reconstituted in vitro by Traub and Nomura in 1968. Reconstitution of a 50S particle, (from Bacillus stearothermophilus), did not follow until 1973 (Fahnestock et al., 1973) by which time significant characterization of the assembly of 30S particles was already complete. This included optimization of the assembly process using conditions of 20 mM Mg^{++} ions, 0.37 M ionic strength, and temperatures of 40 to 50°C (Traub and Nomura, 1969). The strict specificity for ionic strength observed was suggested as reflecting the specific nature of the RNA-protein and protein-protein interactions required for the assembly process (Nomura and Held, 1974). Kinetics of assembly were observed to be first order (Traub and Nomura, 1969), suggesting that

the rate determining step was a unimolecular reaction. This was explained by the presence of inactive intermediates in incubations not heated to the optimum temperature. These reconstitution intermediates (RIs), once heated, became active RI* intermediates capable of forming active subunits. Therefore the sequence:

16S RNA + r-proteins ==> RI

RI --heat--> RI*

RI* --r-proteins--> 30S subunit

provided a unimolecular structural rearrangement explaining the observed kinetics (Nomura and Held, 1974).

The cooperative nature of the assembly process was first illustrated by experiments in which specific proteins were omitted from the mixture. These showed that there was an interdependence between proteins for proper subunit assembly, and led to the first map of the process (Mizushima and Nomura, 1970). This map represents the temporal flow of key interactions in assembly, based largely on the dependence by many proteins on prior interactions of others. S20 is among 6 proteins in the small subunit capable of binding independently to 16S rRNA (the others are S4, S7, S8, S15 and S17). As such, these "primary binding proteins" are located upstream in the assembly map, representing the earliest interactions of the process. Their interactions with 16S rRNA have therefore been most thoroughly characterized and will be discussed below (section e).

As previously discussed, isolated 16S rRNA is itself a highly ordered structure. In fact, isolated rRNAs have been found to assume tertiary structures producing shapes similar to those of their corresponding complete subunits (Vasiliev et al., 1986). Addition of those core proteins capable of independent RNA binding can, however, result in even more compact folding, virtually identical to that seen in situ (Vasiliev et al., 1986). It seems likely then, that various conformations of rRNA will prove to be involved in the different stages of subunit assembly. Garrett (1979) has suggested that such structures may be represented by the metastable RNA conformations resulting from gentle acid isolation techniques (Hochkeppel et al., 1976). Also, in the process of total reconstitution (Traub and Nomura, 1969) the presence of intermediates (RIs) has been shown to be the result of necessary conformation changes (Nomura and Held, 1974). Finally, conformational switches are also likely to prove essential in certain aspects of ribosome function (Brimacombe et al., 1986).

(e) RNA-Protein Interaction in the Ribosome

With recent discoveries of new enzymatic activities for RNA in self-splicing (Kruger et al., 1982) and ribonuclease P function (Guerrier-Takada et al., 1983),

there is rising expectation that catalytic participation of rRNA in peptide bond synthesis may soon be found (Moore, 1988). However, an important architectural role for rRNA also remains clear, with the basic structure of rRNA providing the theme for subunit structure. The basis of that structure is the non-covalent association of protein and RNA.

The interaction of protein and RNA bears more similarity to that of protein and protein than protein and DNA. Although they are alike in both being nucleic acids, RNA behaves more like protein than DNA structurally in its tendency to fold into globular tertiary structures (Wickens and Dahlberg, 1987). Some of the structural features in RNA which have been found to be important for protein recognition include primary sequences in regions which are single-stranded, and the presence of bulged residues located in paired regions or in combination with stem-loops (Wickens and Dahlberg, 1987).

The process of ribosome assembly is a combination of the folding of RNA into higher order configurations (as dictated by its primary sequence), interspersed with the sequential association of various r-proteins. As mentioned above, those proteins most integral to ribosome structure probably bind earliest in assembly, and are also capable of binding independently to "naked" RNA in reconstitution experiments. This property has

facilitated efforts to determine the locations of their binding sites, as a prelude to eventually determining the structural features of the RNA responsible.

These interaction sites have primarily been mapped by three means: nuclease protection, chemical modification and covalent linkage. Some r-proteins protect very large discontinuous segments of RNA in nuclease protection experiments, while a few others protect small, specific fragments (Fig. 2) (reviewed in Zimmermann, 1980). Those protecting discontinuous spans of rRNA probably do so as a result of long range RNA interactions in the regions of binding. A good example is the small subunit protein S4, whose nuclease protection footprint includes most of the 5' domain of 16S rRNA. This interaction has been refined to a few specific sequences by the application of chemical modification and primer extension (Stern et al., 1986), as indicated in Fig. 2. Other applications of chemical probing are reviewed in Garrett et al. (1984). Nuclease protection has also been extended to include other r-proteins which do not bind independently to rRNA. Such studies utilize reconstituted complexes containing groups of r-proteins in nuclease digests with results for added or omitted proteins being derived from the extension or depletion of protection so produced (Gregory et al., 1984; Wiener et al., 1988).

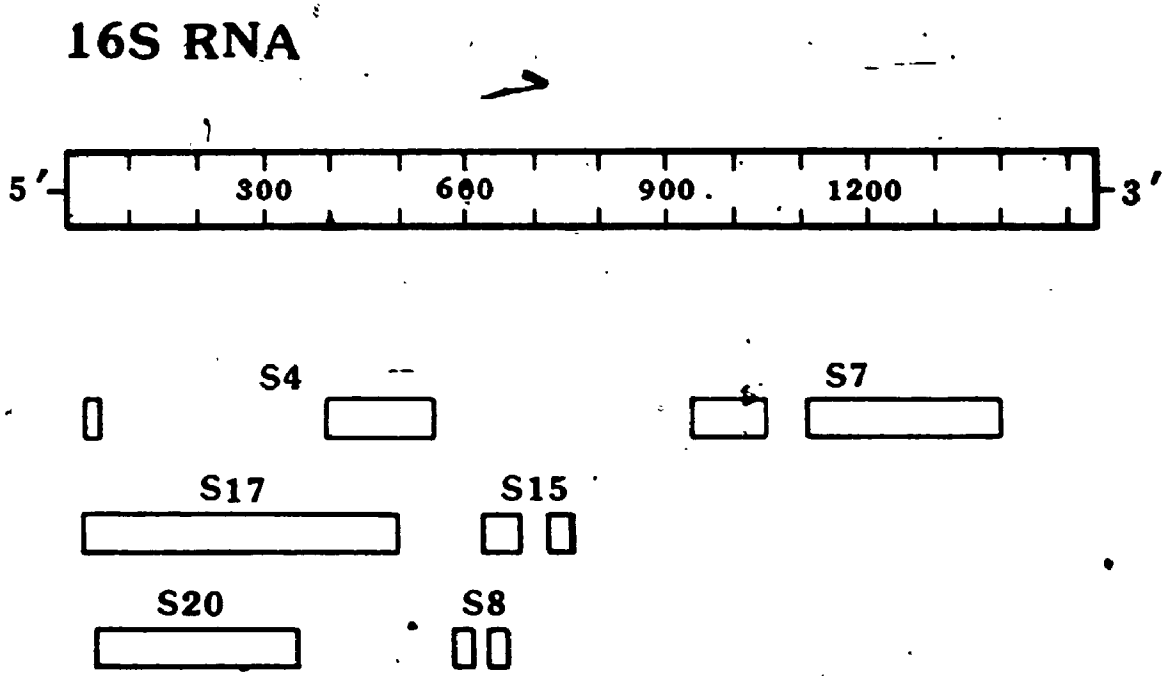

Figure 2. Location of protein binding sites on the 16S RNA. The bars represent protein-specific RNA fragments aligned according to the complete 16S rRNA sequence. Numbers within the 16S RNA denote nucleotide distances from the 5' terminus. From Zimmermann, 1980; Gregory et al., 1984 and Stern et al., 1986.

Another widely used method for assessing RNA-protein association is the use of covalent linkage, which has already been discussed above in the context of RNA-RNA association (section c). Common cross-linking methods include UV irradiation and a variety of bifunctional chemical reagents (Brimacombe et al., 1983). The determination of precise points of cross-linking on r-proteins has proven extremely difficult, but much more success in localizing cross-link sites on the RNA have been provided by partial nuclease digestion followed by 2-dimensional electrophoresis (Brimacombe et al., 1986). In the 30S subunit, only S7 can be consistently linked to 16S rRNA using very low doses of UV irradiation, and its cross-link point has been exactly defined as U_{1240} (Zwieb and Brimacombe, 1979). A second link (generated chemically) using 2-iminothiolane was found to be C_{1379} (Wower and Brimacombe, 1983). Among the remaining 30S subunit proteins, both S20 and S4 have been linked by UV irradiation to 16S rRNA, S20 to the fragment spanning residues 211 to 279 and S4 to residues 423 to 499 (Ehresmann et al., 1977). In these examples, linkage was found to occur within the classically defined binding sites, but with others such as S17 and L23 (Brimacombe et al., 1986) linkages occurred elsewhere.

It is important to bear in mind that cross-linking experiments of this kind provide only topographical information, and do not imply the presence of physical

interactions at cross-link points (Brimacombe and Stiege, 1985). Thus, the occurrence of a cross-link indicates only that the participating structures occupy the same molecular neighbourhood, and this can itself provide unique insights into 3-dimensional environments.

(f) Ribosome Production

It has been known for some time that there is a direct, linear relationship between growth rate and quantity of ribosomes in dividing E. coli cultures (Nomura, 1984). To support faster growth the cell must be capable of increasing its capacity for protein synthesis, and it does this by raising the number of ribosomes per unit of cell mass. When growing rapidly, ribosomes may constitute up to 40% of that mass (Nomura et al., 1984), and therefore the system for producing the components for new ribosomes must be both very efficient and responsive. In fact, when the rates of synthesis of ribosomal components are measured, they are found to be balanced both with respect to one another and coordinated in response to the cell's external environment. (Dennis, 1974). The mechanisms by which E. coli coordinates the divergently located sequences coding for ribosome production are the subject of the following section (g).

The genes for the many protein and RNA constituents of the E. coli ribosome are scattered throughout the bacterial genome as illustrated in Fig. 3. Cellular rRNA is transcribed from seven operons designated rrnA to rrnH (rrnF was removed due to a mapping error [Ellwood and Nomura, 1982]) which are clustered in the region near the bacterial origin of replication. Each shows the general structure Promoter - 16S rRNA - 23S rRNA - 5S rRNA (Morgan, 1982). In addition, the rRNA operons also include from one to three "spacer" tRNA genes located between 16S and 23S RNA or distal to 5S RNA. All seven operons are transcribed from two functional promoters P1 and P2, which produce 30S precursor transcripts for subsequent processing into the individual species (Apirion, 1983). These promoter regions show a large degree of sequence similarity from operon to operon, with two loosely grouped families showing the greatest homology (Lindahl and Zengel, 1986). It appears that the two promoters are subject to different controls (Glaser et al., 1983), and P1 has been shown to be dominantly expressed in vivo (de Boer and Nomura, 1979). Also, upstream 'enhancer' sequences capable of increasing transcription efficiency have been detected in the rrnB operon (Gourse et al., 1986b). Fragments containing this region of DNA show aberrant mobility on acrylamide gels, suggesting an abnormal conformation of the DNA helix such

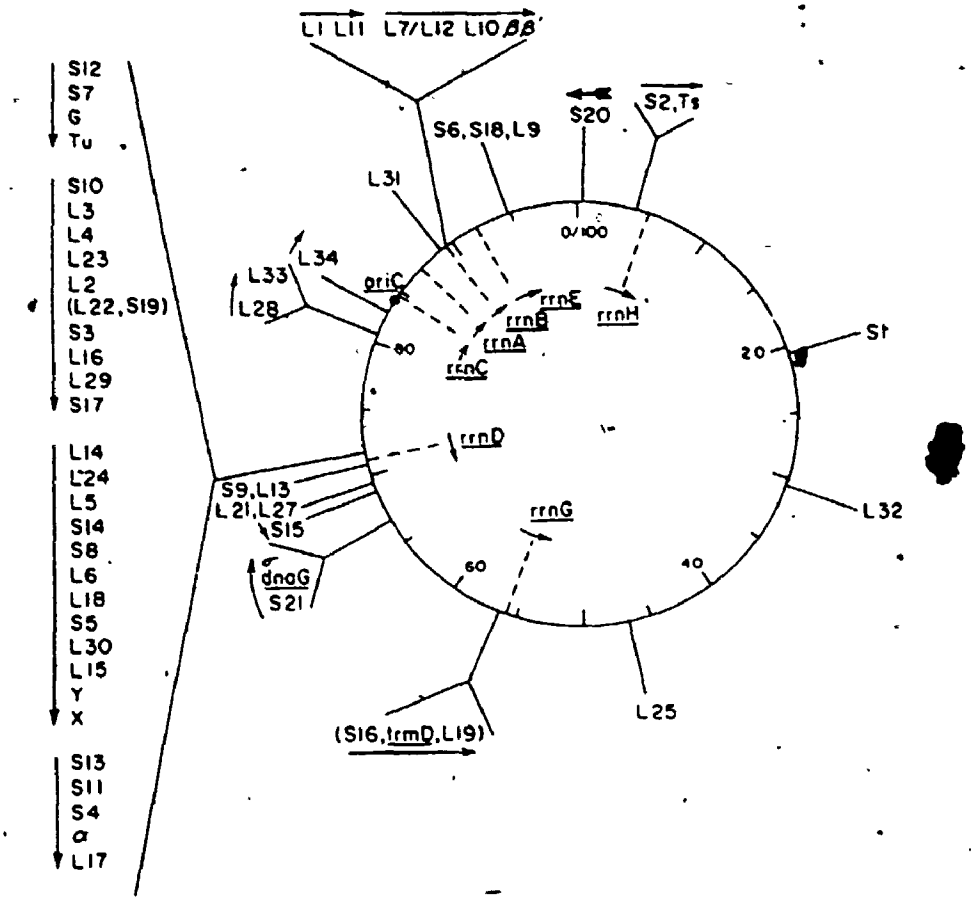

Figure 3. Genetic map of E. coli showing the locations of r-protein and rRNA genes. Genes for r-proteins are represented by the protein product. The genes for a number of cotranscribed proteins are included. The directions of transcription where known are included. From Nomura et al., 1984.

as a bend (Wu and Crothers, 1984) might be involved in this enhancement effect.

The genes for the r-proteins are also shown in the map of Fig. 3, with each gene being represented by its protein product. Genes for ribosomal proteins have traditionally proven difficult to manipulate since the protein products lack identifiable enzymatic activities. Early mapping was performed largely with standard genetic methods using resistance to antibiotics as markers (Davies and Nomura, 1972). Their genes were not identified and characterized until the development of gel systems capable of resolving their products (Kaltschmidt and Wittmann, 1970), and of specialized transducing bacteriophages providing for their isolation and expression (Jaskunas et al., 1975). All of the r-protein genes have now been mapped, and as can be seen from Fig. 3, they show pronounced clustering around two points on the map. These are designated str-spc and rif because these loci contain sites of mutation providing resistance to, or dependence on, the indicated antibiotics (Davies and Nomura, 1972).

(g) Mechanisms of Regulation

The ability to respond to changes in its nutritional environment is critical to the survival of the bacterial

cell. Regulation of the rate at which ribosomes are produced in response to such changes is referred to as growth rate-dependent regulation. This type of control has recently been proposed to be effected at the level of rRNA synthesis through negative feedback inhibition (Gourse et al., 1986b). DNA sequence requirements for this inhibition were found to be restricted to the -35 regions of the rrn operon P1 promoters, with the -10 regions also being important but not as critical. The effector for feedback inhibition has to date proven elusive, but is now generally expected to involve free ribosomes and/or cellular levels of ppGpp (Gourse et al., 1986a; Baracchini and Bremer, 1988). Other determinants of rRNA synthesis levels include rrn leader sequences which enable efficient transcription of the entire rrn operons (antitermination) (Holben and Morgan, 1984), and upstream sequences responsible for the extremely high rates of transcription supported by the rrn promoters (Gourse et al., 1986b).

Likewise, a great deal of progress in determining the mechanisms by which r-protein production are regulated has also been made recently, particularly with the realization that such control is apparently exerted at the level of translation. Early evidence for post-transcriptional regulation of r-protein synthesis came from two sources. First, RNA-DNA hybridization experiments utilizing transducing lambda phage as probes

specific for r-protein sequences, found that changes in expression during nutritional shift up were controlled not only by regulation of available mRNA but also by a second mechanism influencing its efficiency of translation (Dennis and Nomura, 1975). Second, gene dosage experiments in which extra copies of r-protein operons were introduced into E. coli strains on multicopy plasmids or phage, resulted in large increases in cellular levels of mRNA for the reiterated operons while failing to increase levels of their protein products proportionally (reviewed by Nomura et al., 1984).

These first clues that regulation was occurring at a post-transcriptional step were corroborated by in vitro transcription-translation studies in which exogenously added r-proteins were found to be capable of inhibiting r-protein production (Yates et al., 1980; summarized by Nomura et al., 1984). However, it was also observed that only one r-protein per operon was capable of producing this effect, and these were usually found to be those that bind rRNA independently in each subunit. Evidence that the translational repressors so identified function in vivo was derived from operon fusion experiments, in which specific r-protein genes were placed under the control of inducible promoters such as those for the lac and ara operons. Overproduction of the repressor proteins by induction was found to decrease the synthesis

of other r-proteins encoded in their corresponding operons (reviewed by Lindahl and Zengel, 1982).

From these studies a mechanism for the translational control of r-protein production has developed, in which one protein product from each operon may either be sequestered by rRNA in ribosome assembly, or in the absence of available rRNA for ribosome production, may interact with the mRNA for its own operon to repress further translation of those products. Figure 4 summarizes the operons known to be so regulated and their effectors. This process appears to function both in providing a balance between the rates of expression of all 52 r-proteins and in linking control of r-protein output as a whole to the growth rate-dependent control of ribosome production through the rate of rRNA production (Gourse et al., 1986a).

These two regulatory loops, however, are not solely responsible for the versatility with which ribosome production is managed (Mager, 1988). For example, expression of r-proteins will also be affected by such additional factors as variation in the stability of r-protein mRNAs (sometimes as a consequence of autogenous regulation), as well as modulation of the initiation of transcription of r-protein mRNAs (Lindahl and Zengel, 1986). 'Down-regulation' of transcription initiation occurs particularly during the cell's reaction to amino acid starvation, known as the 'stringent response'

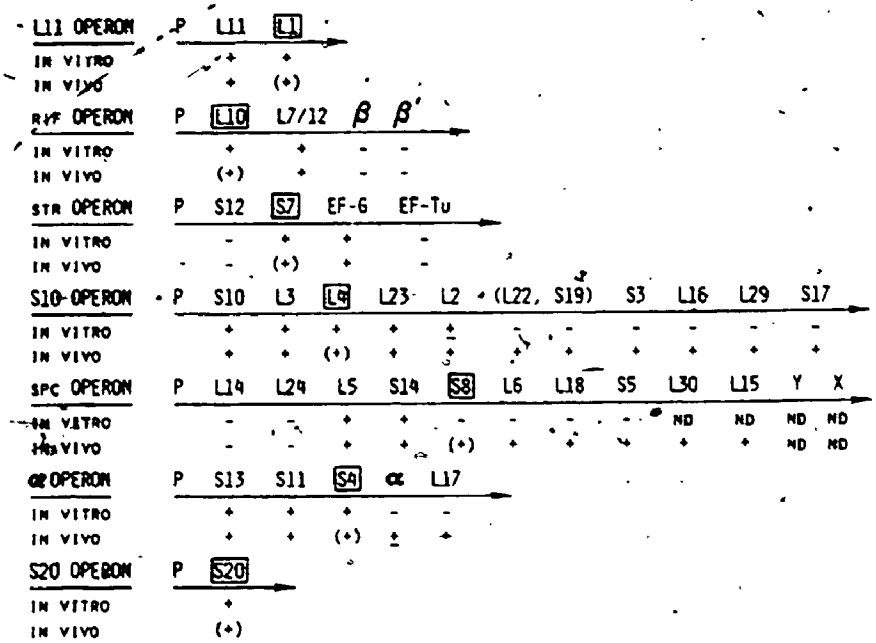

Figure 4. Regulation of gene expression *in vivo* and *in vitro*, by the identified repressor r-protein. Genes are represented by the protein product, and the direction of transcription from the promoter (P) of each operon is indicated by the arrow. Regulatory r-proteins are indicated by the boxes, and the effects of the boxed proteins on the *in vitro* or *in vivo* synthesis of proteins in the same operon are indicated. Symbols: +, specific inhibition of synthesis; -, no significant effect on synthesis; ±, weak inhibition of synthesis; (+), inhibition presumed to occur *in vivo*; ND, not determined. Each operon includes all the cistrons shown for it in Fig. 3. From Nomura *et al.*, 1984.

(Gallant, 1979). This control has been attributed to the presence of a conserved sequence in the promoters of operons coding for components of the translational apparatus, located immediately downstream of the Pribnow box (the 'stringent discriminator') (Travers, 1980; 1984).

Stringent control and the previously mentioned growth rate control have recently been unified under the effects of the 'RNA polymerase partitioning hypothesis' as proposed by Baracchini and Bremer (1988). They have suggested that interaction of ppGpp with RNA polymerase results in its partitioning into two forms with differing affinities for stable RNA and mRNA promoters. In this view, the correlation between ppGpp levels and stable RNA gene activity observed in stringent response and shift-up experiments is a cause-effect relationship. However, the ultimate control mechanism for those levels of ppGpp remains unknown (Baracchini and Bremer, 1988).

In the specific case of the S10 operon, stringent control has been found to depend entirely on sequences in the promoter, encompassing those of the consensus discriminator (Freedman et al., 1985). The S10 operon is, however, apparently unique in that autogenous regulation by r-protein L4 is exerted not only at the translational level but also at transcription, by suppression of readthrough at an attenuator region in the S10 operon leader (Lindahl et al., 1983). During a

nutritional shift-up (growth-dependent regulation), while most r-protein genes respond through autogenous control, the S10 operon responds mainly by increasing its rate of transcription. This occurs not only through a decrease in the rate of attenuation, but also through an increase in the differential rate of transcription initiation (Zengel and Lindahl, 1986).

Conversely, experiments with the L11 operon have shown that abolition of autogenous translational regulation results in the elimination of both growth rate-dependent and stringent controls (Cole and Nomura, 1986). Whether the S10 operon will prove to be anomalously coordinated within the global regulatory system as a result of its transcriptional control remains to be seen, but it is clear that a wide range of interacting signals are required to pace ribosome production with the cell's needs.

(h) Regulation of the Biosynthesis of S20

The gene for ribosomal protein S20 is located at approximately 0.5 min. on the E. coli chromosomal map of Fig. 3. Unlike all other ribosomal constituents it is monocistronic, with transcription governed by 2 tandem promoters (P1 and P2), and a rho-independent terminator just 50 base pairs downstream of the coding region

(Mackie, 1981). Sequence analysis also reveals that the 86 amino acid coding region is initiated by an unusual UUG start codon, and that S20 is a very basic molecule, with high percentages of lysine, alanine, and arginine.

The assembly mapping experiments of Mizushima and Nomura (1970) showed S20 to be among those r-proteins which are capable of binding independently to isolated rRNA (primary binding proteins). The apparent affinity of S20 interaction with 16S rRNA has been measured by Schwarzbauer and Craven (1981) and was determined to be approximately $1.4 \times 10^7\ M^{-1}$ using a filter binding assay. Regions of RNA interacting with the protein have been examined by nuclease digestion of RNA-protein complexes followed by identification of the protected 16S sequences. S20 protects a 5' fragment of 16S rRNA approximately 300 nucleotides in length, stretching from residue 57 to 354 (Ungewickell et al., 1975). Since it is physically unlikely that a small protein like S20 (MW = 9600 daltons), might interact with and directly shield so large a region of RNA, the protein more likely binds several smaller sites within the protected area, thereby maintaining features of secondary and tertiary structure essential for nuclease resistance. The site identified for S20 by this means was also found to overlap with the much larger 500 bp region protected by S4 (Zimmermann et al., 1972; Ungewickell et al., 1975; Mackie and Zimmermann, 1978). UV cross-linking experiments with S20

are consistent with these results, producing an S20-16S rRNA cross-link to a fragment encompassing residues 210 to 297 within the 5' 16S rRNA sequence (Ehresmann et al., 1977).

Since S20 is known to bind 16S rRNA independently in vitro (Mizushima and Nomura, 1970), it is therefore potentially capable of acting as an autogenous regulator of its own synthesis. Experiments using F' factors or high-copy plasmids carrying the S20 gene have in fact shown that increased copy number results in proportionate levels of mRNA for S20, but only small increases in the amount of S20 protein levels (Geyl and Bock, 1977; Mackie and Parsons, 1983). In other words, S20 expression is gene dosage-independent and is also likely to be autoregulated.

Evidence for autoregulation was first obtained in vitro by Wirth and Bock in 1980, who observed that S20 production was reduced by the addition of exogenous S20 or stimulated by the addition of 16S rRNA. Added 16S rRNA was proposed to stimulate S20 production by sequestering excess S20, and in fact, newly synthesized S20 was found to be complexed with 16S rRNA. Further experiments using an uncoupled transcription-translation system provided in vitro evidence that regulation occurs at the level of translation (Wirth et al., 1981).

By conventional views of translational control, these activities imply that S20 is capable of binding

either to 16S rRNA for assembly, or to its own mRNA to effect its inactivation. It is generally thought that such regulatory proteins by and large employ a single site for both functions, thereby leading to the corollary that similar nucleic acid sites be targeted both for assembly and regulatory binding. This postulate is not necessarily critical though, and it remains possible that different RNA binding sites are recognized by two differing protein domains (Mager, 1988). However, most attempts at identifying such translational operators on mRNAs have generally focused on finding sequence homologies with known functional interaction sites (Nomura et al., 1980).

For the case of S20, the most significant such homology encompasses 10 of 12 nucleotides from residue 198 to 209 of 16S rRNA, directly adjacent to the 5' end of the fragment cross-linked to S20 by UV irradiation (Ehresmann et al., 1977). The homology includes 7 consecutive residues spanning most of the region between the Shine-Dalgarno site and UUG initiation codon of the S20 mRNA (Mackie, 1981). However, any potential significance for these similarities is at best speculative in light of the finding that similar homologies in at least one other operon have proven to be merely coincidental (Deckman and Draper, 1985). In the case of the α operon, S4 is believed to recognize a very complex tertiary structure containing several regions of

very weak homology spread out over a large region of rRNA (Deckman and Draper, 1987).

(i) Objectives

Prior to this work, most efforts aimed at delimiting the r-protein domains responsible for RNA binding and other functions were based on a proteolytic approach. R-proteins were fragmented by proteolytic or chemical digestion and the resulting products then tested for residual binding or other activities. This approach has provided significant successes, (summarized in Chapter 2), particularly in the case of S4, but is ultimately limited by the number of chemical and enzymatic cleavages available.

Two separate experimental approaches have implied that the amino terminus of ribosomal protein S20 contains residues essential for its binding to 16S rRNA. In the first, Paterakis et al. (1983) found that two proteolytic fragments of E. coli ribosomal protein S20 lacking 14 or 35 amino acids from its N-terminus exhibited reduced or no 16S rRNA binding activity, respectively. In a second, an amino terminal fragment of S20 up to 50 residues in length cosedimented with 16S rRNA after the latter had been incubated with crude extracts of heat-shocked cells (Mackie, 1977a). In neither of the above cases were

quantitative measurements obtained. Therefore, we have employed here a comprehensive means of obtaining an assortment of deletions at the C-terminus of the S20 protein, without proteolysis. Mutation is accomplished at the DNA level, and altered peptide products are generated by coupled in vitro transcription-translation of the new sequences.

This approach was undertaken with the potential for integration with a parallel study of binding activities with S20 mRNAs. Vectors for the controlled transcription of specific RNAs can now provide sufficient volumes of product for conventional binding studies (Melton et al., 1984), as will be discussed further in Chapter 3. Comparison of 16S rRNA and S20 mRNA binding activities with the S20 deletions discussed above, would provide an excellent means of determining the extent to which the two activities utilize common peptide structures.

The broader question of S20 mRNA structure and its effect on regulation has also become accessible through the application of site-directed mutagenesis (Zoller and Smith, 1984). Ongoing experiments in the laboratory have been directed toward dissecting the role of the unusual UUG start codon of S20 and S20 mRNA-16S rRNA homologies in the autoregulatory mechanism of S20 (Parsons et al., 1988). Alterations to sequences directing translation are tested for regulatory effects by measurement of whether normal S20 gene dosage compensation is

maintained. Most such mutations have been found to also produce significant effects on translational efficiency. Within the scope of this thesis, application of the transcription-translation methods developed can be used to assess relative translational efficiencies *in vitro* of the site-directed mutants created.

CHAPTER 2

BINDING OF S20 DELETION MUTANTS TO 16S rRNA

INTRODUCTION

Purified ribosomal protein S20 binds to 16S rRNA independently in the high salt reconstitution buffer of Traub and Nomura (1969) with a K_a of 1.4×10^7 M^{-1} (Schwarzbauer and Craven, 1981). This interaction has been shown to occur specifically in the 5' domain of the 16S RNA molecule (Zimmermann, 1974), presumably as one of the early interactions of 30S subunit assembly.

Previous attempts to delineate the interactive regions of the protein have consisted of cleaving purified S20 proteolytically and testing the resulting fragments for residual binding activity (Paterakis et al., 1983). C-terminal fragments resulting from digestion of S20 with chymotrypsin and staphylococcus aureus protease were tested for binding with 16S RNA extracted by phenol (Kurland, 1960) or by acetic acid (Hochkeppel et al., 1976). Loss of 35 N-terminal residues abolished all binding, while the loss of just 14 left detectable but reduced binding to acetic acid extracted RNA only. Bound fragment was detected on polyacrylamide gels and was not quantified.

The use of chemical and proteolytic methods for isolation of functional r-protein domains has proven most successful in studies with S4. Cleavage of S4 at asparaginyl-glycyl bonds with hydroxylamine (Changchien and Craven, 1986), at tryptophan with dimethyl sulfoxide

and hydrogen bromide (Changchien and Craven, 1985), at cysteine with 2-nitro-5-thiocyanobenzoic acid (Changchien and Craven, 1978), and partially with trypsin (Changchien and Craven, 1976), yields large peptide fragments of varying activities which led to the following deductions. S4 contains a subdomain encompassed by residues 47 to 124 which is responsible for specific 16S rRNA recognition. The C-terminal portion of the molecule (S4 contains 203 amino acids), is required for promoting a conformational change in the assembling 30S particle in vitro. Residues 32 to 46 were found to be important for the assembly of a number of other 30S proteins, and the N-terminal 31 residues were required for binding of tRNA by the ribosome (Changchien and Craven, 1985).

The functional domains of S1 have similarly been localized using cyanogen bromide cleavage (Subramanian et al, 1981), trypsin digestion (Suryanarayana and Subramanian, 1979), and isolation of mutant forms of the protein (Subramanian and Mizushima, 1979). Two distinct structural and functional domains were revealed, with residues 1 to 170 encompassing the ribosome binding site, and the remainder (171 to 557) containing the nucleic acid binding function of S1 (Subramanian, 1983).

Other less exhaustively studied r-proteins which have been examined for functional fragments include S8 (Paterakis and Littlechild, 1982; Bruce et al., 1977), L18 (Newberry et al., 1978), and S13 (Schwarzbauer and

Craven, 1985). S13 was proposed to have a C-terminal domain for RNA recognition and an N-terminal region for interaction with protein S19.

This chapter outlines our attempts to delineate the regions of S20 required for 16S rRNA binding activity using a molecular approach. An unlimited range of 3' deletions in the coding region for S20 can be created using the double strand-specific exonuclease BAL 31. Several internal deletions can also be produced using 3 in-frame Sau3A restriction sites in the S20 gene. Deleted sequences are then expressed in vitro by coupled transcription-translation, yielding labelled S20 mutant proteins deleted internally or at the C terminus. These products are then testable without further purification for RNA binding ability to assess the nature of sequences necessary for RNA binding.

MATERIALS AND METHODS

(i) Enzymes and Chemicals:

All chemicals used were of reagent grade. Phosphoenolpyruvate (PEP) for in vitro transcription-translation was from Calbiochem. Radiochemicals were obtained from New England Nuclear. Restriction enzymes were purchased from Pharmacia, Boehringer Mannheim, and

Bethesda Research Laboratories. Nuclease BAL 31 was obtained from Bethesda Research Laboratories.

(ii) Strains and Plasmids:

The source plasmid (pGM24) from which S20-containing sequences were originally derived was described by Mackie and Parsons (1983). It contains residues 232 to 551 of the S20 sequence (see Appendix A for numbering). This includes the entire leader and coding sequence, but lacks both promoters and the transcriptional terminator. Fig. 1(a) shows pCD2, a derivative of this plasmid which carries the same S20 sequences with a new BamHI site inserted next to the existing one for EcoRI. The source of S20 containing fragments for these experiments was pCD2.

The vectors used for cloning and expressing mutant sequences are shown in Figs 1(b) and (c). Plasmid pKK223-3 (Brosius and Holy, 1984) was obtained from Pharmacia. PCD0 is a derivative of the vector pCQV2 described by Queen (1983), which was obtained from Dr. D.T. Denhardt. Host strains were JM103 (Δ[lac, pro], thi, strA, endA, sbcB15, hspR4; SupE, F', traD36, proAB$^+$, lacI^q-ZΔM15) (Messing and Vieira, 1982) and MM294 (endA1, thi-1, hsdR17, supE44; from M. Meselson) respectively. Strains used for cell-free extracts were RD100 (rns$^-$, pnp$^-$, met$^-$, trpD9778, relA, lacZ; from M. L. Pearson) and BU8049 (F$^-$, Δ[lac, pro] strA, recA, lon$^-$) from the Bukhari

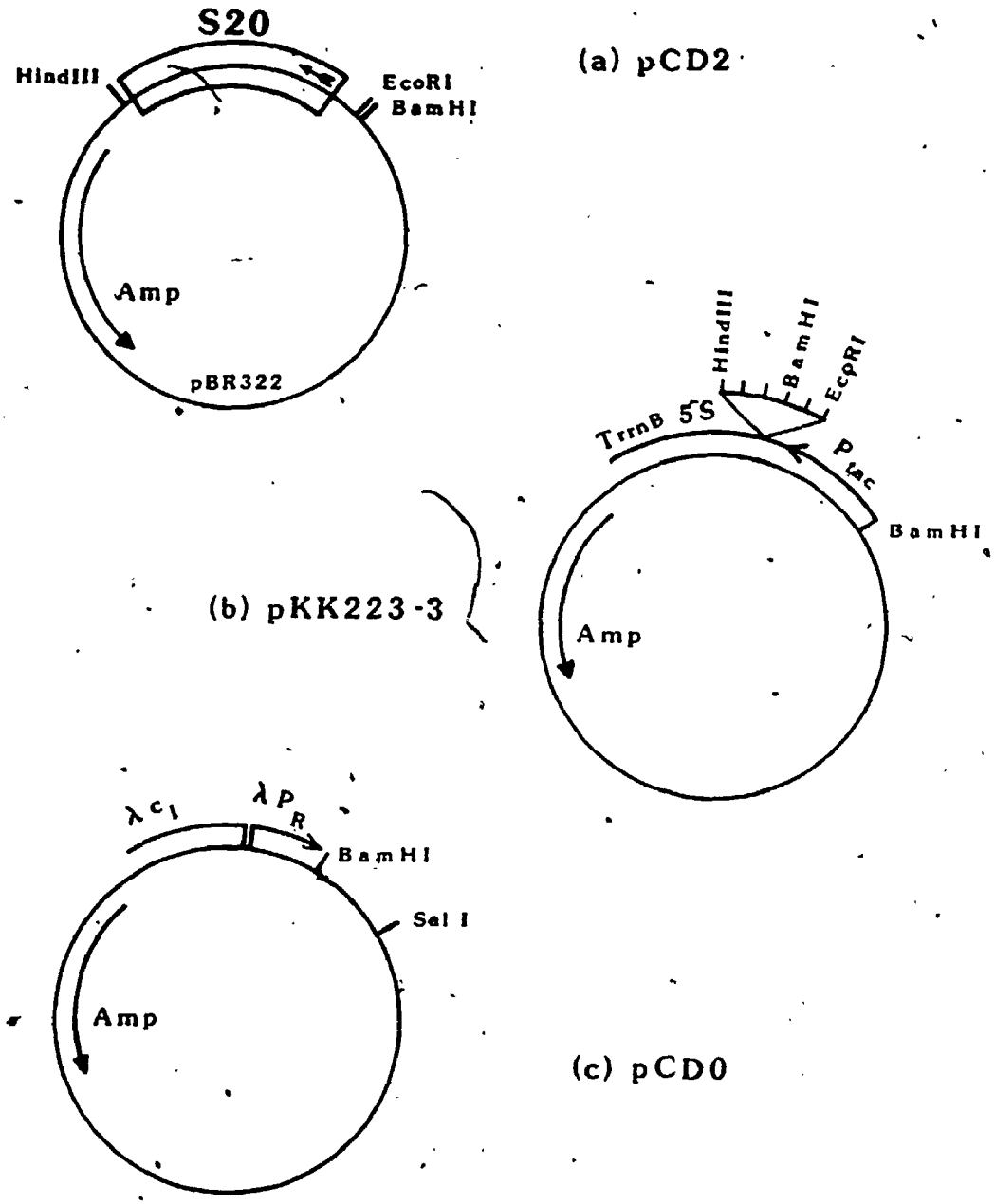

Figure 1. Physical maps of the S20 source plasmid and expression vectors. (a) pCD2; the orientation of the S20 gene is shown by an arrow. (b) pKK223-3; P_{tac} = hybrid trp-lac promoter and T_{rrnB} = transcriptional terminators from the rrnB ribosomal RNA operon. (c) pCD0; P_R = promoter and ribosome binding site of the phage lambda cro gene and C_I = temperature sensitive repressor of the P_R promoter. Directions of transcription from the P_{tac} and P_R promoters are marked by arrows.

collection (obtained through Dr. G. Chaconas). All sequencing was performed in the bacteriophage M13mp8 (Messing and Vieira, 1982), using JM103 as the host.

Plasmid DNA was isolated from saturated cultures of the appropriate strains to which 175 mg/l chloramphenicol had been added at mid-log phase (A_{600} = 0.6). Closed circular DNA was isolated by dye-buoyant density centrifugation of the cleared lysate (Clewell, 1972) followed by 2 precipitations from sodium acetate with 2.5 volumes of ethanol (Maniatis et al., 1982). Plasmid DNA was stored in 10 mM Tris pH 7.6, 1mM EDTA (TE buffer) at 4°C.

(iii) BAL 31 Nuclease Treatment and S20 Fragment Isolation:

BAL 31 nuclease was titrated in the buffer recommended by the supplier (B.R.L.) using the EcoRI-HindIII fragment of pCD2 (Fig 1[a]). Digestions were separated on a 6% polyacrylamide gel in TBE buffer (100 mM Tris-borate pH 8.3, 2.5 mM EDTA) and visualized by staining with 0.5 µg/ml ethidium bromide.

Fragments for cloning were prepared by treating HindIII-cut pCD2 with BAL 31 in the recommended buffer for either 7 or 15 minutes at 37°C. The enzyme-to-fragment ratio was 2 x 10^{-2} units/pmole using a fragment concentration of 50 nM (termini concentration of 100 nM). Reactions were quenched by extraction with equal volumes

of phenol saturated with TE buffer and DNA subsequently precipitated with 2.5 volumes of ethanol.

Fragment ends were repaired at 8°C for 1 hour with 1 U *E. coli* DNA polymerase I (large fragment) in a 30 µl reaction containing 60 mM Tris pH 7.6, 6 mM $MgCl_2$, 1.5 mM dithiothreitol and 2.5 mM deoxyribonucleotide triphosphates. HindIII linkers labelled with [^{32}P]-ATP were ligated to the fragments in 60 µl of the above buffer (plus 1.0 mM ATP) at 15°C for 12 hours with 2 U of T4 DNA ligase. This was followed by digestion with HindIII and EcoRI (or HindIII and BamHI) before finally purifying the S20 deletions on a 6% polyacrylamide gel. DNA fragments were eluted from the gel by the method of Maxam and Gilbert (1980).

(iv) Internal Deletions of the S20 Gene:

DNA fragments from pCD2 (Fig. 1[a]) were prepared for Sau3A digestion by the following method. 5 µg of pCD2 was digested with EcoRI and HindIII and then electrophoresed on a 0.8% agarose gel in TAE buffer (40 mM Tris pH 8.0, 20 mM sodium acetate, 1 mM EDTA) overnight at 40 V. DNA was visualized by staining with 0.5 µg/ml ethidium bromide, and the EcoRI-HindIII DNA fragment electroeluted from the gel by the method of Maniatis *et al.* (1982). The purified fragment was then digested with Sau3A and prepared for ligation by

extraction with phenol-chloroform and ethanol precipitation.

(v.) Cloning S20 Mutants in Expression Vectors:

Vectors digested with the appropriate enzymes were prepared for ligation by treatment with calf intestinal alkaline phosphatase to reduce spurious positives in transformations. Restricted plasmid (5 µg) was incubated at 37°C for 1 hour with 0.001 U of enzyme in 100 µl of 50 mM Tris-HCl (pH 9.0), 1 mM $MgCl_2$ and a 1:20 dilution of enzyme diluant containing 100 mM glycine-KOH (pH 10.2), 1 mM $MgCl_2$, and 0.1 mM $ZnCl_2$. Reactions were terminated by two extractions with equal volumes of phenol-chloroform and two extractions with ether, followed by precipitation of the DNA with ethanol.

Ligations were performed as recommended by the enzyme supplier (Boehringer Mannheim) using fragment to vector ratios of 10:1 for single fragments with differing ends. This ratio was increased up to 20:1 for 3 component ligations.

Transformations were performed by the standard $CaCl_2$ method of Cohen et al. (1972). Ampicillin-resistant clones of interest were screened by restriction digestion of DNA isolated by rapid alkaline lysis of 2 ml cultures (Maniatis et al., 1982).

(vi) Sequencing:

Sequencing of deleted S20 sequences was carried out by the modified dideoxy technique of Biggin et al. (1983). The 17-base pair M13 "universal" primer was utilized for sequencing fragments cloned in the vector M13mp8 (Messing and Vieira, 1982).

(vii) Coupled Transcription-Translation In Vitro:

Coupled transcription-translation reactions were carried out essentially as described by Zubay (1977) and modified by Mackie (1977b). Cell-free extract (S-30) was prepared from cultures of RD100 or BU8049 grown in rich medium with vigorous shaking. Best yields of the mutant proteins were obtained when S-30 was prepared from cells harvested in early log phase ($A_{600} \leq 0.8$). Optimum Mg^{++} and Ca^{++} concentrations were determined for each extract using a β-galactosidase coding template. A plasmid fusing the coding region of β-galactosidase to the P2 promoter, leader, and first six codons of S20 (pGP9) was utilized for this purpose (Parsons et al., 1988). 100 µl aliquots of S-30 were stored at -70°C until used and were never refrozen. 100 µl aliquots of premixed components (except PEP, $CaCl_2$, poly(ethylene glycol) and [^{35}S]-methionine) were also stored at -70°C until use.

The concentrations of plasmid in transcription-translation incubations were limited to about 5 µg per ml. The reactions were performed at 34°C for 30 minutes

and included 20 µCi [^{35}S]-methionine for labelling. Aliquots were immediately frozen at -70°C.

Experiments utilizing protease inhibitors included leupeptin (2-4 µg/ml) or phenylmethylsulfonyl fluoride (2-4 mM) before S-30 was added. 2-phenanthroline (8 mM) was added to incubations after 20 minutes.

Yields of S20 were assessed as follows. A fraction of each incubation was precipitated with 5 volumes of acetone and applied to a 16.25% polyacrylamide slab gel (0.75 mm thick) based on the SDS/urea system developed by Swank and Munkres (1971). These contained 0.1% SDS and 6 M urea in 0.1 M sodium phosphate at pH 7.2. A 3.5% polyacrylamide upper gel was poured to facilitate removal of the comb. The gels were normally run at 60 V overnight using 0.1% SDS, 0.1 M sodium phosphate pH 7.2 running buffer. Wet gels were processed for fluorography and then dried and exposed. Slices containing S20 or its derivatives were excised and rehydrated in 50 µl ddH_2O. After 1 hr, 10 mls of a mixture of 3% Protosol in Econofluor (NEN) was added and the vials incubated at 37°C overnight before counting. This method was suggested by New England Nuclear. Another sample from each incubation was counted directly to obtain the specific activity of methionine, from which yields of S20 were derived.

(viii) Isolation of 16S rRNA:

Crude ribosomes were isolated from strain MM294 (section ii) essentially as described by Zimmermann et al. (1972) and frozen at -70°C. RNA was isolated from 70S ribosome pellets by resuspending them in buffer containing 0.1 M LiCl, 0.5% SDS, 10 mM Tris pH 7.5 and 1 mM EDTA (Fellner, 1969) and then centrifuging the suspension through a 5 to 20% sucrose gradient in a similar buffer containing 0.1% SDS. One culture was labelled with 100 µCi [^{3}H]-uridine per 200 mls of culture. Labelled RNA was diluted with unlabelled to yield approximately 660 DPM per µg of 16S rRNA.

(ix) RNA-protein Association:

Samples of [^{3}H]-16S rRNA (11 pmoles containing 4000 DPM) were incubated at 37°C in 40 µl of TMK buffer (50 mM Tris pH 7.6, 20 mM $MgCl_2$, and 350 mM KCl) containing 6 mM β-mercaptoethanol for 30 minutes, and then chilled. Aliquots of the in vitro translations were thawed immediately before use and centrifuged for 30 seconds at 10,000 x g to remove precipitates. Protein, RNA, and 2 µg bovine serum albumin (BSA) were incubated for 30 minutes on ice in a total volume of 50 µl. Incubations were immediately loaded onto Bio-Gel A-0.5m columns (Garrett et al., 1971) equilibrated with TMK buffer containing 6 mM β-mercaptoethanol and 10 µg per ml BSA and eluted with the same buffer. Bio-Gel A-0.5m wa

found to give the best separation between 16S rRNA and unbound proteins and unincorporated [^{35}S]-methionine from the in vitro translation. Twelve fractions of 7 drops each were collected and counted directly in 2.5 ml PCS (Amersham). In each case a blank reaction (minus RNA) was run to quantify the radioactivity coeluting with 16S rRNA.

(x) Dual Label Scintillation Counting:

Quench curves were generated for [^{3}H] and [^{35}S] on a Beckman model 3801 scintillation counter. All scintillation counting was performed with [^{35}S] spill calculated and corrected by a dual counting program.

RESULTS

(i) Characterization of S20 deletions:

Deletions in the 3' region of the S20 gene were generated by digestion with exonuclease BAL 31 and cloned into expression vectors. This strategy relies upon appropriate vector supplied sequences to prevent run-on translation from the randomly terminated S20 coding sequence. This function was provided by a pBR322 derived fragment which contains three closely spaced stop codons immediately adjacent to the deleted termini. An outline of the manipulations followed in the generation of 3'

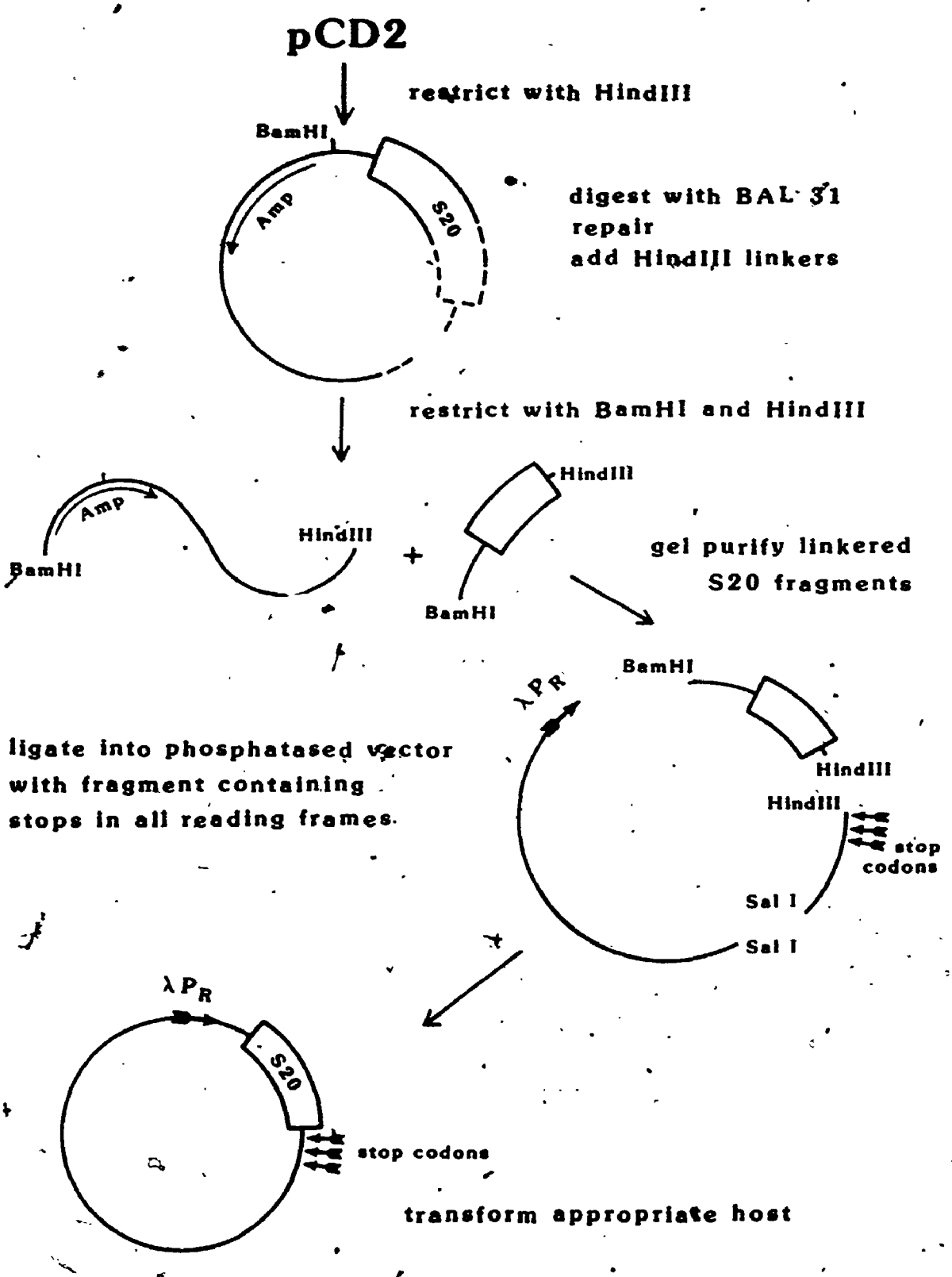

Figure 2. Generation of 3' deletions in the gene for S20. See the text (section i) for details.

deletions is presented in Fig. 2. The deletions were confirmed by hybridization to S20 sequences and then characterized by sequencing.

Exonuclease BAL 31 was titrated with a sample of the EcoRI-HindIII fragment removed from pCD2 as shown in Fig. 3. Digestion times are given in the figure legend and the times chosen for use in further experiments were 7 and 15 minutes at the highest level of the enzyme tested. For convenient cloning into pCD0, the fragment actually utilized for BAL 31 mutagenesis was the slightly larger BamHI-HindIII fragment of pCD2. Fig. 4(a) shows the 6% polyacrylamide gel from which the shortened fragments were removed for cloning.

Vector pCD0 was prepared for ligation with the deleted fragments by digestion with BamHI, SalI and alkaline phosphatase. Ligation and transformation produced large numbers of ampicillin resistant colonies, 60 of which were screened by quick alkaline lysis preparation of DNA from 2 ml cultures and subsequent digestion with BamHI and HindIII. Fig. 4(b) shows a sample polyacrylamide gel from the screening in which a variety of deletion sizes is evident.

Internal deletions were prepared by Sau3A digestion of an isolated EcoRI-HindIII fragment from pCD2 (Fig. 1). The fragments were ligated as an unfractionated mixture into pKK223-3 previously digested with EcoRI and HindIII. Ligations were used to transform JM103. DNA prepared by

Figure 3. Titration of BAL 31 nuclease. pGM24 was digested with HindIII and then aliquots treated with either 2 x 10^{-2} (a-e), 6 x 10^{-3} (f-j), or 2 x 10^{-3} (k-n) units of BAL 31 per pmole of DNA. Digestion times at 37°C were: (a) 10 min, (b) 7 min, (c) 3 min, (d) 2 min, (e) 1 min, (f) 10 min, (g) 7 min, (h) 3 min, (i) 2 min, (j) 1 min, (k) 10 min, (l) 7 min, (m) 3 min, (n) 1 min. Aliquots were then digested with EcoRI before electrophoresis on a 6% polyacrylamide gel. A set of size standards produced by HinfI digestion of pBR322 are marked on the right side. The arrow on the left shows the expected size of the EcoRI-HindIII fragment of pGM24. (Digestion with EcoRI apparently failed in sample lane k)

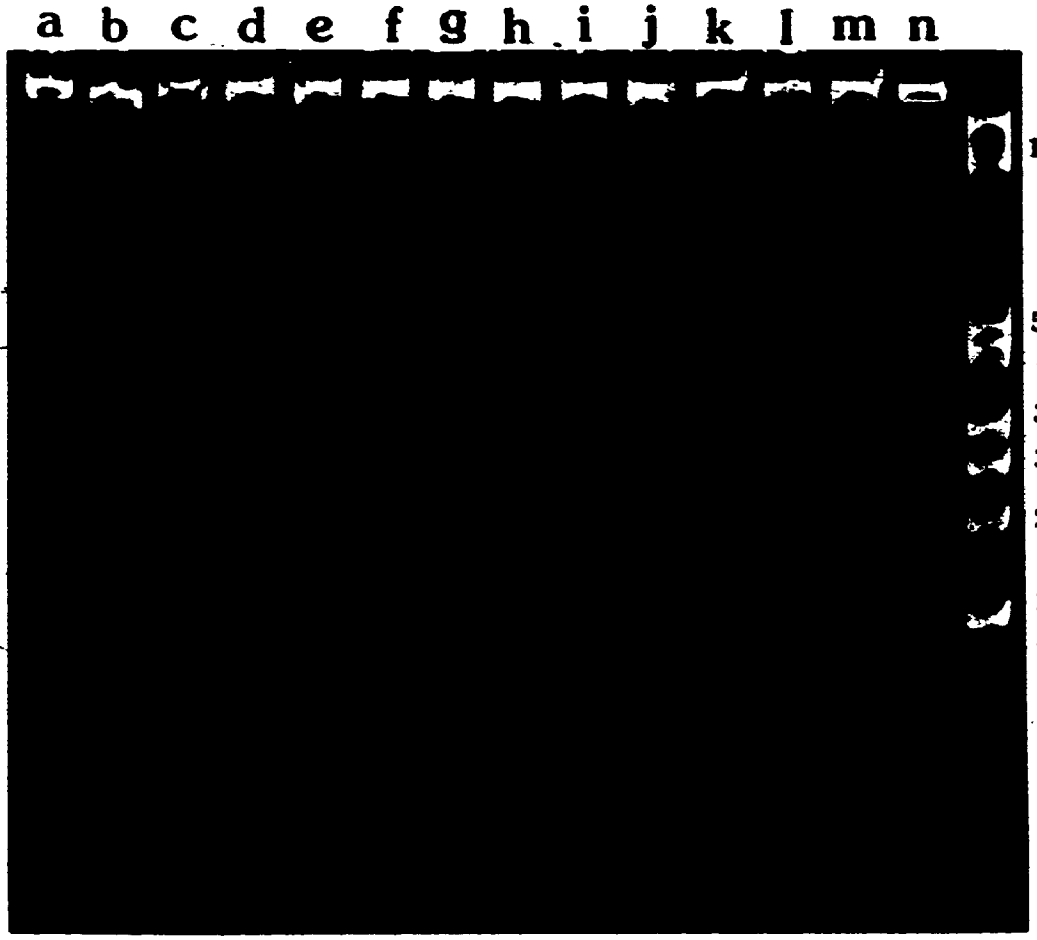
a b c d e f g h i j k l m n
1632
517
/506
396
344
298
221
/220
154

Figure 4(a). BAL 31 digestion of the S20 encoding BamHI-HindIII fragment of pCD2. Lane (a) contains a set of size standards as marked on the left. Lane (b) contains the full length BamHI-HindIII fragment of pCD2 (marked by the arrow on the right). Lanes (c) and (d) contain the same fragment treated with BAL 31 as described in Materials and Methods for 7 and 15 minutes respectively.

Figure 4(b). Screening of putative S20 deletion plasmids DNA prepared by alkaline lysis from ampicillin resistant transformants was digested with BamHI and HindIII before electrophoresis on 6% polyacrylamide gels. Three fragments resulting from the vector and their sizes are marked on the left. The range of deleted S20 fragments is shown on the right. Size standards (arrow) are as in (a).

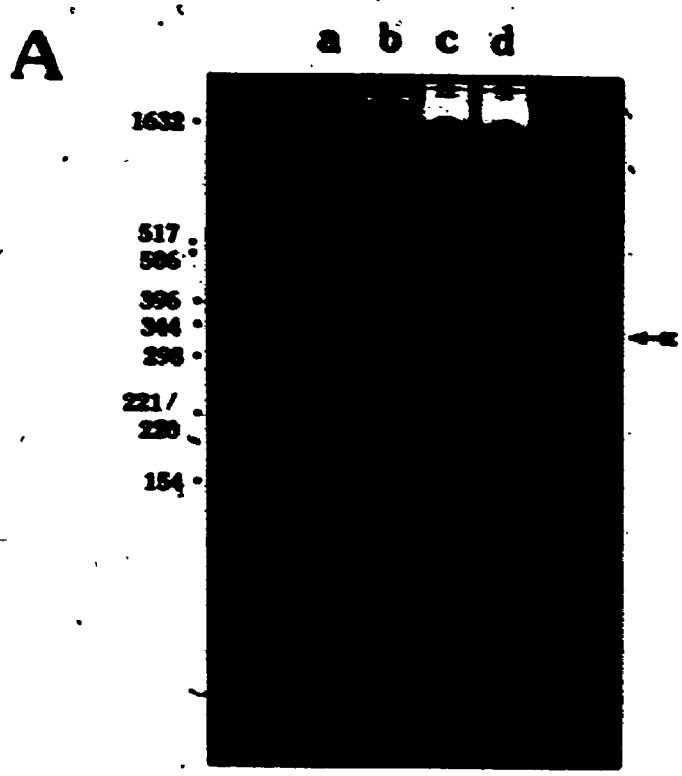
A
a b c d
1632
517
506
396
344
298
221/
220
154

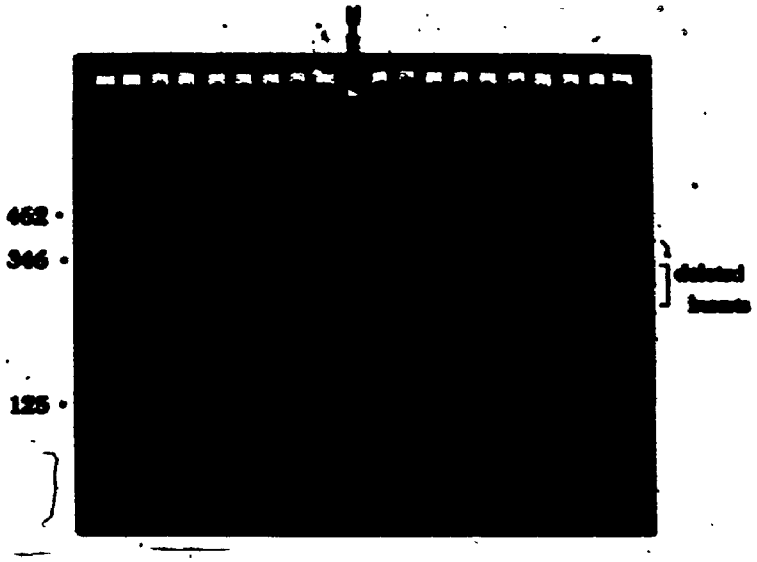
B
468
396
125

quick alkaline lysis was digested with EcoRI and HindIII and sized on polyacrylamide gels to screen for the range of possible deletions.

The identities of the sequences cloned were confirmed by Southern blotting as S20 by hybridization with an S20 probe (data not shown) before characterization.

The S20 sequences from a selected group of deletions were cloned as EcoRI-HindIII fragments into the sequencing vector M13mp8. Sequencing was performed by the method of Biggin et al. (1983) and a sample gel is illustrated in Fig. 5. Results of sequencing indicated that the final S20 residue in each of the clones is as listed in Table 1. Determination of the exact residue to which each gene was deleted also revealed the reading frame in which sequences downstream of S20 will be translated in each clone. Each reading frame is terminated by a different stop codon found in the downstream fragment, producing 3 different run-ons or tails of 3, 5, or 10 amino acids (Table 2). Fig. 6(a) summarizes the C-terminal deletions produced in S20.

Internal mutants were sequenced to determine the order of internal fragments resulting from random ligation. Fig. 6(b) summarizes the four clones selected, which yielded the 3 possible deletions plus a deletion-insertion in which the downstream Sau3A fragment was

Figure 5. Sequencing of various deletions of the S20 gene. The illustrated gel shows the sequences of the 3' deletions pCD104, 105 and 301 whose end points are residues 474, 453 and 508 respectively. The internal deletion pCD12, which is missing the 3' Sau3A fragment between residues 471 and 520, is interpreted in the region of the deletion. "Stop" marks the normal stop codon of S20, and the Sau3A recognition sequence representing the deletion site is shown.

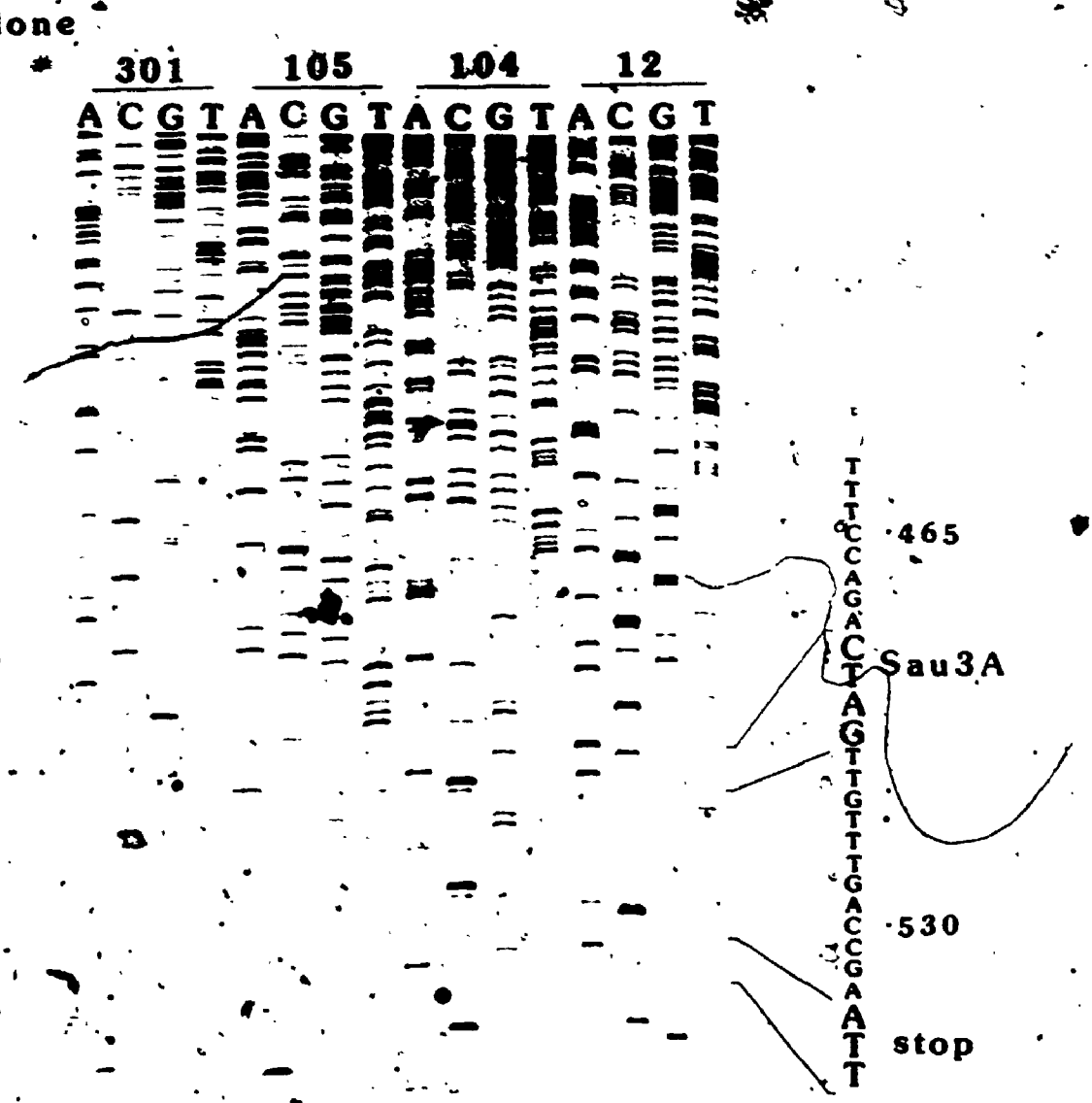
clone
301
105
104
12
A C G T A C G T A C G T A C G T
TTCCAGACTAGTTGTTTGACCGAATT
465
Sau3A
530
stop

Table 1. Positions of deletions in nucleotide and amino acid sequences for S20 C-terminal mutants.

Plasmid	Last S20 Nucleotide Remaining[a]	Last S20 Amino Acid[b]	Resulting Amino Acid 'tail'[c]
pCD6	-	86	-
pCD101	531	85	3
pCD102	513	79	3
pCD103	483	69	3
pCD104	474	66	3
pCD105	453	59	3
pCD106	438	54	3
pCD107	411	45	3
pCD201	512	79	10
pCD202	503	76	10
pCD301	508	78	5

a. The numbered nucleotides represent the last remaining nucleotide of the S20 sequence as shown in Appendix A.

b. The listed residues represent the last remaining amino acid in each translated S20 deletion peptide. Full length S20 has 86 amino acid residues.

c. These are the C terminal extensions of 3, 5 or 10 amino acid residues (see Table 2) added to the deleted S20 when the natural stop codon is removed.

Table 2. Sequences of possible S20 C-terminal run-ons.

Run-on length	Sequence
3 residues	-(x) lys leu stop
5 residues	-gln ala leu met arg stop
10 residues	-ala ser phe asn ala val val tyr his ser stop

x = gly, ser, cys, or arg.

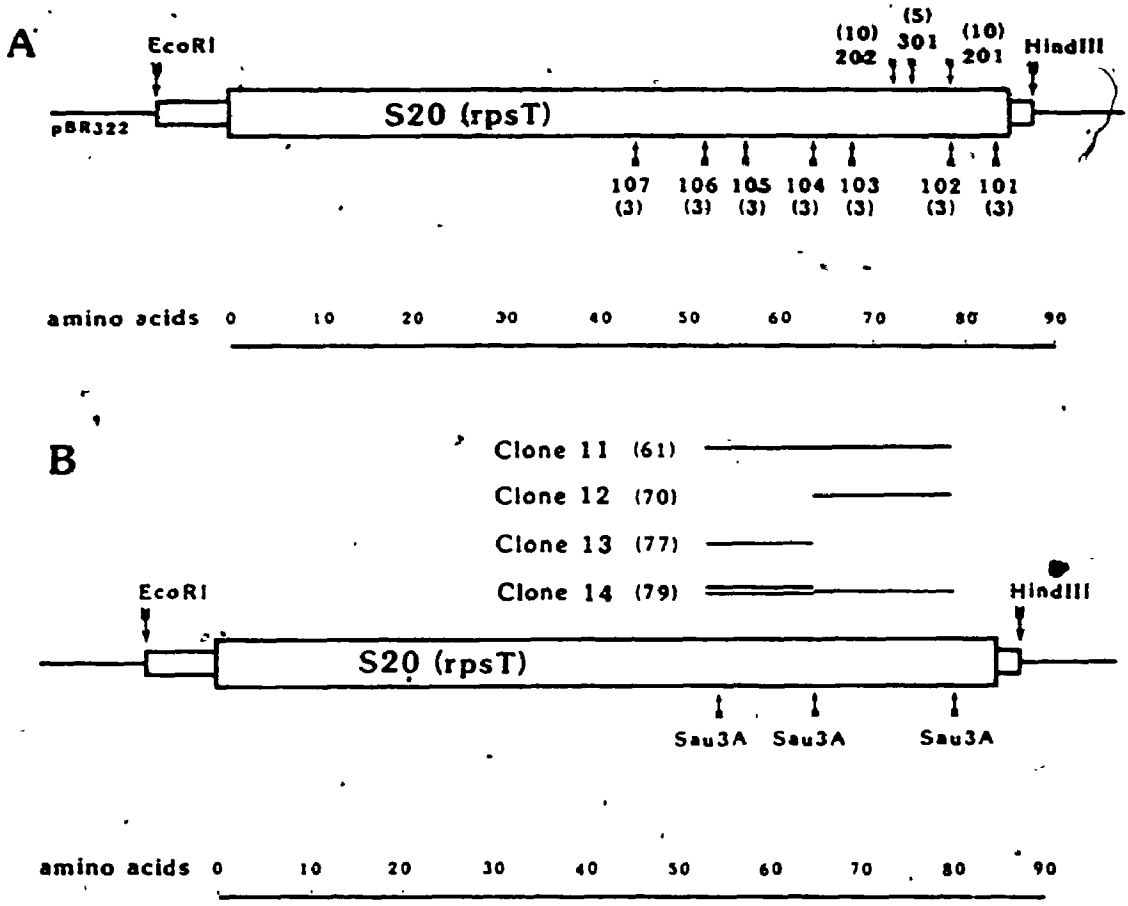

Figure 6(a). Map of C-terminal deletions of ribosomal protein S20. The end points of each of the characterized BAL 31-generated deletions shown in Table 1 are marked. Numbers in brackets indicate the tail size (Table 2). The plasmid carrying the full-length EcoRI-HindIII insert in pKK223-3 is designated pCD6..

Figure 6(b). Map of internal deletions of ribosomal protein S20. The locations of the three Sau3A restriction sites used in constructing the deletions are indicated. Deleted sequences are represented by single lines (——), while a duplicated sequence is shown by a double line (═══). Numbers in brackets indicate the number of amino acid residues remaining in each mutant.

deleted and replaced by a second copy of the upstream one.

(ii) Optimization of S20 Yield:

Expression of S20 products in in vitro transcription-translation was monitored by electrophoresis of the reaction products on polyacrylamide gels containing SDS and urea, followed with detection by autoradiography. An example exposure of such a gel on Kodak XAR-2 film is shown in Fig. 7. Yields of S20 products were assessed by cutting and counting the appropriate bands as indicated in Materials and Methods. Calculation of the efficiency of detection of radioactivity by this method was accomplished by the casting of minigels uniformly impregnated with [^{35}S]-protein and subsequent processing by the same method. The efficiency of detection was determined to be approximately 60%, and yield calculations were corrected accordingly.

Yields of S20 products were optimized in the cell-free system by several means. S-30 extracts for transcription-translation were prepared from cultures at various stages of growth, with the highest yields of final products resulting from S-30 cultures at $A_{600} \leq 0.8$. A lon$^-$ strain (BW8049) was utilized for the production of an S-30 extract in an attempt to reduce protein degradation. No improvements in the yields of mutant proteins over those obtained with extracts from

Figure 7. Products of coupled transcription-translation *in vitro* of S20 deletion mutants. Polyacrylamide gels containing SDS and urea (Materials and Methods) were used to resolve the products of *in vitro* transcription-translation. Reactions programmed by the following plasmid templates are shown: (a) pCD101, (b) pCD102, (c) pCD103, (d) pCD104, (e) pCD105, (f) pCD106. Lane (g) contains an S20 standard. The 3 major products are marked on the right, with the third arrow showing a small peptide associated with resistance to tetracycline.

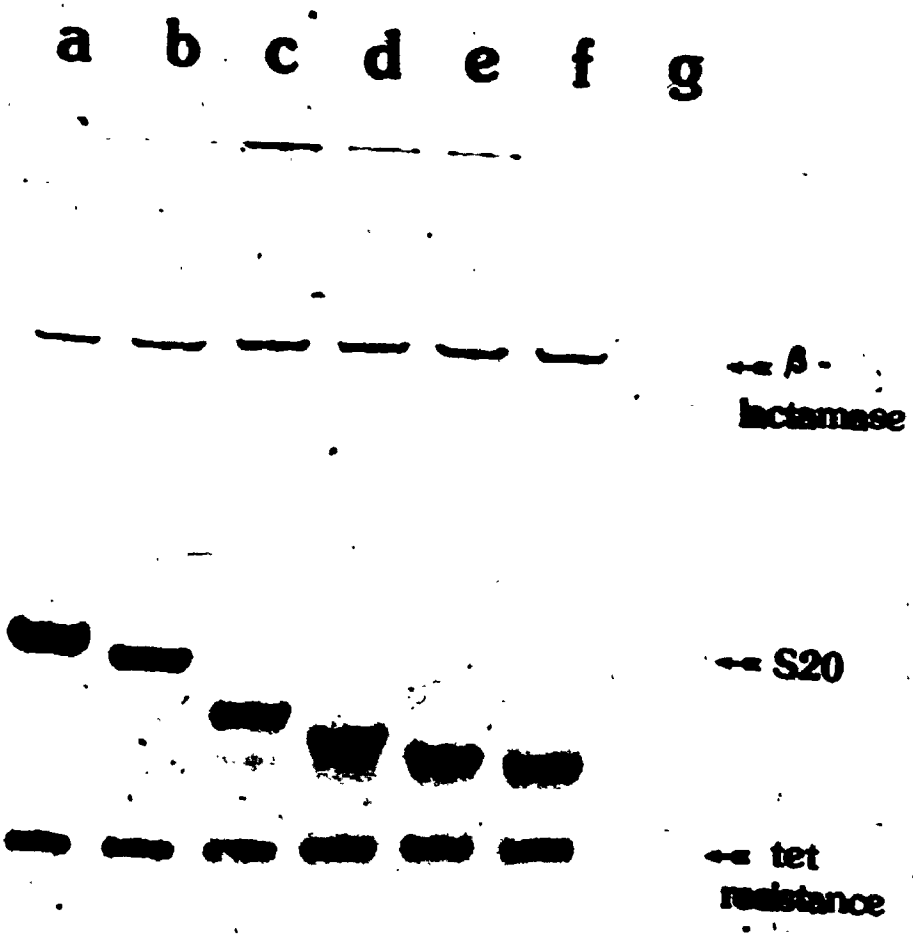
a b c d e f g
β-lactamase
S20
tet resistance

RD100 were observed. Optimal levels of both Mg^{++} and Ca^{++} were determined for each S-30 extract and the quantities of magnesium acetate and calcium chloride in the cell-free system adjusted according to the extract used.

Both the time and the temperature employed for in vitro reactions were varied to determine the maximum yield of a model altered S20 from clone 103. A temperature of 34°C produced the greatest quantity of product as monitored by SDS-urea polyacrylamide gels, and yield was not found to increase significantly after 30 minutes at this temperature. Attempts to improve the yields of the shorter mutant proteins by the addition of various protease inhibitors including leupeptin, phenylmethylsulfonyl fluoride and 2-phenanthroline were unsuccessful.

In general, it was found that the shorter the S20 coding sequence remaining, the lower the final yield of peptide produced in the cell-free system. Actual yields varied from as high as 425 pmoles per pmole of template with full length S20, to as low as 60 pmoles of mutant peptide per pmole of template with shorter clones such as 106 and 107. It is unclear if this effect is a result of lower translational efficiency or increased proteolytic breakdown. The greatly reduced yields of these proteins observed with cell extracts of stationary phase cultures (A_{600} = 1.5) could indicate breakdown is the cause, since

these extracts would be expected to differ most prominently from log phase ones in the presence of increased levels of cellular proteases (Goldberg and St. John, 1976). However, these also resulted in lower levels of complete S20, which should be rather resistant to degradation.

(iii) Optimization of the Protein-RNA Binding Assay:

The assay utilizes gel filtration for the separation of bound and unbound protein (Garrett et al., 1971). Bio-gel A-0.5m (Bio-Rad) provided the widest separation between RNA and the large quantities of unincorporated [^{35}S]-methionine from the in vitro translation. The presence of this spurious [^{35}S] also precluded simpler procedures such as the use of spun columns (Worthington Inc.) as its contamination of the RNA fraction is unavoidable. 16S rRNA elutes at the void volume with this grade of gel, providing minimum dilution of the fraction and the shortest run times. However, a significant number of spurious [^{35}S] counts also elute here, presumably because they are associated with whole ribosomes from the S30 extract. A short high-speed centrifugation (250,000 x g) was found to be effective at removing these flow-through counts from the in vitro reaction products, but also resulted in appreciable loss of S20 products. Therefore, a blank reaction with no 16S rRNA was processed along with each binding sample, and

the radioactivity in the void volume subtracted from calculations.

(iv) S20 Binding to 16S rRNA:

The binding of protein (P) to RNA (R) to give the complex R-P can be written as P + R <--> R-P. For this reaction, the number of moles of protein bound per mole of RNA (v) may be defined as $v = nK(A) / [1+K(A)]$ where K is the apparent association constant, n is the number of independent binding sites on the RNA, and (A) is the molarity of unbound protein (Schwarzbauer and Craven, 1979). This expression may be rewritten as $1/v = 1/[nK(A)] + 1/n$ such that a double reciprocal plot of 1/v versus 1/(A) gives a line with a slope of 1/nK and a y intercept of 1/n.

Protein-RNA complexes between S20 and 16S rRNA were formed and separated from free S20 as described. The variables include the concentration of 16S RNA, the concentration of S20, and the yield of bound S20. The ratio of bound S20 to 16S RNA is equal to v and (A) is the total S20 minus the bound S20. These values are displayed in Appendix B.

A binding curve for complete S20 synthesized in vitro from plasmid pCD6 is plotted from the data of Appendix B in Fig. 8. Fig. 9 shows the double reciprocal plot of the same data. A line generated by linear regression analysis was used to calculate n and K from its y intercept and slope, and an apparent binding

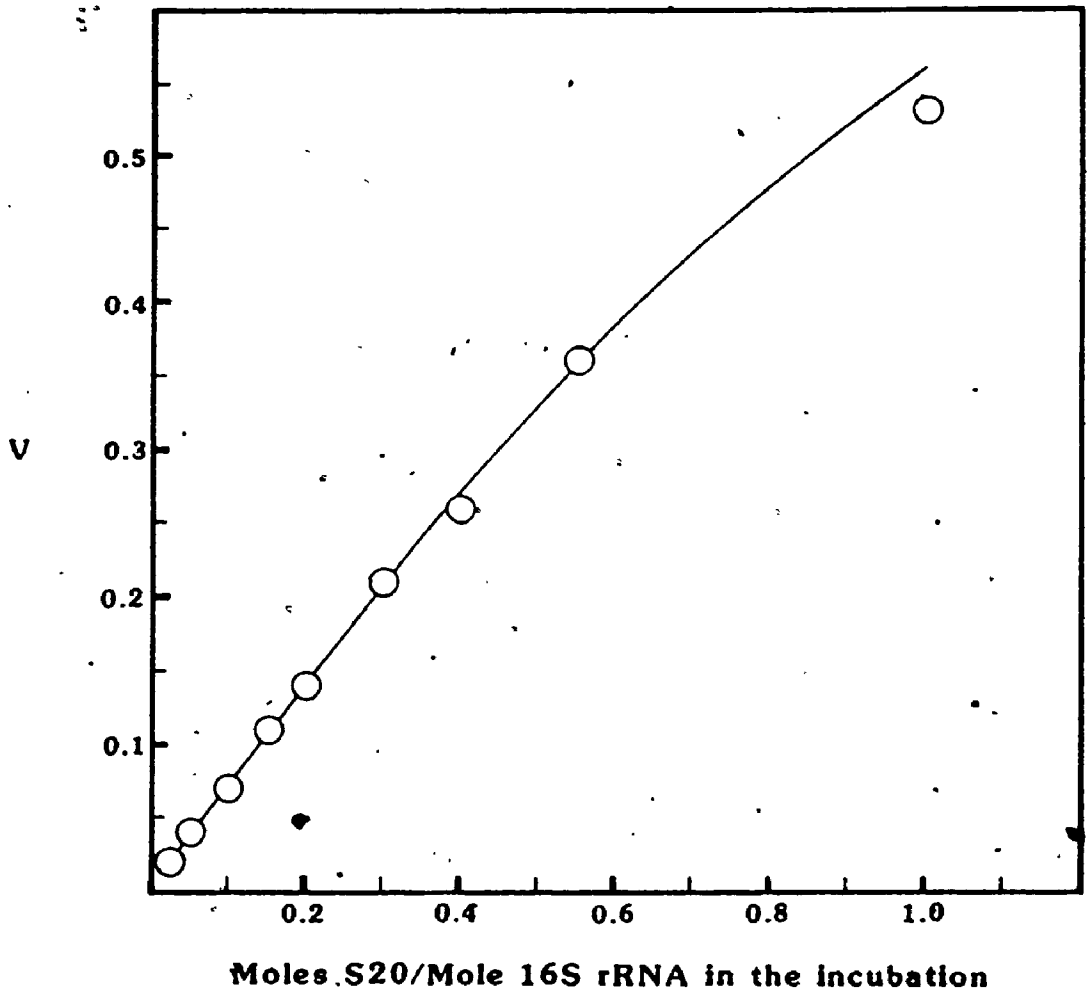

Figure 8. Binding curve for ribosomal protein S20 with 16S rRNA. Increasing amounts of a [^{35}S]-labelled, pCD6 directed, in vitro translation were reconstituted with purified [^{3}H]-labelled 16S rRNA as described in Materials and Methods. v = moles of S20 bound / mole RNA.

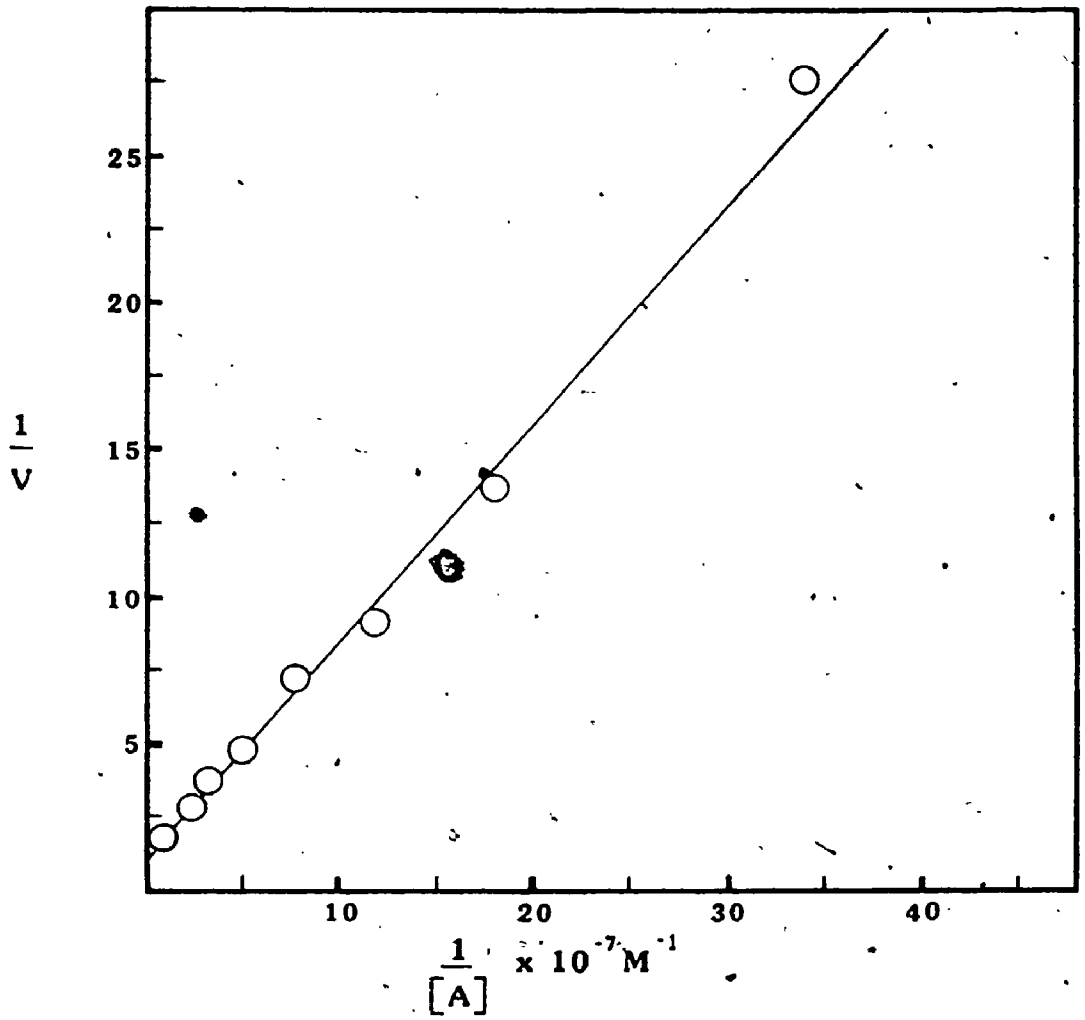

Figure 9. Double reciprocal plot of S20 binding to 16S rRNA (from Fig. 8). [A] is the molar concentration of unbound S20; the $^1/_v$ intercept is $^1/_n$; the slope is $^1/_{nK}$ where n is the number of binding sites and K is the apparent association constant.

constant (K) of 1.2×10^7 (M^{-1}) was obtained (with the number of binding sites equal to 1.1). This compares favourably with an equilibrium value of 1.4×10^7 (M^{-1}) obtained by Schwarzbauer and Craven (1981) using a nitrocellulose binding method for measuring complex formation.

All of the data tabulated in Appendix B represent incubations utilizing protein derived from a single translation. Although some variations in binding activity among the products of individual translations were found to occur, numerous different in vitro translations of normal S20 yielded no products with measured K_a values less than 1.0×10^7 (M^{-1}).

Specificity for S20 binding to 16S rRNA was established by several means. First, authentic unlabelled S20 competed for binding with labelled S20 that was produced in vitro: 30 pmoles of unlabelled S20 reduced the binding of 2 pmoles of [^{35}S]-S20 to 11 pmoles 16S rRNA in the standard assay by 50%. Secondly, analysis of proteins coeluting with 16S rRNA from Bio-Gel columns showed S20 to be the only labelled protein present. Also, S20 synthesized in vitro was shown to have a low affinity for an unrelated RNA (clover yellow mosaic virus RNA). Finally, saturation of 16S rRNA at higher protein/RNA levels was demonstrated as shown in Fig. 10. To obtain these levels, a lower concentration of RNA than that used in the standard assay was

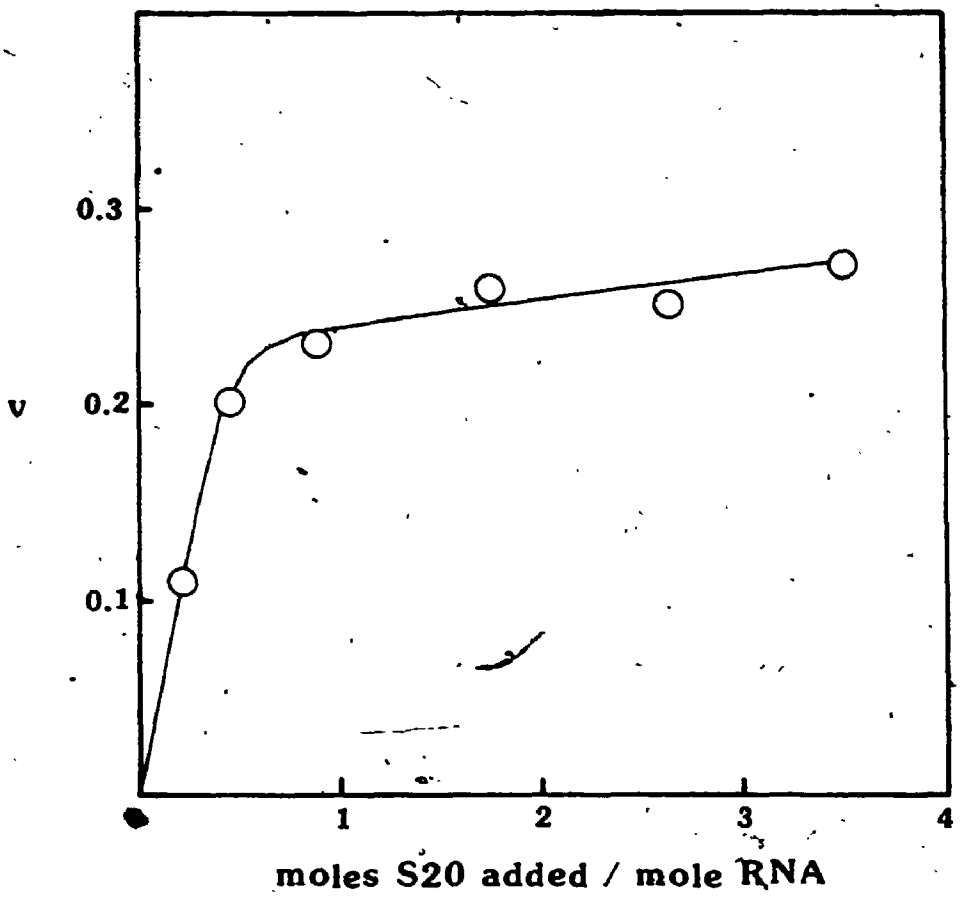

Figure 10. Saturation of 16S rRNA by S20 produced in vitro. Approximately 2.5 pmoles of 16S rRNA were mixed with increasing quantities of pGP11-directed translation products in 25 µl volumes. Complexes were analyzed as in the standard assay (Materials and Methods).

necessary, which may have resulted in the low stoichiometric ratio of around 0.3 pmoles of S20 per pmole of 16S rRNA that was obtained.

To verify that the RNA remained intact through the standard assay, denaturing agarose gel analysis of 16S rRNA from an example binding was performed after separation of the complexes. As can be seen in Fig. 11 no visible degradation was observed.

(f) Binding of S20 Derivatives to 16S rRNA:

The ability of mutant S20 proteins synthesized in vitro to bind to 16S rRNA was assessed in the standard assay. The data are summarized in Appendix C. A plot of the level of binding by 1 pmole of each mutant S20 to 11 pmoles of 16S rRNA is graphed against the sizes of the mutant proteins in Fig. 12. These data show that the removal of any residues from the C-terminus of S20 results in an immediate drop in its ability to bind to 16S rRNA. The loss of only 6 C-terminal residues (clone 102) eliminated most of the normal activity, and the loss of another 14 (clone 104) completely removed it. A third clone, (202), which carries the longest amino acid run-on, is in fact of the same size as normal S20 and differs from it only in the identity of the last 10 residues. This derivative displayed less than 4% of the binding of normal S20. Examination of the activity of a second similarly sized deletion carrying the alternative 5'

Figure 11. Denaturing agarose gel analysis of 16S rRNA after the standard assay. 16S rRNA from a standard assay was recovered by ethanol precipitation rather than collected and counted in PCS as usual. The RNA was glyoxylated in 50% DMSO and electrophoresed on a 1% agarose gel in 0.01 M sodium phosphate buffer, pH 7.0 (lane (b)). Lane (a) contains a similar starting sample of 16S rRNA glyoxylated directly. Size markers shown on the right side are: (c) human RNA, (d) RsaI-digested pBR322, and (e) PstI/BamHI-digested pBR322.

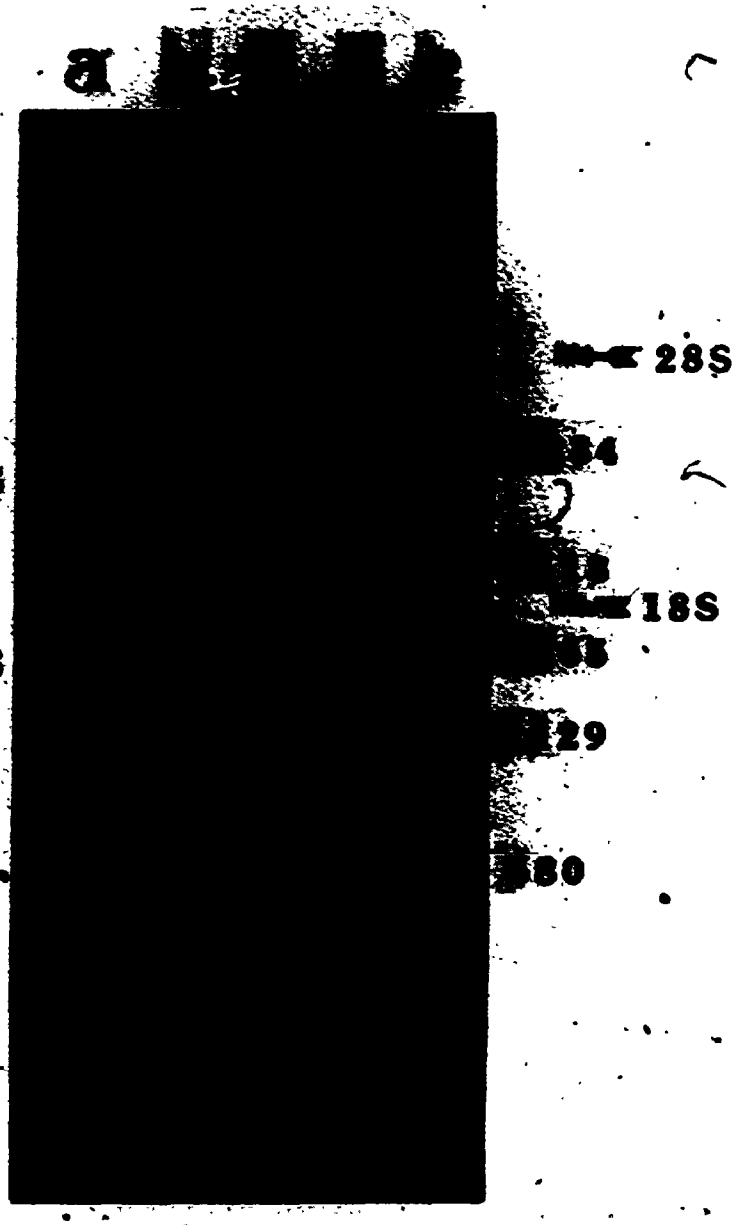
a
28S
23S
18S
16S
29
80

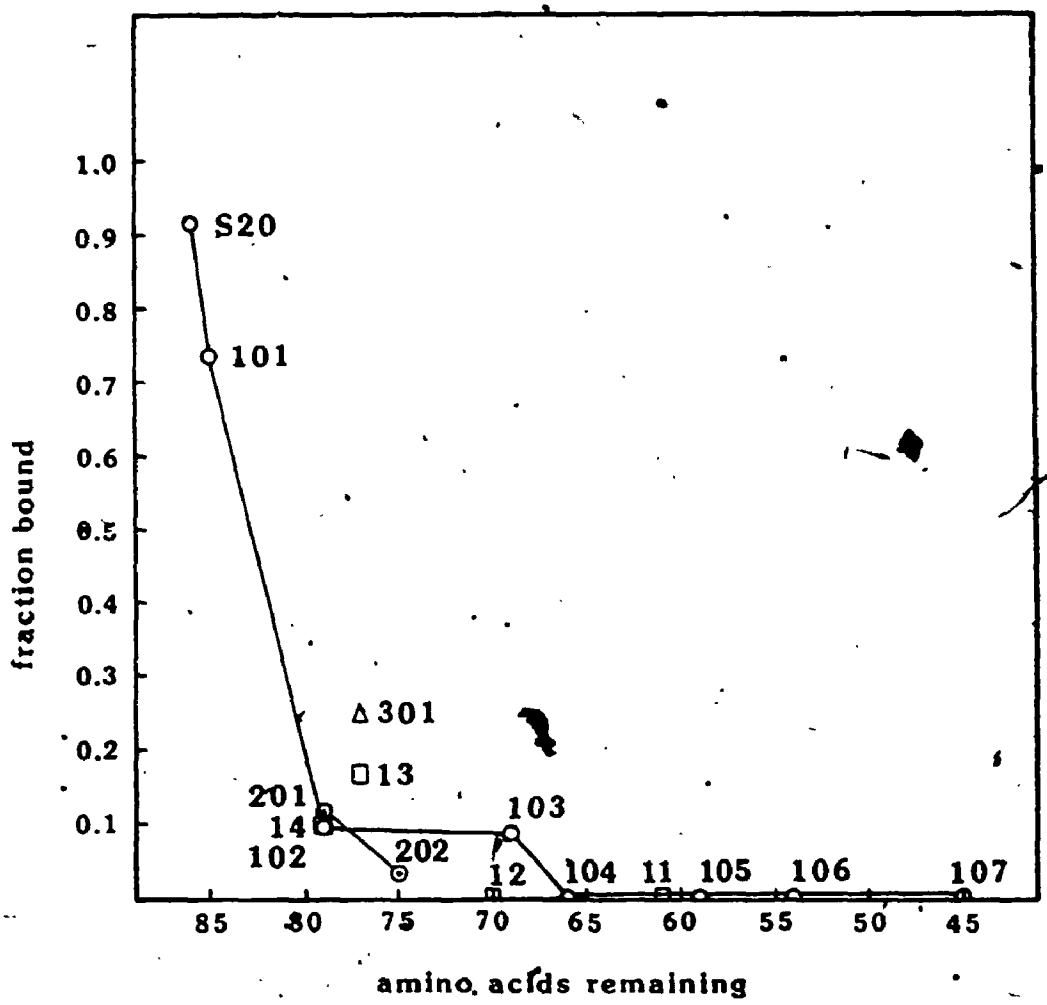

Figure 12. Binding of mutant S20 polypeptides to 16S rRNA as a function of deletion size. The graph shows the fraction bound of each peptide to 11 pmoles of 16S rRNA in the standard assay. Input of protein is constant at 1 pmole and the levels are plotted against the number of amino acid residues remaining in the peptide. Each family of amino acid run-ons (Table 2), is represented by a different symbol: ○ = 3 amino acids, Δ = 5 amino acids, ⊙ = 10 amino acids, □ = internal deletions.

residue run-on (clone 301), shows that this "tail" can confer an intermediate level of binding activity relative to the longer, but less active 10 amino acid version. The significance of these "tail" effects will be discussed below.

Among the internal deletions, removal of the entire region bounded by the Sau3A sites, or just the downstream half resulted in a total loss of measurable binding. However, after removal of only the upstream fragment (clone 13), an intermediate level of activity remained. Again, the extreme C-terminal region was critical. Replacement of the deleted downstream fragment with a duplication of the upstream Sau3A fragment (clone 14) generated a mutant S20 slightly less active than that in clone 13.

DISCUSSION

The molecular method presented here for studying protein structure-function relationships is significant in its utilization of mutant polypeptides derived by in vitro synthesis for binding studies. There are several advantages realized by this approach. First, manipulation of DNA provides a more versatile means of implementing changes in protein structure. Potential alterations available through DNA mutation are not

restricted by the defined repertoire of chemical and protease cleavages available. Second, this approach enables the testing of potentially labile protein conformations without any requirement for purification, which frequently entails denaturation or other harsh treatments. This method also provides proteins labelled to sufficient specific activity that they are detectable in very small quantity, again without the need for purification. Finally, generation of partially active proteins in vitro makes it possible to study mutations which could be impossible to generate or purify in vivo. This is particularly true if loss of function is very deleterious to the organism or if the purification process utilizes a functional aspect of the protein.

The presence of other labelled proteins and unincorporated [^{35}S] in our standard assay precludes the use of filter binding methods for measuring protein-RNA association. A limitation of the alternative gel filtration method is the inability to measure equilibrium values. This is probably of minor significance in the case of a strong interaction with a large electrostatic component such as that of 16S rRNA binding a very basic ribosomal protein like S20, but weaker mutant interactions might be more strongly affected. For weaker binding mutants, the possibility that cooperative interactions might be necessary to observe better binding was tested by addition of a mixture of proteins S4, S5,

S16 and S17 along with 16S rRNA. These proteins bind in the same domain of the RNA as S20, but produced no effect on the binding activities of several mutant S20s.

An analysis of the amino acid sequence of S20 by the method of Garnier et al. (1978) predicts that S20 may be composed of 3 major helical segments, with the C-terminus representing a region of high probability for α helix (Fig. 13). This is in contrast to circular dichroism measurements (Giri et al., 1984) suggesting S20 has a low α-helical content. A similar analysis of the mutant sequences indicates that while the shortest 3 residue run-on is effectively neutral, the 5 and 10 residue "tails" favour helical and extended conformations respectively. The loss of virtually any residues from the C-terminus (as represented by clones 101-107), results in an immediate deterioration of 16S rRNA binding, leading to its complete elimination after the loss of more than 17 amino acids. There could be two primary explanations for this. First, these residues could form part of the RNA binding site of S20 itself, with the result that their elimination leads to the loss of direct RNA-protein contacts. Alternatively, if an intact network of interactions is required to maintain the integrity of an entire region of the protein (a 'domain'), then a disruption anywhere within that region which alters its overall structure could

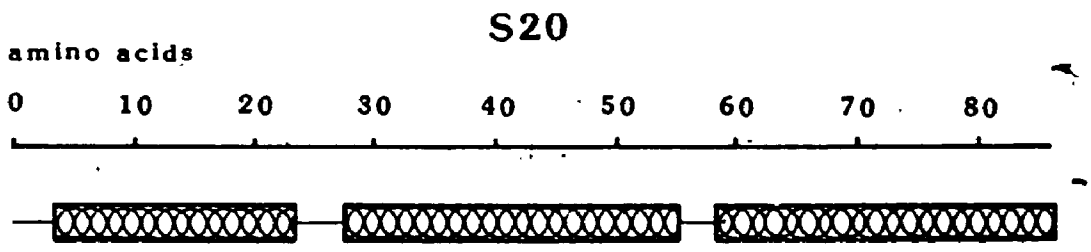

Figure 13. Analysis of potential α-helical regions within S20 by the method of Garnier et al. (1978). ▓▓▓ = alpha helix. The helical segments are 5.0 times more probable than any other structure.

inactivate the site of binding, while not actually being within it.

Substitution of the 10 C-terminal residues of S20 with a random sequence favouring an extended configuration (clone 202), also led to the loss of binding activity. However, an intermediate level of binding activity, more than six times greater than this, was produced by substituting the 5 residue helical "tail" in another deletion missing a similar number of normal S20 residues (clone 301 compared to 202). This may imply that a helical structure is important here.

Manipulations of internal S20 sequences are also consistent with the significance of the C-terminus. The two segments delimited by Sau3A restriction sites in the S20 coding region each represent essentially one half of the third helical region of the protein. Removal of this whole region or the downstream half (clones 11 and 12) resulted in total loss of measurable binding, while the loss of just the upstream fragment (clone 13) left an intermediate amount of activity. Replacement of the deleted downstream fragment with a duplication of the upstream one (clone 14) failed to restore more than a low level of activity.

These data suggest that C-terminally deleted mutants of S20 are not significantly capable of binding 16S rRNA due to the absence of a critical region proximal to the normal C-terminus. This region could be essential for

the integrity of the secondary and tertiary structure of S20, or perhaps be part of the RNA binding site itself. In view of the earlier data of Paterakis et al. (1983), it seems likely that N and C terminal segments of S20 interact with each other to generate a conformation of the protein capable of binding to 16S rRNA. This work has been summarized in Donly and Mackie, 1988.

CHAPTER 3

INTERACTION OF RIBOSOMAL PROTEIN S20 WITH RNA TRANSCRIPTS PREPARED IN VITRO

INTRODUCTION

Regulation of gene expression at the initiation step of translation (translational control), is now recognized as a relatively common regulatory strategy (Gold et al., 1981). In the simplest model of such a process, a protein product might bind reversibly to its own ribosome binding site (Shine-Dalgarno sequence) to control its own synthesis (autogenous translational control). This kind of mechanism is particularly suited to the control of free intracellular concentrations of proteins required for multiprotein complexes, such as ribosomes (von Hippel and Fairfield, 1983). The idea is predicated on the partitioning of the product into a functional fraction sequestered by the assembly of the complex, and a free intracellular pool capable of repressing further expression of its mRNA by interaction with it.

Many ribosomal proteins have been proposed to be regulated directly or indirectly through such post-transcriptional mechanisms (Nomura et al., 1984). Most of the proteins which regulate their own expression directly are known RNA binding proteins (eg. S4, S8, S20, L4). However, in only two cases have actual interactions between a regulatory r-protein and its target mRNA been documented. In the first, Johnsen et al. (1982) demonstrated that the L10-L12 protein complex is able to retain RNA transcripts of the L10 operon on

nitrocellulose filters. These RNAs were generated by transcription of circular plasmid templates *in vivo* with *E. coli* RNA polymerase. Because of the heterogeneity of the RNA, no binding affinities of the L10/L12-mRNA complex could be determined. The site of binding was narrowed by RNase protection to a fragment of approximately 85 nucleotides in the L10 leader. This binding was correlated with regulation of the operon by verifying that RNAs containing any one of several point mutations in the L10 leader known to cause loss of autoregulation also failed to interact with L10/L12 on filters (Christensen *et al.*, 1984).

In the second case, specific interactions between S4 and RNA transcripts of the α operon were quantified using a nitrocellulose filter binding assay (Deckman and Draper, 1985). This interaction was found to occur with an affinity of approximately 2×10^7 M^{-1} and was further characterized using mRNA fragments of various sizes prepared by *in vitro* transcription (Deckman *et al.*, 1987). Binding of S4 was ultimately proposed to occur in a region of complex structure containing a stable helix and loop resulting in a "pseudo-knot" configuration (Fig. 1). Evidence for this structure was obtained by studying its susceptibility to nucleases specific for single- or double-stranded RNA (Deckman and Draper, 1987). The primary structural feature responsible for S4 binding was however proposed to be the main helix in Fig. 1.

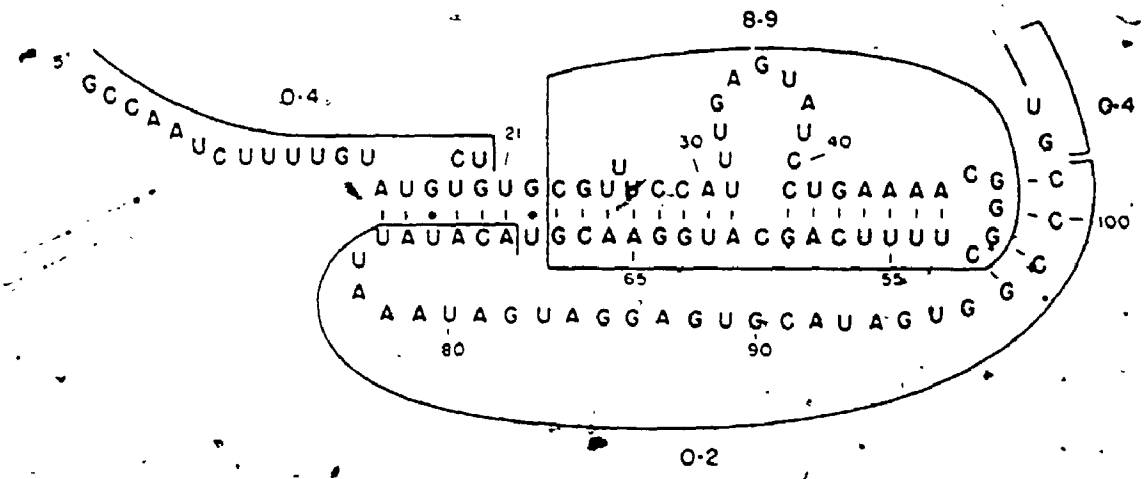

Figure 1. Model for the secondary structure of the leader of α-operon mRNA when complexed with S4. The approximate free energy contributions S4 derives from the interaction are marked for each region. Taken from Deckman and Draper (1987).

The study of mRNA-protein interactions has been greatly facilitated by the recent introduction of vectors providing for *in vitro* synthesis of pure single-stranded RNAs (Melton *et al.*, 1984). The specificity necessary to produce pure RNA products results from the use of bacteriophage RNA polymerases which initiate transcription exclusively at phage promoters. The two promoter-polymerase systems most frequently employed are those of the *E. coli* bacteriophage T7 (McAllister *et al.*, 1981) and phage SP6 of *Salmonella typhimurium* (Kassavetis *et al.*, 1982). Their utilization makes it possible to generate the microgram quantities of specific RNAs necessary for most physical studies of RNA-protein interactions. This applies to both the mRNAs of cloned ribosomal protein genes as well as for cloned rRNA genes or portions thereof.

This chapter will deal with the application of these systems to the gene for r-protein S20 and portions of the sequence of 16S rRNA. Ensuing studies of S20-RNA interactions made possible by these methods will also be addressed.

MATERIALS AND METHODS

(i) Enzymes and Plasmids

Enzymes and materials for transcription gave comparable results when obtained from either Pharmacia or Promega. RNase-free deoxyribonuclease I was obtained from Pharmacia.

The vector used for *in vitro* transcription of S20 sequences (pCD20) is shown in Fig. 2. It is a derivative of the plasmid pSP65 developed by Melton *et al*. (1984), which was obtained from Promega. S20 sequences were derived from the plasmid pGM34, which contains residues 163 to 690 of the S20 gene including the proximal P2 promoter, leader, coding sequence and transcriptional terminator (Appendix A). This entire fragment is contained in the plasmid pCD20.

Transcription vectors containing portions of the 16S rRNA sequence were obtained from Dr. D. Draper (The Johns Hopkins University). These are shown in Fig. 2. pCD15 is a derivative of BRL expression plasmid pT7/T3-18 which contains the entire 5' domain of 16S rRNA (residues 1-614) under the control of a T7 promoter. The deletion pCD16 is the same insert missing bases 116 to 288 of the 16S rRNA sequence cloned in the U.S. Biochemicals vector pT7-1. Its expression is also controlled by a T7 promoter.

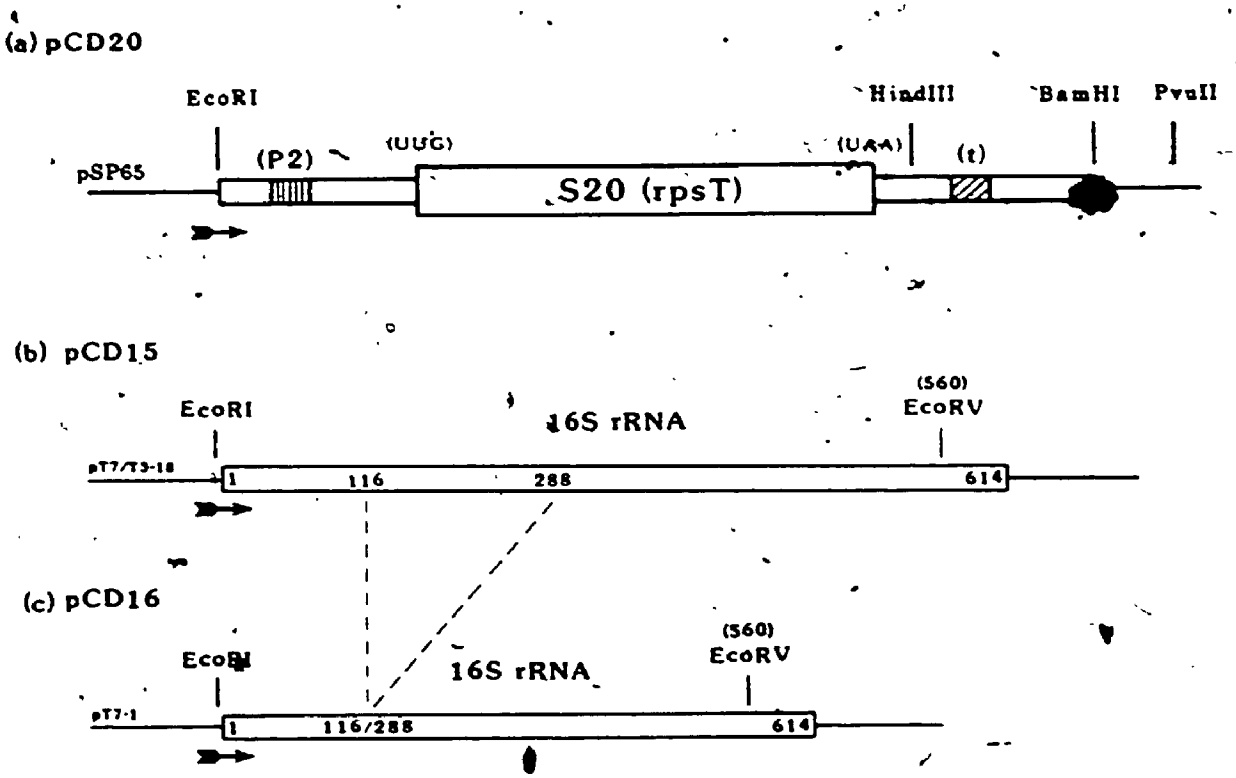

Figure 2. Maps of templates for in vitro transcription. (a) pCD20 contains residues 163 to 690 of the S20 gene (Appendix A) adjacent to an SP6 promoter. (P2) is the second S20 promoter, while (t) is the S20 terminator. (b) pCD15 contains residues 1 to 614 of 16S rRNA adjacent to a T7 promoter. (c) pCD16 contains the same segment as (b) but deleted for residues 116-288. Arrows mark the approximate start points of transcription.

(ii) Transcription In Vitro:

Transcription reactions were carried out essentially as suggested by Promega. Final ribonucleotide triphosphate concentrations of 0.7 mM were utilized when maximum RNA yield was desired. 1 µCi of [^{3}H]-UTP or [^{35}S]-CTP per 50 µl reaction was included for labelling. Template was eliminated from the reaction products by a 10 minute digestion at 37°C with DNase I (Pharmacia). RNA was normally collected by extraction of the products (after a 1:1 dilution with water) using 1 volume phenol-chloroform followed by ethanol precipitations from ammonium acetate and then sodium acetate.

RNA for filter binding was further purified by passage over disposable reverse-phase columns (NENSORB) obtained from NEN Research Products. The instructions of the manufacturer were followed throughout with elution of the RNA being accomplished with 50% ethanol in water. Transcripts treated this way were considered to be free of unincorporated nucleotides.

(iii) Electrophoresis of RNA on Denaturing Gels:

The integrity of all RNA transcripts was checked in one of two ways. Approximately 1 µg of RNA was denatured with glyoxal in 50% DMSO and electrophoresed in a 1.5% agarose gel (Maniatis et al., 1982). Gels were soaked for 15 minutes in 50 mM NaOH, before staining for 45 minutes in 0.5 M ammonium acetate containing 0.25 µg/ml

ethidium bromide. Destaining in the same solution minus ethidium bromide for at least another 45 minutes produced clean backgrounds.

Labelled RNA was also analyzed by electrophoresis on 5% (29:1) polyacrylamide gels containing 8 M urea. Samples were first heated to 90°C in 90% formamide containing 0.1% xylene cyanol and 0.1% bromophenol blue, and then immediately loaded on gels and electrophoresed by standard techniques (Maniatis et al., 1982). Wet gels were processed for fluorography before being dried and exposed to Kodak XAR-2 film.

(iv) RNA-Protein Association:

Binding of S20 to various RNA transcripts was assayed by three different methods.

(a) Mobility shift assay: Approximately 6 pmoles of RNA transcript was allowed to renature for 20 minutes at 37°C in 20 µl of either TMK buffer or low magnesium (LM) buffer containing 4 mM $MgCl_2$, 200 mM KCl and 30 mM Tris pH 7.6. Meanwhile, 16 pmoles of purified S20 in 5 µl of similar buffer was also heated to 37°C for 20 minutes. RNA and protein were mixed on ice and left 20 minutes. Samples were mixed with 2 µl of glycerol and loaded on 5% polyacrylamide gel (75:1) at 4°C. Electrophoresis was conducted at 4°C in 1x TBE buffer for 9 hours at 200 V. Wet gels were processed for fluorography, dried and exposed to Kodak XAR-2 film.

(b) Gel filtration: RNA-protein association was assayed essentially as in Chapter 2 with these changes. The incubation contained a total of 6 pmoles of transcript in a total volume of 25 µl. 20 U of RNase inhibitor (RNA Guard, Pharmacia) was added to the RNA before protein from *in vitro* transcription-translation. Scintillation counting was in 2.5 ml PCS (Amersham) as before.

(c) Filter binding: Approximately 1 pmole of RNA transcript was allowed to renature in 5 µl of buffer at 37°C containing 20 mM Tris pH 7.8, 5 mM $MgCl_2$, 150 mM KCl and 6 mM β-mercaptoethanol. Meanwhile, purified S20 (a kind gift from Dr. R.A. Zimmermann) which had been dialyzed into TMK was renatured in 5 µl of the above buffer at 37°C for 15 minutes. Each was cooled to room temperature briefly and then mixed on ice. After 15 minutes, the mixtures were filtered through nitrocellulose circles (Schleicher and Schuell BA85) prewet in degassed binding buffer and held on a glass frit with light suction (Draper *et al.*, 1988). The filters were dried without washing and counted in 2.5 ml toluene/omnifluor (NEN Research Products). In each case a sample of RNA with no added protein was processed to determine the background RNA retention of the filters, and a similar sample spotted directly on a filter to assess the total counts present.

RESULTS

The most obvious means of assaying for S20-mRNA interactions was to employ the gel filtration system used in Chapter 2 for measuring S20-16S rRNA association. However, this method measures binding under non-equilibrium conditions which may be poor at detecting interactions of more transient duration. Therefore, gel retardation and filter binding were also utilized here for measurements with minimal time during which separation of bound from unbound protein occurs. Positive and negative controls for all the assays were obtained in the form of 16S rRNA sequences with and without the S20 binding region to independently check the performance of each.

i) Products of Transcription In Vitro:

The RNA products of *in vitro* transcription are generally in the form of 'run-off' transcripts: the plasmid template is cleaved by restriction with a suitable enzyme prior to use with the result that RNA polymerase molecules run off the end of the template strand. This results in populations of RNA molecules of uniform size which may be analyzed by gel electrophoresis to assess their integrity. Both polyacrylamide and agarose gels were utilized with RNA denatured in urea/formamide or glyoxal respectively.

When pCD20 was prepared as a template, it was cleaved either at the HindIII site just downstream of the S20 stop codon or at the BamHI site, such that the S20 transcriptional terminator is included (Fig. 2). Fig. 3 shows an agarose gel of transcription products from these templates which have been denatured with glyoxal in 50% DMSO. The expected sizes of the products are 403 residues (lane 1 - HindIII-cut template) and 545 residues (lane 2 - BamHI-cut template). The SP6 polymerase unexpectedly showed a tendency to terminate at the natural S20 terminator, as evidenced by a band of 436 residues in the products from the BamHI-cut template.

Electrophoresis of transcripts on denaturing polyacrylamide gels containing 8 M urea was also employed to assess their integrity. A group of transcripts from various templates are shown on such a gel in Fig. 4. Once again, the RNA produced by termination at the S20 terminator in pCD20 is evident as approximately 20% of this template's products. Overall, these products can all be seen to be free of significant degradation.

The yields of RNA transcribed in *in vitro* reactions were estimated by calculating the specific activity of the labelled nucleotide triphosphate in the reaction and measuring the number of counts incorporated into acid precipitable material by the RNA polymerase. Typical yields were in the range of 5-10 pmoles of transcript per pmole of template added.

Figure 3. Denaturing agarose gel of transcription products of pCD20. Lane (a), pCD20 (HindIII) and lane (b), pCD20 (BamHI). Size markers shown in the right margin are: (c) PstI/BamHI/HindIII digested pBR322, (d) RsaI digested pBR322, and (e) total E. coli RNA (16S and 23S RNA sizes are approximate). Transcript sizes are as marked in the left hand margin. Lane (b) also shows a band (436 residues) corresponding to transcripts terminated at the natural S20 terminator.

a b c d e

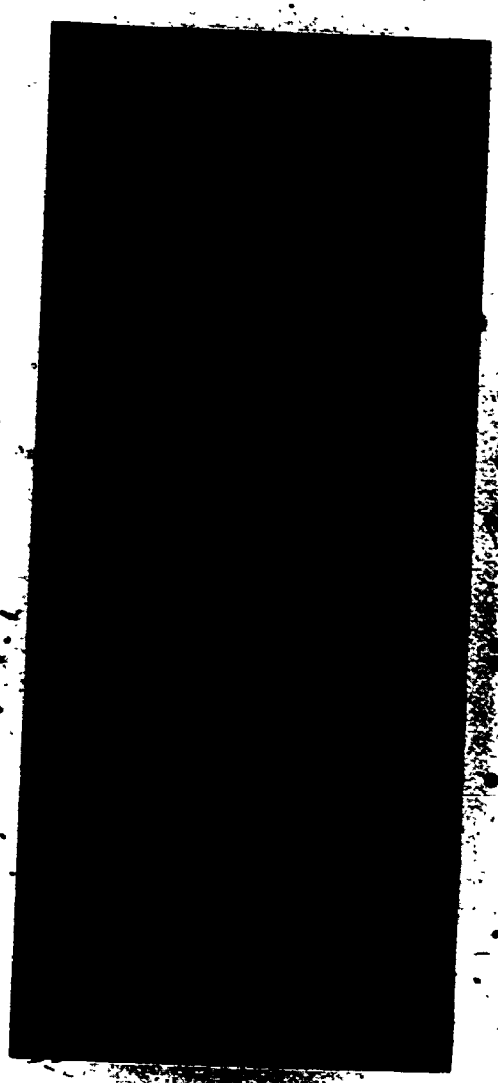

3234
2900
2118
1565
1540
783
680
346
545
403

Figure 4. Denaturing polyacrylamide gel of RNAs transcribed *in vitro*. Approximately 2 x 10^4 [^{35}S] DPM or 4 x 10^4 [^{3}H] DPM of acid-precipitable transcription products from each template were electrophoresed on a 6% polyacrylamide gel containing urea. Lane (a), size markers; lane (b), pCD20 (*Bam*HI); lane (c), pCD20 (*Hind*III); lanes (d) and (e), pCD15 (*Eco*RV); lanes (f) and (g), pCD16 (*Eco*RV).

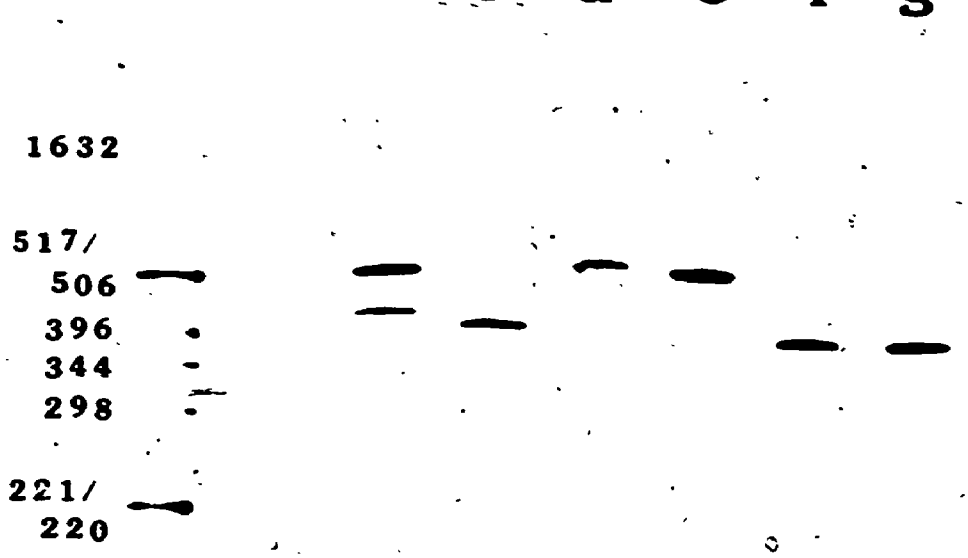
a
b
c
d
e
f
g
1632
517/
506
396
344
298
221/
220
154
75

(ii) Mobility Shift Assay:

RNA transcripts from the 16S rRNA deletion-carrying plasmid pCD16 were used to characterize the behaviour of RNAs produced in vitro in the gel system employed. Various conditions of buffer and temperature were used for renaturation of identical samples as shown in Fig. 5. Quite unexpectedly, it was observed that incubation of pCD16 transcripts at 37°C in either MS (lane d) or TMK (lane e) buffers (conditions employed to allow RNA to assume natural secondary and tertiary structures). resulted in its conversion to a slower migrating form on the gels. This conversion appeared to correlate with the amount of Mg^{++} present, possibly representing formation of dimers of the RNA transcripts.

Assays performed in the presence of S20 consequently utilized a low magnesium (LM) salt buffer to minimize this electrophoretic heterogeneity. A gel showing the assay of 3 transcripts for S20 binding by mobility shift is shown in Fig. 6. When added, S20 was in a 2.5:1 excess over RNA. All showed conversion to their slower migrating forms in (LM) buffer, both in the presence or absence of S20, with pCD20 showing a similar conversion for both S20 transcripts present. No new bands correlated with the presence of S20. Therefore, it was concluded that if S20 interacts with any of these RNAs, it does not alter their conformations sufficiently to

Figure 5. Non-denaturing polyacrylamide gel of RNA transcripts of pCD16. Equal aliquots of pCD16 transcription products were treated before electrophoresis as follows: lane (a), diluted in formamide; lane (b), diluted in TE at 0°C for 30 min; lane (c), diluted in TE at 37°C for 30 min; lane (d), diluted in MS at 37°C for 30 min; lane (e), diluted in TMK at 37°C for 30 min; lane (f), diluted in TMK at 37°C for 30 min with 6 pmoles of a mixture of ribosomal proteins. Samples were then loaded on a 5% polyacrylamide gel (75:1) and run as described in Materials and Methods. Band 2 marks the slower migrating form of RNA.

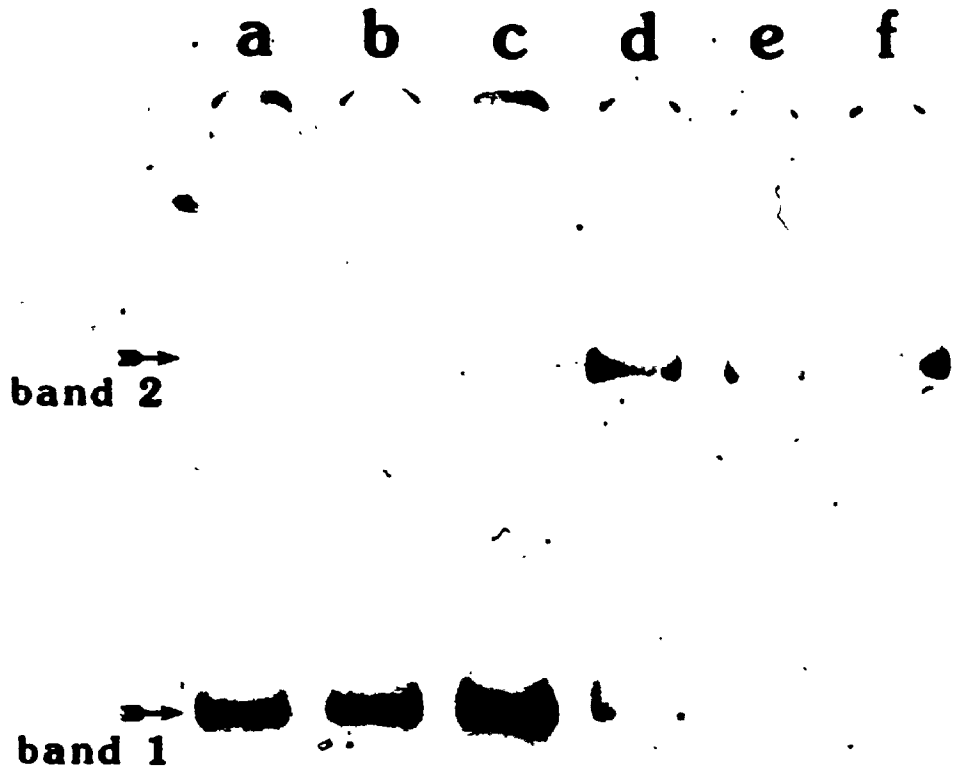
a b c d e f
band 2
band 1

Figure 6. Mobility shift assay of S20 binding to RNA transcripts of pCD15, pCD16 and pCD20. 6 pmole samples of each transcript were prepared 3 different ways for electrophoresis. One was diluted in TE (lanes [a], [d] and [g]), one incubated for 30 min at 37°C in LM buffer (lanes [b], [e] and [h]), and a third also incubated in LM buffer before being mixed with 15 pmoles of S20 on ice for 30 min (lanes [c], [f] and [i]). Samples were loaded on a 5% polyacrylamide gel (75:1) and run as described in Materials and Methods.

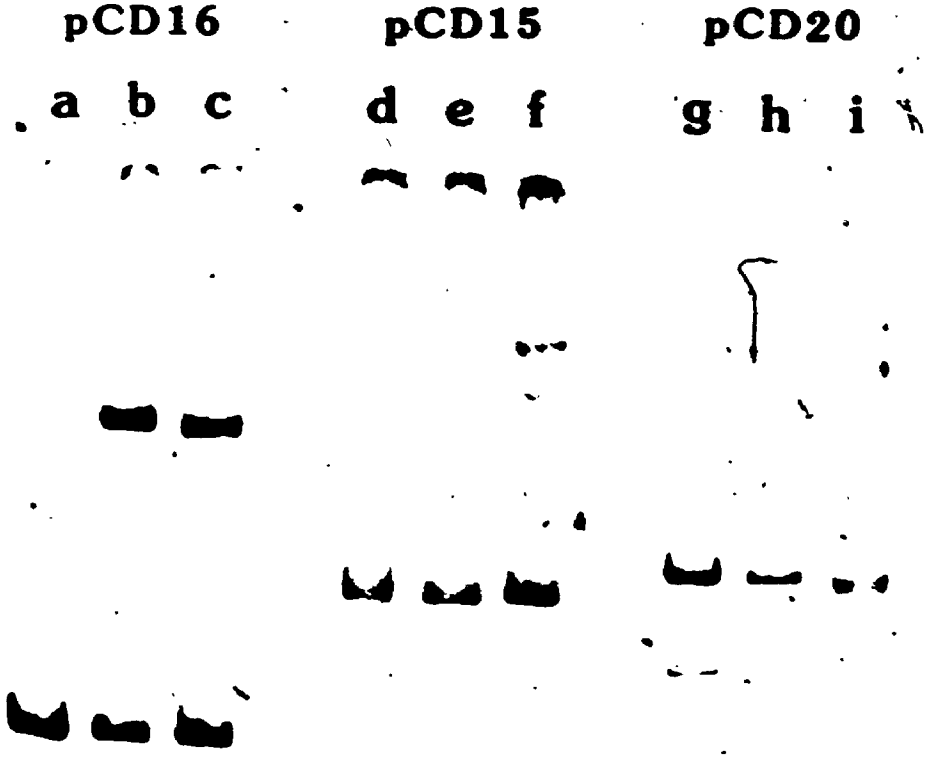
pCD16
pCD15
pCD20
a b c d e f g h i

produce a detectable reduction in their mobility in this gel system.

(iii) Gel Filtration:

Association of RNA transcripts with S20 protein synthesized in vitro was assayed essentially as described in Chapter 2 with the changes noted in Materials and Methods. Plasmid pCD15 contains the entire region of 16S rRNA believed to be involved in S20 binding and this transcript was therefore selected as the positive control for binding of RNA synthesized in vitro in this assay.

In comparison with experiments using isolated 16S rRNA (Chapter 2), transcripts of the pCD15 plasmid gave significantly lower RNA recoveries from the Biogel A-0.5m columns, most likely due to non-specific retention. Therefore, calculations of the pmoles of S20 bound/pmole of pCD15-RNA (v) were made using the actual values of RNA recovered. The data are compiled in Appendix D. These calculations yielded an apparent association constant $k = 1.2 \times 10^7\ M^{-1}$. The binding curve in Fig. 7 clearly demonstrates that this interaction shows saturation at higher protein/RNA levels.

The deletion plasmid pCD16 produces an RNA transcript missing the central region of the putative S20 binding site on 16S rRNA. Therefore, this transcript was expected to have little or no affinity for S20 and this was in fact found to be the case. No binding of S20,

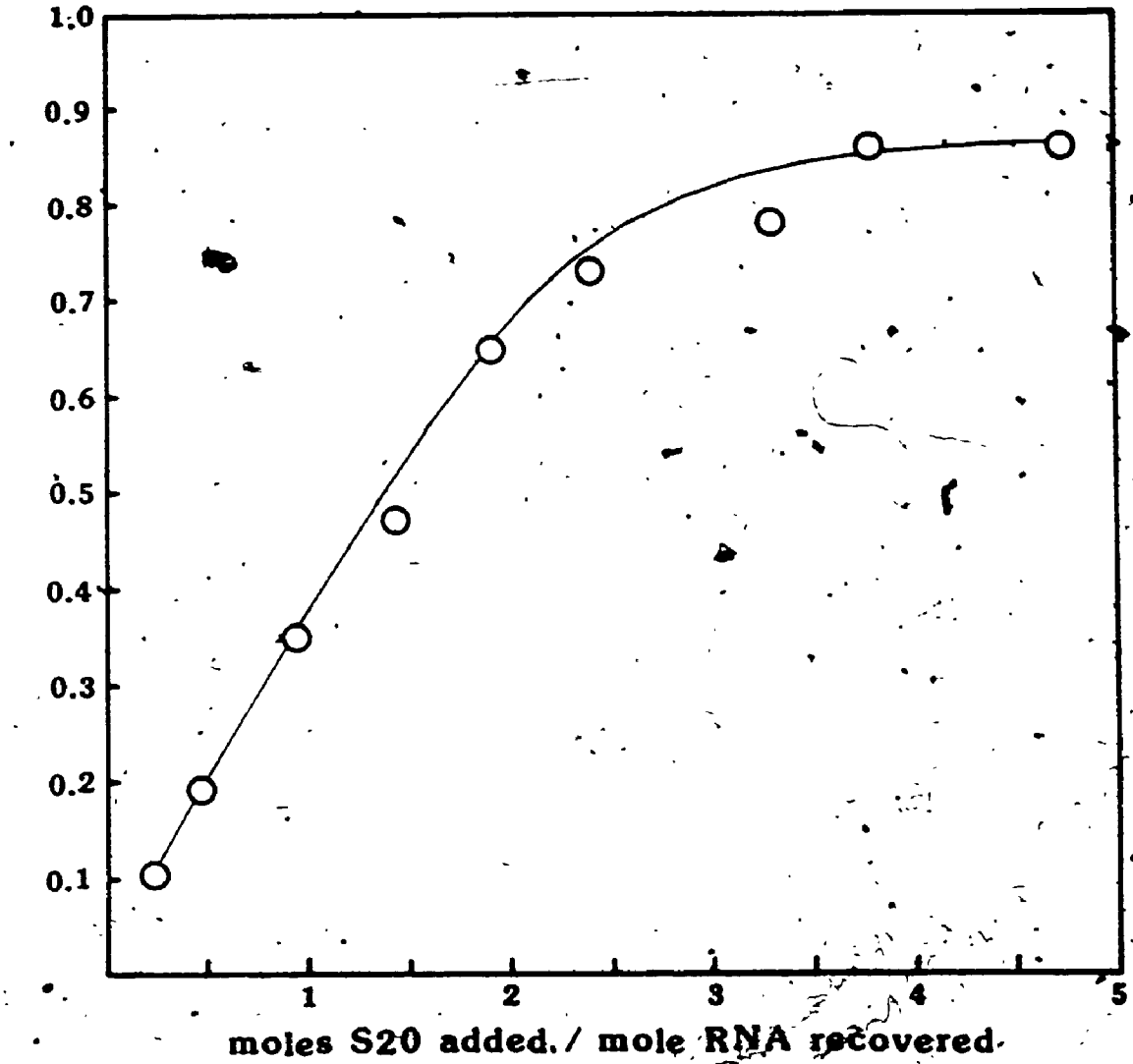

Figure 7. Binding curve for S20 with the 5' region of 16S rRNA (transcribed *in vitro* from pCD15). Increasing amounts of [^{35}S]-labelled, pGP11-directed, *in vitro* translation were mixed with 6 pmoles of [^{3}H]-labelled RNA transcribed *in vitro* from pCD15. Association was assayed as described in Materials and Methods. V was calculated using moles S20 bound / mole of RNA recovered due to the low recovery of RNA from columns as explained in the text.

even at a 4:1 molar excess, to pCD16 RNA was detectable in the same assay as that used for pCD15 transcripts.

In a similar assay, no binding of S20 to pCD20-directed RNA transcripts was detected either. In their studies of the binding of S4 to α operon mRNA, Deckman and Draper (1985) also utilized a moderate salt (MS) buffer, consisting of 30 mM Tris pH 7.6, 8 mM $MgCl_2$, 140 mM KCl and 20 mM NaCl, to approximate in vivo ionic conditions. Substitution of this buffer into the S20 binding assay with pCD20-directed RNA transcripts still resulted in no binding.

The possibility that the RNA substrate might be degraded by enzymes in the cell-free extract resulting in its inactivation was also tested. Six pmoles of pCD20-directed RNA transcripts were incubated in TMK buffer with unlabelled cell-free protein products, and applied to a Biogel A-0.5m column. Material eluting in the void volume was collected and precipitated with ethanol rather than counted in PCS. The RNA was then analyzed by denaturing agarose gel electrophoresis and blotting to Biodyne (Pall) nylon membrane. An exposure to Kodak XAR-2 film is shown in lane (b) of Fig. 8, demonstrating that the RNA is intact, but recovered in lower quantity as pointed out above. It was therefore concluded that S20 binds to the model in vitro RNA (pCD15-directed RNA transcripts) with a comparable affinity as to that for

Figure 8. Denaturing agarose gel of pCD20 transcripts after gel filtration. A 6 pmole sample of [^{3}H]-pCD20 (HindIII) RNA transcript was incubated in TMK buffer with unlabelled cell-free extract before passage over Biogel A 0.5m. The eluted RNA fraction was precipitated and analyzed by denaturing gel electrophoresis. After blotting to nylon, it was exposed directly to Kodak XAR-2 film, lane (b). Lane (a) contains an identical sample denatured for electrophoresis directly. The arrow shows the expected size of intact transcripts (403 residues).

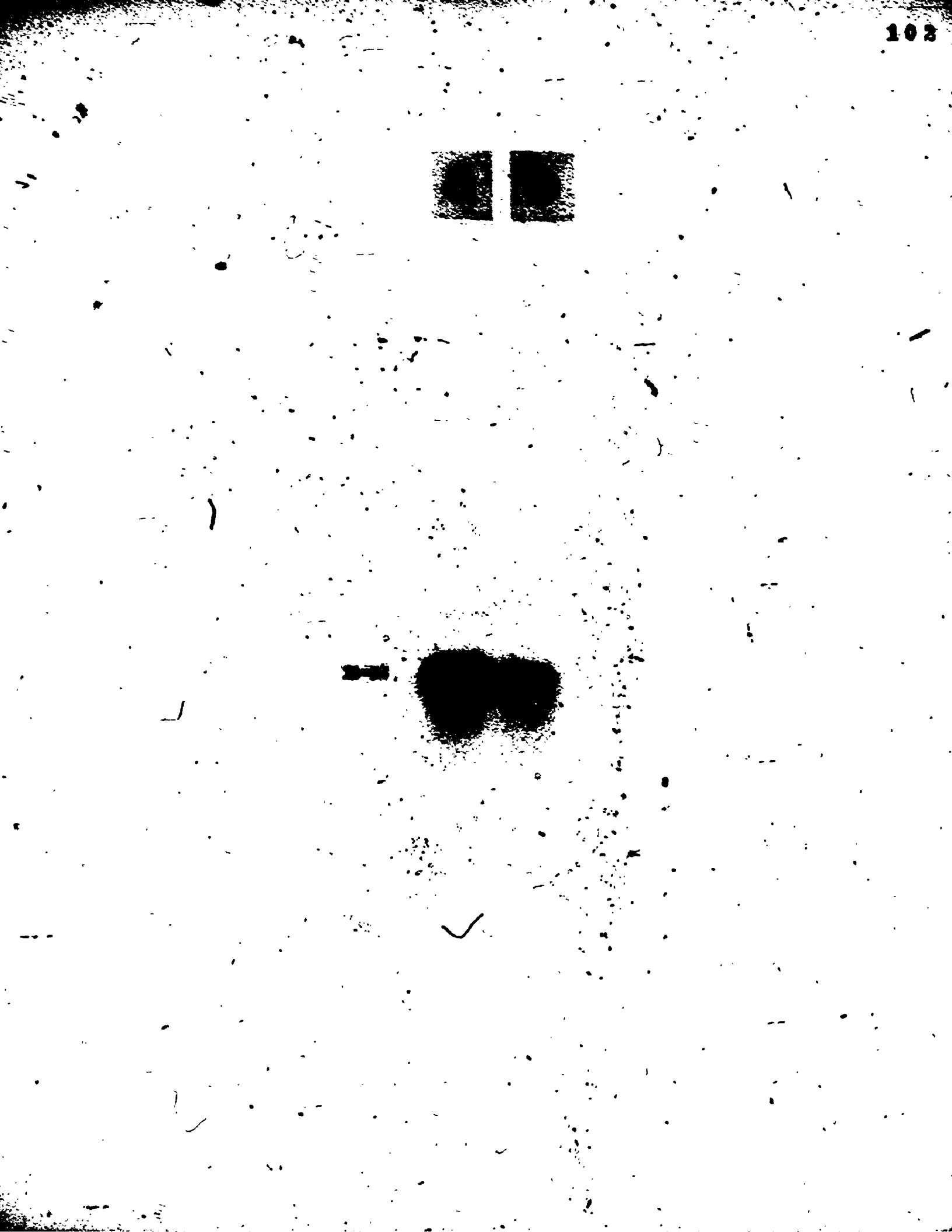

16S rRNA. There was no detectable binding by S20 to transcripts of S20 mRNA.

(iv) Filter Binding:

Two control filters were prepared for each series of filtrations: one containing the complete reaction mix without any S20, and the other with 1 pmole of the renatured RNA spotted directly on it. From these numbers the background retention of RNA in the absence of protein can be determined. This level was found to vary from 25 to 40% with different RNA preparations purified on disposable NENSORB columns. This level was significantly higher than expected and was not reduced by increasing the filtration rate, increasing the volume used, or raising the ionic strength of the buffer.

Using 1 pmole of RNA in 10 µl volumes, each of the 3 transcripts was tested with a range of S20 inputs from 1 to 20 pmoles as detailed in Materials and Methods. Values of the quantities of [^{35}S] label retained on each filter are expressed graphically as percentages of input counts in Fig. 9. Each of the RNAs tested showed increased counts retained with increasing S20 concentrations. PCD16 and pCD20 failed to show saturation even at protein to RNA ratios of 20:1. Specific binding with pCD15 was apparently obscured by the high basal RNA retention level and non-specific interactions. However, the equivalence of the pCD16 and

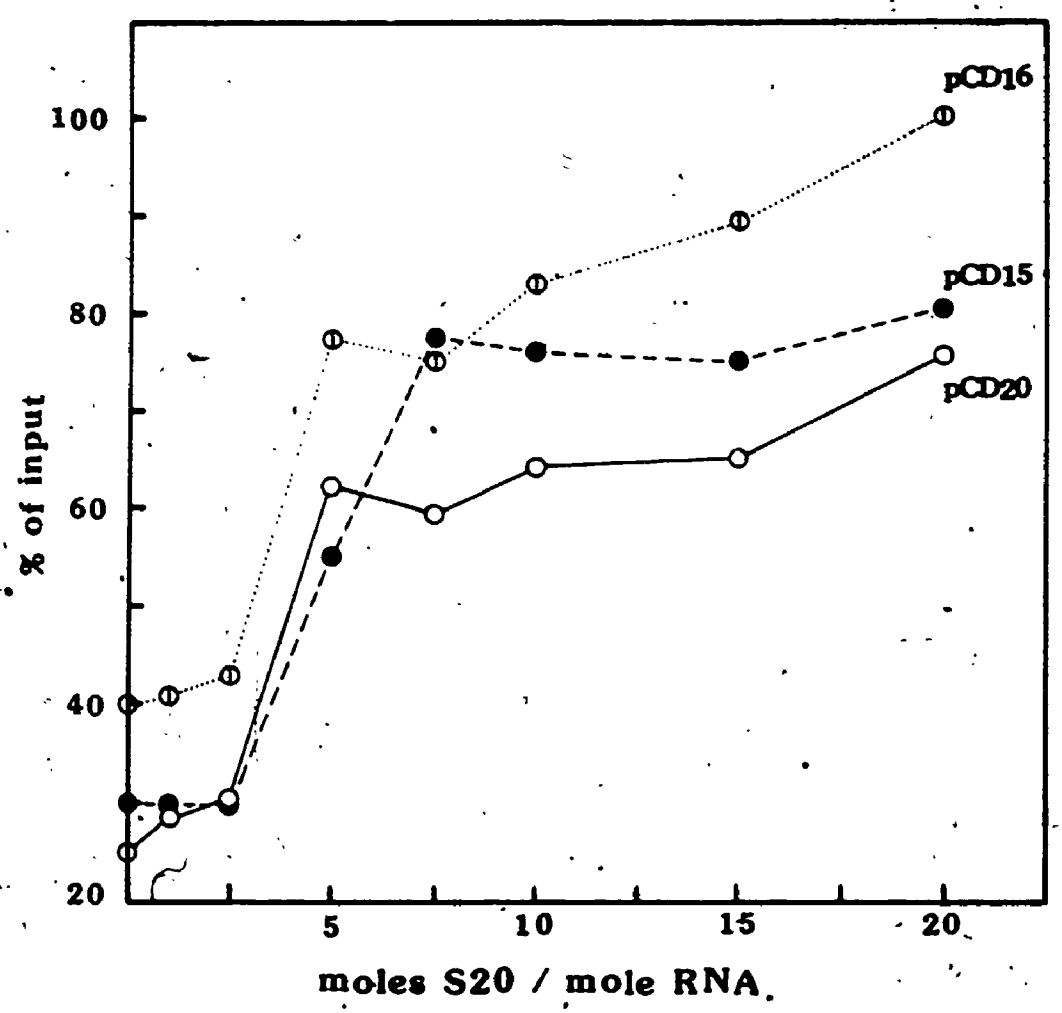

Figure 9. Filter binding of purified S20 and transcribed RNAs in vitro. 1 pmole aliquots of [^{35}S]-labelled RNAs were mixed with increasing quantities of unlabelled purified S20 as described in Materials and Methods. After filtration, filters were dried without washing and counted. % of input equals the counts retained on the filter / input counts for each point. % of input is plotted against the ratio of input S20/RNA

pCD20 curves suggest that any interaction with the S20 mRNA is undetectable over the level of non-specific binding anyway.

DISCUSSION

Binding of S20 to a 16S rRNA transcript produced *in vitro* was used as a test of the three assays employed. Due to technical problems with two of the assays, binding of the positive rRNA control (pCD15) could not be detected to purified S20. (The purified S20 was previously found to be active in 16S rRNA binding by competition with labelled S20 produced *in vitro* [Chapter 2]). In the first case (gel retardation), the mobilities of the RNA transcripts were unexpectedly found to be altered simply by incubation at 37°C in either of the buffers employed. In addition, the S20 protein itself may have proven too small at 10,000 daltons to visibly alter the migration of the RNAs on these gels unless it were to induce a significant change in conformation. In the second case (filter binding), the level of background binding by NENSORB-purified RNAs to nitrocellulose was found to be much higher than expected. This level may have been sufficient in combination with non-specific binding to effectively obscure specific binding by pCD15 transcripts. As a result, these methods failed to provide a valid means of assessing the binding activity

of the S20 messenger RNA.

The gel filtration assay employed in Chapter 2 however, was capable of detecting specific binding of pCD15-directed RNA transcripts with S20 produced in vitro. This interaction was measured as having an apparent affinity of 1.2×10^7 M^{-1}. This result should probably not be compared directly to the measured k_a of 1.2×10^7 M^{-1} for S20 binding to 16S rRNA in Chapter 2 though because of the large differences in efficiency of recovery of the two RNAs. But it is sufficient to demonstrate that RNAs produced in vitro can specifically bind S20 produced in vitro, and that this binding can be detected by the assay. Transcripts of the deletion clone pCD16, which lacks the S20 binding region of 16S rRNA, produced no detectable binding when assayed by gel filtration. This establishes the specificity of both the assay and the interaction of pCD15-directed RNA transcipts with S20 above. Future work could define the S20 binding site on rRNA through a systematic investigation of deletions and point mutations in residues 1 to 614.

When transcripts of the S20 mRNA (pCD20) were tested in this system, they showed the same levels as the deletion pCD16. Therefore, S20 is judged by this means to show no specific affinity for its own mRNA. No change was observed when reconstitution buffer (TMK) was replaced by one containing an ionic strength closer to

that *in vivo* (MS buffer of Deckman and Draper, 1985).

One difficulty in using the gel filtration approach is that during the course of time over which separation of bound from unbound protein occurs (approximately 20 minutes) dissociating protein normally exchanged in equilibrium will be left behind by the migrating RNA fraction. The result of such non-equilibrium measurement is that an interaction with a very high exchange rate might be misinterpreted as having a low affinity, as could be occurring with S20 and S20-mRNA. However, as mentioned in Chapter 2, this is probably of lesser significance in the case of strongly electrostatic interactions such as would be expected with the highly charged S20 molecule. Moreover, rapid association-dissociation of protein and nucleic acid is apparently not characteristic of interactions of known regulatory significance (Barkley and Bourgeois, 1978; Chadwick *et al.*, 1970).

Convincing evidence exists that S20 is capable of self-regulation at a post-transcriptional step (Wirth *et al.*, 1982; Parsons and Mackie, 1983). In view of our inability to detect an interaction by S20 with its mRNA which might provide for this activity, it is tempting to suggest an alternative mechanism. Most prominent is the idea that S20 might recognize and bind an intermediate in the initiation of its own synthesis. Such a model could be provided for by the lower affinity start codon of S20

(UUG), which would in effect provide a pause in initiation through which S20 might effect a sensitive step such as formation of a tertiary complex. However, significantly greater evidence for the existence of such complexes will be required to substantiate this mechanism.

CHAPTER 4

TRANSLATIONAL EFFICIENCY OF S20 LEADER MUTANTS

INTRODUCTION

The 5' non-coding sequence of S20 mRNA shows a region of apparent homology with the sequence of 16S rRNA in the area of the rRNA protected by binding of S20 (Parsons and Mackie, 1983, and Fig. 1). As mentioned earlier (section h of Chapter 1), this site, which includes the unusual UUG start codon of S20, has been proposed as the potential target for S20-mediated translational repression. The site-directed mutagenesis technique of Zoller and Smith (1984), was utilized to introduce limited changes in nucleotide sequence into the initiation codon and adjacent sequences of S20 mRNA to test their involvement in translation and autoregulation (Parsons et al., 1988). A number of deletions of the S20 leader created with BAL 31 nuclease (Parsons and Mackie, unpublished results) were also tested for their effects on translational efficiency.

Post-transcriptional regulation can be readily assessed by measuring whether dosage compensation is maintained for sequences present on multicopy plasmids. Dosage compensation is monitored by comparison of the relative in vivo levels of mRNA and protein product which result. However, other factors affecting mRNA and product levels include the half life of the mRNA produced and the efficiency of its translation into the protein product. These factors may vary significantly with

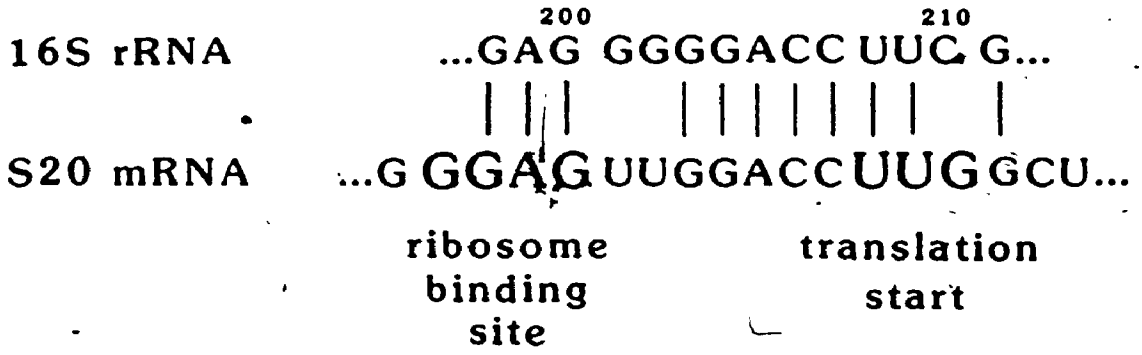

Figure 1. Homologous sequences found in the S20 mRNA and in the 5' third of 16S rRNA. Residues identical in the two sequences are joined. Bold letters denote the Shine-Dalgarno sequence and initiation codon of S20 mRNA.

different structural changes in the 5' untranslated portion of a mRNA (Hall et al., 1982; Belasco et al., 1986). Therefore, mRNA half life and translational efficiency must also be measured for each mutation to assess its level of autoregulation. This chapter will address the question of the relative translational efficiencies measured in vitro that result from mutations of the S20 leader.

MATERIALS AND METHODS

(i) Strains and Plasmids:

The host strain for plasmids used was GM323, a derivative of JM109 described in Parsons et al. (1988). Plasmids incorporating mutations in the gene for S20 were derivatives of the expression vector pKK223-3 (Chapter 2, Fig. 1(b)). Fig. 2 indicates the general structures of these plasmids while Table 1 details their partial nucleotide sequences in the region of translation initiation.

(ii) Transcription-Translation In Vitro:

DNA-directed protein synthesis was carried out as described in Chapter 2 for deletions of the S20 leader. Site-directed mutants were expressed using a modification of this method, designed to translate the mutant

transcripts in competition with an excess of β-lactamase mRNA. Duplicate incubations of 20 µl each were programmed with 400 ng of plasmid DNA including either 4 ng or 16 ng of the S20 test plasmid. The remainder in each case was pBR322, which primarily directs the synthesis of β-lactamase. Incubations at 34°C were performed for 30 minutes in the presence of 1 µCi [^{35}S]-methionine and 2.4 µg 16S rRNA to sequester newly synthesized S20 (Wirth and Bock, 1980). Incubations were terminated by precipitation with 5 volumes of acetone and the products subsequently resolved on 16.25% polyacrylamide gels containing SDS and urea (Swank and Munkres, 1971). Yields of S20 and β-lactamase were determined by elution from the gels as explained in Chapter 2, or by scanning autoradiograms produced from them with an LKB Ultroscan XL scanning densitometer. Values for S20 were normalized relative to the recoveries of β-lactamase.

(iii) Measurement of S20 mRNA Synthesized In Vitro:

Incubations similar to those used for S20 synthesis (above) were prepared without any added [^{35}S]-methionine. After incubation at 34°C, 100 µl samples were diluted with 4 volumes of 6.5 mM EDTA and 0.25% SDS before being extracted twice with equal volumes of phenol-chloroform and precipitated with 2.5 volumes of ethanol. Pellets

were reprecipitated once from 100 µl of 0.25 M sodium acetate.

A fraction of each RNA extract equal to approximately 5 µg was denatured with glyoxal in 50% DMSO and resolved on a 1.5% agarose gel (Maniatis et al., 1982). The RNA was then blotted by standard Northern transfer methods (Maniatis et al., 1982) to a Biodyne A nylon membrane (Pall) and fixed by UV irradiation (Church and Gilbert, 1984). Blots were probed with an antisense RNA from the S20 coding region of plasmid pGM49, which has been described by Mackie (1986), using denaturing conditions outlined there. Finally, RNA was quantified by densitometry of Kodak XAR-2 films exposed for 4-6 hours to the dried blots.

RESULTS

(i) Mutations of the S20 Leader Region:

All mutations were cloned in the expression vector pKK223-3 for the purpose of testing the resulting effects on translational efficiency and regulation of S20 synthesis. The general structures of these plasmids are illustrated in Fig. 2 (Parsons et al., 1988; Parsons and Mackie, unpublished results). The prototype plasmid used in these experiments (pCD6), contains the untranslated leader and coding regions of S20 under the control of the

inducible tac promotor (Table 1 and Fig. 2). A series of S20 leader deletions were also cloned in pKK223-3 in the same way. These plasmids, (pGP243, 251, 258, and 261), all contain deleted versions of the same S20-encoding EcoRI-HindIII fragment as pCD6. In each case the numbered residue indicates the most 5' residue of the S20 leader remaining.

Two different site-directed mutations were made in the original plasmid pCD6 to test specific features of the S20 gene. Plasmid pGP12 changes residues 269 and 270 from GA to CT, disrupting the largest region of homology with the S20 binding region of 16S rRNA (Fig. 1). In pGP13, residue 273 which codes for the first T of the initiation codon of S20 was changed to an A, creating an AUG start.

As an alternative approach to identifying features of the S20 gene required for translational control, the entire S20 leader and start codon were replaced with a synthetic DNA, yielding plasmid pGP11 (Fig. 2). This was accomplished by synthesizing two complementary oligonucleotides that when annealed produced a double-stranded fragment with an EcoRI end immediately adjacent to an artificial AUG start. The fragment extended to the Dde I site early in the S20 coding sequence (Parsons et al., 1988). This was cloned along with the remainder of S20 into pKK223-3 such that translation is initiated at a Shine-Dalgarno sequence provided by the vector and an AUG

Table 1. Partial structures of deletion and site-directed mutants of the S20 leader region.

Plasmid	Partial DNA Sequence[a]
pGP11	.. aggaaacagAATTCATGGCTAA ..
pGM70	.. aggaaacagAATTCTTGGCTAA ..
pGP12	.. TGGGAGTTGCTCCTTGGCTAA ..
pGP13	.. TGGGAGTTGGACCATGGCTAA ..
	240 260 280
pCD6	.. gaattccCCTTTGAATTGTCCATATAGAACACATTTGGGAGTTGGACCTTGGCTAA ..
pGP243	.. ttccTCCATATAGAACACATTTGGGAGTTGGACCTTGGCTAA ..
pGP251	.. ttccGAACACATTTGGGAGTTGGACCTTGGCTAA ..
pGP258	.. ttccTTTGGGAGTTGGACCTTGGCTAA ..
pGP261	.. ttccGGGAGTTGGACCTTGGCTAA ..

a. The DNA sequences shown include the start codon and Shine-Dalgarno site of each plasmid (underlined). Point mutation base changes are boxed. Lower case letters indicate sequences derived from the vector pKK223-3. Plasmids pGP12 and pGP13 contain the same 5' junction with the vector as pCD6.

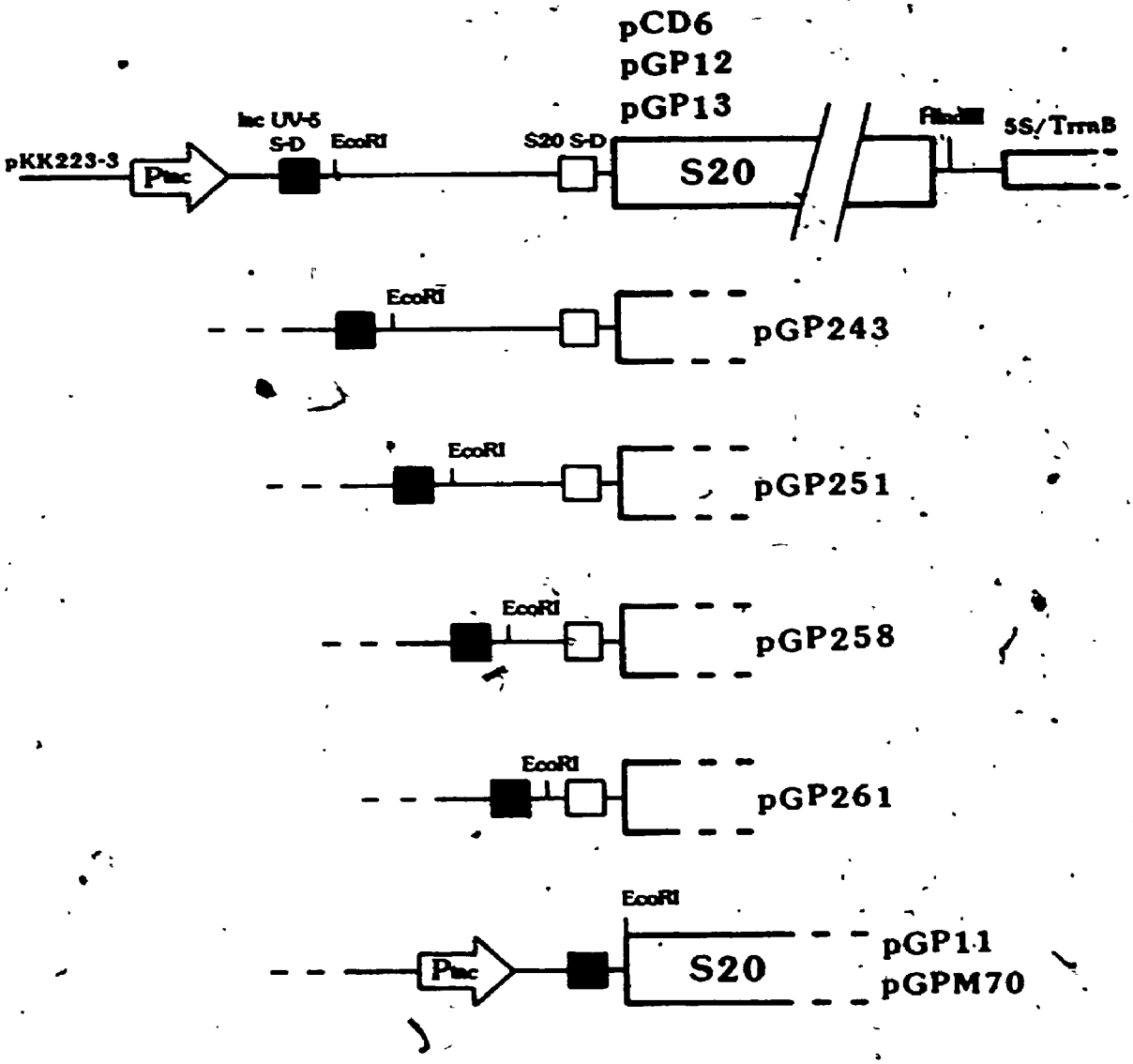

Figure 2. General structures of plasmids carrying mutations in the leader and initiation codon of the S20 gene. All plasmids are based on the vector pKK223-3 sequences (Chapter 2, Fig. 1). pGP12 and pGP13 contain point mutations relative to pCD6 located in the region of the Shine-Delarno sequence and initiation codon (refer to Table 1). pGP11 and pGM70 utilize the lacUV-5 Shine-Dalgarno site contributed by the vector pKK223-3 for translational initiation. The remaining plasmids utilize the S20-supplied Shine-Dalgarno site. P_{tac} is the tac promoter. T_{rrnB} is a ribosomal RNA operon terminator and 5S codes for 5S RNA (which cannot be processed from the transcript).

codon derived from the synthetic DNA. A final mutant, pGM70, changes this AUG back to a UUG in the context of the pKK223-3-derived leader sequence.

(ii) Translational Efficiencies In Vitro:

The translational efficiency of each of the S20 leader mutants was measured in vitro by coupled transcription-translation. Deletions of the S20 leader were tested simply by expressing them in vitro (as in Chapter 2) and measuring the relative levels of S20 by laser densitometry of autoradiograms from 16.25% polyacrylamide gels on which translation products had been resolved. Fig. 3 shows an example of such a gel. Table 2 displays the quantified values for synthesis of S20, which show that in comparison to the prototype plasmid (pCD6), the three proximal deletions (pGP251, 258, and 261) all resulted in a reduced capacity of the template to direct the synthesis of S20. Plasmid pGP261, which shows the least activity, deletes up to just one base short of the GGAG of the S20 Shine-Dalgarno site. Quite surprisingly, the fourth mutant (pGP243), produced an increase of about 70% in S20 level over pCD6. This effect has also been observed in vivo (Descary and Mackie, unpublished). The increase may have resulted from a specific change in conformation of the mRNA, or from the chance placement of a significant sequence in the pKK223-3 vector, producing the increased efficiency.

Figure 3. Coupled transcription-translation products of plasmids carrying S20 leader deletions. Transcription-translation reactions programmed by various plasmids were resolved on 16.25% polyacrylamide gels containing SDS and urea as described in Chapter 2. The lanes are as marked: (a) pGM24, (b) pGP12, (c) pGP11, (d) pCD6, (e) pGP243, (f) pGP251, (g) pGP258, (h) pGP261. The major products, β-lactamase and S20, are shown by arrows.

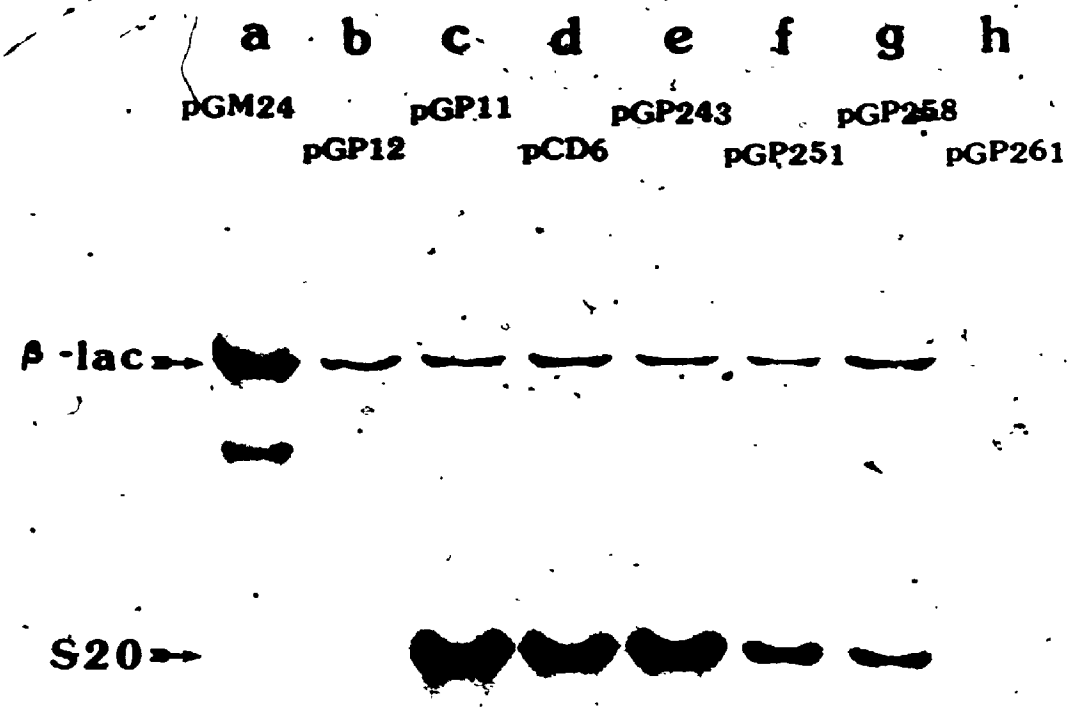
a b c d e f g h
pGM24
pGP12
pGP11
pCD6
pGP243
pGP251
pGP258
pGP261
β-lac
S20

Table 2. S20 synthesis directed *in vitro* by plasmids carrying deletions of the S20 leader.

Plasmid	Relative Synthesis of S20[a]
pCD6	1.0
pGP243	1.7
pGP251	0.65
pGP258	0.26
pGP261	0.11

a. Synthesis of S20 was measured by scanning densitometry of autoradiograms made from gels resolving the products of coupled transcription-translations. Both β-lactamase and S20 were measured, and the S20 values normalized to β-lactamase production. Values are expressed relative to the prototype plasmid pCD6.

The remaining mutants were tested by a modification of this method, in which the S20-encoding plasmids were transcribed and translated in the presence of a large excess of pBR322 (100:1 or 25:1 by mass). Titration experiments demonstrated that S20 synthesis was linear with the concentration of template in this range. In this way, the S20 mRNA synthesized during the incubations was limiting and had to compete for translation with an excess of other RNAs (such as those for β-lactamase). The yields of S20 therefore provided a measure of the translational efficiency of the S20 mRNA transcribed from each template. Table 3 shows the data for S20 mRNA and protein levels obtained for this group. S20 mRNA is given as the average peak area from scans of autoradiograms (Fig. 4) obtained from two RNA blots. Table 3 also shows that except for pGM70 there were no significant differences among the levels of S20 mRNAs which accumulated during the incubations. S20 and β-lactamase proteins were quantified by solubilization and scintillation counting of the corresponding bands from dried SDS-urea polyacrylamide gels (Fig. 5). The numbers in the table represent average raw yields resulting from the two template concentrations (100:1 and 25:1). The S20 values were normalized to those of β-lactamase to account for differences in translation capacity in each reaction.

Table 3. Coupled transcription-translation of templates containing mutations in the S20 leader.

Template[a]	Raw Yields[b]		Level of	Relative	Efficiency	Repression
	β-lactamase	S20	S20 mRNA[c]	Efficiency[d]	in vivo[e]	in vivo[f]
pCD6	13,870	1140	1.67	100	0.31	69
pGP13	13,090	2060	1.76	170	0.92	8
pGP12	13,420	200	1.78	17	0.05	[95]
pGP11	13,940	3480	1.44	360	1.00	0
pGM70	13,030	310	3.12	14	0.26	[74]

a. The templates listed were present in limiting quantities relative to pBR322.

b. Raw yields (in cpm) were determined by solublizing and counting the bands corresponding to β-lactamase and S20 from dried gels. Two points in the linear range of the S20 template were averaged.

c. S20 mRNA values are the average peak areas from scans of two autoradiograms obtained from two RNA blots of total RNA extracted from incubations like those for measuring yields of S20.

d. Relative efficiency is the ratio of the yield of S20, normalized for the recovery of β-lactamase, to the level of S20 mRNA, expressed as a percentage of the value for pCD6.

e. Efficiency is given as the ratio of the rate of synthesis of S20 to the steady state level of S20 mRNA *in vivo* as taken from Parsons *et al.* (1988). The values are normalized to that of the derepressed mutant pGP11.

f. Percent repression *in vivo* = (1.0 - efficiency) x 100. PGP12 and pGM70 resulted in S20 levels too low to accurately measure repression.

Figure 4. S20 mRNA levels in coupled transcription-translations. Autoradiograms of total RNA blots hybridized with an S20 probe were scanned as described. RNA was from in vitro translations directed by the following plasmids: (b) pGM70, (c) pCD6, (d) pGP11, (e) pGP12, (f) pGP13. Lane (a) contains total RNA from strain GM325 (which has been transformed with pCD6). The arrow marks the position of the S20 mRNA in the total cellular RNA.


a b c d e f
S20
mRNA

Figure 5. Coupled transcription-translation of S20 leader mutants in the presence of an excess of pBR322. Plasmids carrying mutants in the S20 leader were translated *in vitro* in the presence of either a 25:1 or 100:1 excess of pBR322 as described in Materials and Methods. Products were resolved on a 16.25% polyacrylamide gel containing SDS and urea. Lane (a) and (b), pGP11; lanes (c) and (d), pGP12; lanes (e) and (f), pGP13; lanes (g) and (h), pCD6; lanes (i) and (j) pGM70.

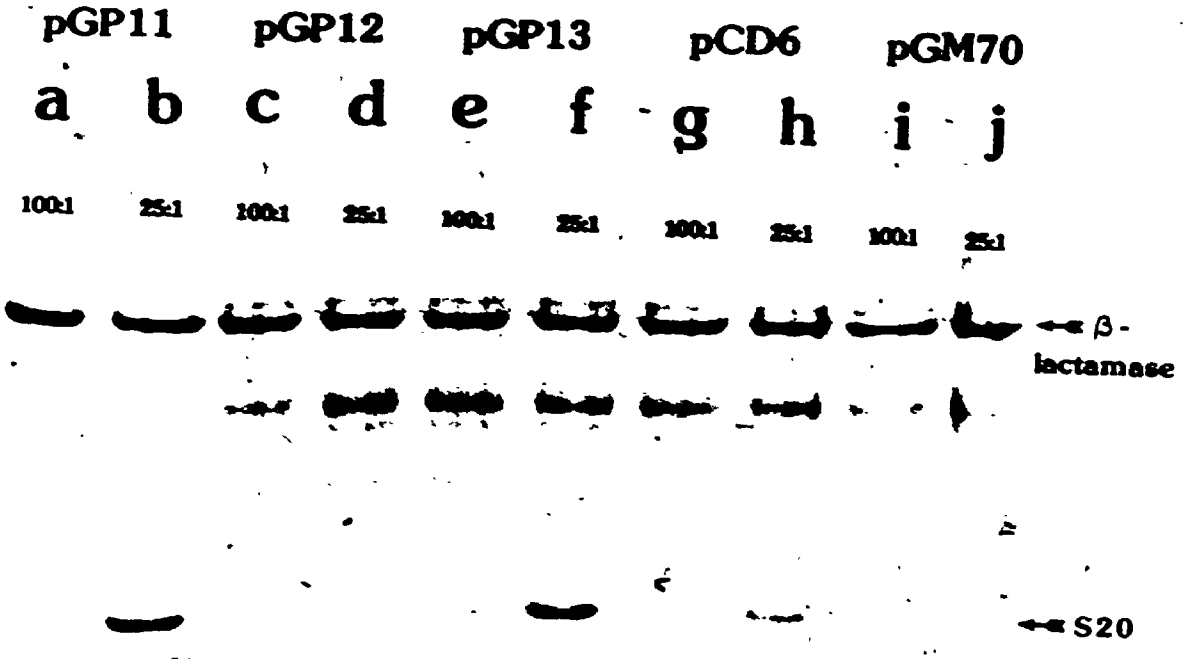
pGP11
pGP12
pGP13
pCD6
pGM70
a b c d e f g h i j
100:1 25:1 100:1 25:1 100:1 25:1 100:1 25:1 100:1 25:1
β-lactamase
S20

The relative translation efficiency for each mRNA was calculated as the ratio of the yield of S20 product (after normalization) to the level of mRNA accumulated. Those values are expressed in Table 3 as percentages of the value for the prototype plasmid pCD6. The templates pGP11 and pGP13 yielded 170% and 360% as much S20 as pCD6 did. In contrast, pGP12 and pGM70 were found to be rather inefficient, yielding only 17% and 14% as much S20 respectively.

Also listed in Table 3 are the values calculated for translational efficiency in vivo, as taken from Parsons et al. (1988). Comparison of these values with that for the derepressed mutant pGP11, permits a relative determination of the percent repression for each. However, this requires a sufficient level of S20 production in vivo to exert a measurable effect. For the very inefficient mutants pGP12 and pGM70, such a level may not have been reached.

DISCUSSION:

It has been shown that S20 is capable of regulating its own synthesis both in vivo (Geyl and Bock, 1977; Parsons and Mackie, 1983) and in vitro (Wirth and Bock, 1980; Wirth et al., 1982) at a post-transcriptional step. This regulation can be assessed by observing whether a

higher dosage of the S20 gene results in proportionally higher levels of mRNA and protein product. Dosage compensation as a measure of translational repression *in vivo* was quantified by Parsons *et al.* (1988) by relating the rate of S20 synthesis to the steady-state level of S20 mRNA (Table 3). The plasmid containing a replacement of the leader and UUG start codon of S20 (pGP11), was assigned an arbitrary value of 1 as being the construction most likely to be completely derepressed. The remaining values were normalized to it. By this method, the level of repression for the normal S20 leader (pCD6) was seen to be approximately 69%. However, the level of repression found for the single base mutation in pGP13 (UUG to AUG) was only slightly lower than that for the total leader replacement in pGP11.

Those mutations which relieved translational repression *in vivo* were also accompanied by large increases in the levels of S20 mRNA and protein *in vivo* (Parsons *et al.*, 1988). Messenger RNA levels were found to be increased as a result of a longer half-life for the hybrids. However, as shown here, these mutations also produce large increases in the inherent translational efficiencies of those mRNAs, from 1.7 to 3.6 fold as measured by coupled transcription-translation *in vitro*. In the absence of any evidence that S20 binds to its own wild type mRNA (Chapter 3), it would appear unlikely that these derepressing mutations function by changing the

affinity of S20 for a binding site on its message. More likely, any mutation increasing the level of S20 mRNA or the efficiency with which it is translated will result in relief of repression, regardless of the mechanism (Parsons et al., 1988). Such an effect has been observed in the case of IF3, in which alterations of the initiation codon from AUU to AUG abolished normal translational repression (Butler et al., 1987; Gold et al., 1984). However it would seem unlikely that the UUG initiation codon alone could be responsible for autogenous translational control of S20 production, and in fact, the two derepressing mutations (pGP11 and pGP13), do produce slightly different levels of relief in vivo. To differentiate between the role of the UUG codon and other leader sequences in this process, the AUG of pGP11 was reverted back to the natural UUG initiation codon (pGM70). Unfortunately, in the context of the ribosome binding and leader regions supplied by pKK223-3, the UUG codon was capable of producing only a very low level of translation activity, as evidenced by an in vitro efficiency value of just 14% of the normal S20 level (Table 3). This amount was not sufficient for an accurate estimate of the level of repression occurring with this transcript in vivo.

The final site-directed mutant (pGP12), contains an alteration in the region of homology shown between the 16S rRNA S20 binding region and the S20 mRNA (Mackie,

1981). Induction of this gene did not result in significant overproduction of S20 as would be expected if an S20 recognition site in the leader had been made unrecognizable to the protein. Instead, the change produced a large drop in the efficiency of synthesis of S20 both *in vivo* and *in vitro*. The conversion of GA at positions -4 and -3 (relative to the initiation codon) to CT would be predicted by Hui *et al*. (1984) and Stormo *et al*. (1982) to be inhibitory to translation. Therefore, the very low translational efficiency observed with the pGP12 transcript *in vitro*, (just 17% of pCD6), is not in itself particularly surprising. However, this level may be insufficient for making enough S20 to produce measurable repression of the hybrid messenger. So, although translation of pGP12 did not result in sufficient S20 production for an accurate estimate of the repression level, it did show that alteration of this site does not result in overproduction of S20.

Deletions of variable segments of the S20 leader (pGP243, 251, 258, and 261), were analyzed less comprehensively than the site-directed mutants above. However, *in vitro* transcription-translation of plasmids carrying these deletions shows that significant determinants of translational efficiency lie outside the boundaries of the Shine-Dalgarno/initiation codon region. In particular, the extremely efficient deletion ending at residue 243 of the leader is somewhat surprising. This

is most likely the result of forming a specific secondary or tertiary conformation in this region or the chance juxtaposition of a particular sequence from the vector with the S20 leader.

Overall, these results fail to support a model for S20 regulation in which free S20 binds to its own mRNA at a site of homology with its 16S rRNA binding site to effect the repression of further translation. Instead, the most important determinant of repression appears to be the UUG initiation codon itself. The remaining residues in the region of 16S rRNA homology and other areas of the leader appear to function in setting the intrinsic translational efficiency of the S20 mRNA. Substantial increases in that efficiency are observed to result in insensitivity to the normal translational control of S20 production. During their examination of a large number of point mutations in the proposed L1 binding site of the L11 leader, Thomas and Nomura (1987) also concluded that regulatory sites overlapped sequences determining translational efficiency. In the absence of any evidence that S20 binds specifically to its own mRNA (when constructed in vitro), it is therefore possible that the target for S20-mediated repression may not be the mRNA alone, but a ribosome-mRNA complex poised at or near the initiation codon.

CHAPTER 5

SUMMARY

Two previous studies relate to the question of whether fragments of S20 are capable of binding to 16S rRNA. The first addressed only the subject of C-terminal fragments and found that very little N-terminal sequence was expendable (Paterakis et al., 1983). The investigation was also limited to a survey of only two fragments. In the second, it was observed that a peptide which was smaller than S20, but apparently identical with its N-terminus, could be isolated by its ability to bind to 16S rRNA (Mackie, 1977a).

The first part of this work was undertaken for the purpose of determining, by a more flexible method, whether mutants of S20 missing C-terminal sequences were still capable of binding 16S rRNA. In fact, the loss of as little as 6 C-terminal residues of S20 was found to result in a sharp loss of 16S rRNA binding ability. This does not explain the property of the peptide studied by Mackie (1977a), but in combination with the results of Paterakis et al. (1983), does lead to the conclusion that the N- and C-terminal regions of S20 may interact to produce a conformation capable of binding 16S rRNA.

A related section of this work was designed to explore the functional basis for S20's ability to regulate its own synthesis at a post-transcriptional step (Geyl and Bock, 1977; Parsons and Mackie, 1983). Most ribosomal proteins have been proposed to be regulated by the process of translational control, which involves the

interaction of a regulatory member of each operon with its mRNA to repress translation. Such interaction has been observed experimentally for only 2 of the ribosomal protein "repressors". Therefore, the ability of S20 to bind to S20 mRNAs produced in vitro was tested. Rather surprisingly, S20 was found to show no specific affinity for an mRNA transcript encompassing the P2 promoter, leader, coding region and terminator of the S20 gene.

This has raised the possibility that S20-mediated repression may utilize alternative targets for S20 binding, such as structures formed during the initiation of S20 translation. Future work in this area might proceed in vitro, with the assay of S20's ability to inhibit preformed complexes composed of purified subunits and factors. Alternatively, footprinting experiments in vivo could clarify the question of what sequences S20 interacts with (and thereby protects) in the process of regulation.

A third facet of this study of S20 protein-RNA interaction involved the role of the leader and initiation codon of S20 mRNA in the process of autoregulation. These were found to be critical determinants not only of the level of autoregulation of the S20 gene, but also of the efficiency with which it is translated. In particular, it was found that alteration of the unusual UUG start codon of S20 to AUG resulted in almost complete relief from autoregulation (Parsons et

al, 1988), as well as a substantial increase in the translational efficiency of the mRNA produced. This dual effect appears to be more than coincidental, and relief from repression was proposed to result from any substantial increase in translational efficiency. The determinants of translational efficiency in the S20 mRNA were further found to be affected by sequences encompassing a large part of the S20 leader as well as the UUG start codon.

The methods and systems developed in the course of the above studies should also provide significant future potential for a number of diverse areas of study. In particular, the use of in vitro translation for the generation of peptides incorporating specific structural alterations has significant advantages over other methods currently available. These products can also be considered for use when partially or completely purified from the cell-free extracts in which they are produced. Their synthesis can be accomplished at levels of nanomoles of protein product per pmole of input template, providing a rich source of very high specific activity product.

The methodology developed in this thesis also holds the potential for more refined characterization of the RNA binding site of S20 on 16S rRNA. Systems for the in vitro transcription of 16S rRNA sequences offer a flexible means of generating an array of truncated RNA

fragments (available from template run-off at alternate restriction sites), as well as a convenient system in which to create and express site-specific alterations of 16S rRNA.

APPENDICES

APPENDIX A. Sequences of the gene for S20 and flanking regions (Mackie, 1981).

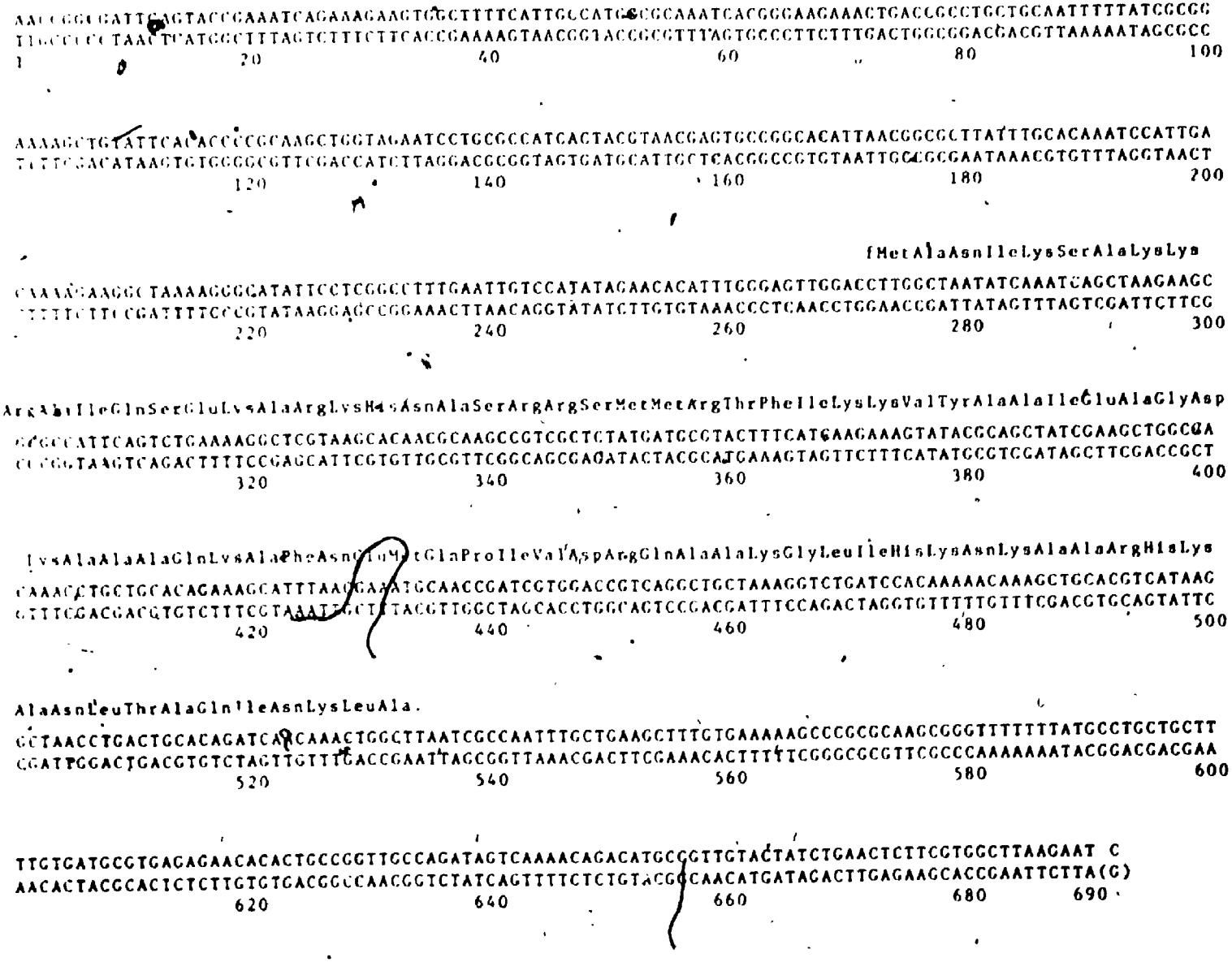

APPENDIX B. Data from S20 binding to 16S rRNA.

S20 Added (pmoles)	S20 Bound (pmoles)	V	$\frac{1}{V}$	Unbound S20 (pmoles)	[A]	$\frac{1}{[A]}$
0.27	0.21	0.02	52.4	0.06	1.24×10^{-9}	8.07×10^{8}
0.54	0.40	0.04	27.7	0.15	2.94×10^{-9}	3.40×10^{8}
1.09	0.81	0.07	13.6	0.28	5.54×10^{-9}	1.81×10^{8}
1.63	1.2	0.11	9.08	0.42	8.44×10^{-9}	1.18×10^{8}
2.18	1.5	0.14	7.18	0.65	1.30×10^{-8}	7.74×10^{7}
3.26	2.3	0.21	4.84	0.99	1.98×10^{-8}	5.03×10^{7}
4.35	2.8	0.26	3.92	1.55	3.10×10^{-8}	3.23×10^{7}
6.00	3.9	0.36	2.81	2.08	4.16×10^{-8}	2.40×10^{7}
11.2	5.9	0.53	1.88	5.34	1.07×10^{-7}	9.36×10^{6}

APPENDIX C. Data for binding of S20 mutants to 16S rRNA.

Plasmid	Type of Deletion	Amount of Peptide Added (pmoles)	Amount of Peptide Bound (pmoles)
pCD101	C-terminal	1.09	0.72
		1.24	0.84
		1.24	0.97
		1.41	1.04
		1.47	0.98
		2.18	1.42
		3.27	2.05
pCD102	C-terminal	0.64	0.09
		0.66	0.05
		0.72	0.05
		0.96	0.05
		1.29	0.15
pCD103	C-terminal	0.53	0.04
		0.96	0.08
		2.11	0.21
pCD104	C-terminal	1.1	0.0
pCD105	C-terminal	0.6	0.0
pCD106	C-terminal	1.1	0.0
pCD107	C-terminal	0.6	0.0
pCD201	C-terminal	0.42	0.05
		0.52	0.04
		0.78	0.08
		0.84	0.11
		1.18	0.15
pCD202	C-terminal	0.23	0.02
		0.72	0.03
pCD301	C-terminal	1.02	0.24
		1.04	0.24
		1.20	0.31
		1.56	0.38
		2.04	0.51
		2.00	0.70
		2.93	0.76
pCD11	Internal	1.2	0.0
pCD12	Internal	2.3	0.0
pCD13	Internal	0.92	0.19
		1.85	0.36
		2.04	0.27
		3.09	0.63
pCD14	Internal	1.10	0.09
		1.58	0.14
		2.20	0.10
		3.50	0.15

APPENDIX D. Data for binding of S20 to the 5'region of 16S rRNA (transcribed *in vitro* from pCD15).

S20 Added (pmoles)	S20 Bound (pmoles)	v[a]
0.55	0.26	0.11
1.1	0.45	0.19
2.2	0.82	0.35
3.3	1.10	0.47
4.4	1.53	0.66
5.5	1.69	0.73
7.7	1.82	0.78
8.8	2.00	0.86
11	2.00	0.86

a. v = pmoles S20 bound / pmole of RNA recovered

REFERENCES

APIRION, D. (1983) RNA processing in a unicellular microorganism: implications for eukaryotic cells. Prog. Nucleic Acids Res. Mol. Biol. 30, 1-40.

BARACCHINI, E. and BREMER, H. (1988) Stringent and growth control of rRNA synthesis in Escherichia coli are both mediated by ppGpp. J. Biol. Chem. 263, 2597-2602.

BARKLEY, M.D. and BOURGEOIS, S. (1978) Repressor recognition of operator and effectors. In "The operon." (Miller, J.H. and Reznikoff, W.S. eds) Cold Spring Harbor Laboratories, Cold Spring Harbor, N.Y. pp 177-220.

BELASCO, J.G., NILSSON, G., VON GABAIN, A. and COHEN, S.N. (1986) The stability of E. coli transcripts is dependent on determinants localized to specific mRNA segments. Cell 46, 245-251.

BIGGIN, M.D., GIBSON, T.J. and HONG, G.F. (1983) Buffer gradient gels and ^{35}S label as an aid to rapid DNA sequence determination. Proc. Natl. Acad. Sci. (USA) 80, 3963-3965.

BRIMACOMBE, R., MALY, P. and ZWIEB, C. (1983) The structure of ribosomal RNA and its organization relative to ribosomal protein. Prog. Nucleic Acids Res. Mol. Biol. 28, 1-48.

BRIMACOMBE, R., ATMADJA, J., KYRIATSOULIS, A. and STIEGE, W. (1986) RNA structure and RNA-protein neighborhoods in the ribosome. In " Structure, function, and genetics of ribosomes." (B. Hardesty, G. Kramer, eds.) Springer-Verleg, New York, pp 184-202.

BRIMACOMBE, R. and STIEGE, W. (1985) Structure and function of ribosomal RNA. Biochem. J. 229, 1-17.

BROSIUS, J., DULL, T.J. SLEETER, D.D. and NOLLER, H.F. (1981) Gene organization and primary structure of a ribosomal RNA operon from Escherichia coli. J. Mol. Biol. 148, 107-127.

BROSIUS, J. and HOLY, A. (1984) Regulation of ribosomal RNA promoters with a synthetic lac operator. Proc. Natl. Acad. Sci. (USA) 81, 6929-6933.

BRUCE, J. FIRPO, E.J. and SHAUP, H.W. (1977) Ribosomal protein - nucleic acid interactions. I. Isolation of a polypeptide fragment from 30S protein S8 which binds to 16S rRNA. Nucleic Acids Res. 4, 3327-3340.

BUTLER, J.S., SPRINGER, M. and GRUNBERG-MANAGO M. (1987) AUU-to-AUG mutation in the initiator codon of the translation initiation factor IF3 abolishes translational autocontrol of its own gene (infC) in vivo. Proc. Natl. Acad. Sci. 84, 4022-4025.

CAPEL, M.S., ENGELMAN, D.M., FREEBORN, B.R., KJELDGAARD, M., LANGER, J.A., RAMAKRISHNAN, V., SCHINDLER, D.G., SCHNEIDER, D.K., SCHOENBORN, B.P., SILLERS, I.-Y., YABUKI, S. and MOORE, P.B. (1987) A complete mapping of the proteins in the small ribosomal subunit of Escherichia coli. Science 238, 1403-1406.

CARBON, P., EHRESMANN, C., EHRESMANN, B. and EBEL, J. (1978) The sequence of Escherichia coli ribosomal 16-S RNA determined by new rapid gel methods. F.E.B.S. Letters 94, 152-156.

CARBON, P., EHRESMANN, C., EHRESMANN, B. and EBEL, J. (1979) The complete nucleotide sequence of the ribosomal 16-S RNA from Escherichia coli. Eur. J. Biochem. 100, 399-410.

CHADWICK, P., PIRROTTA, V., STEINBERG, R., HOPKINS, N. and PTASHNE, M. (1970) The lambda and 434 phage repressors. Cold Spring Harbor Symp. Quant. Biol. 35, 283-294.

CHANGCHIEN, L. and CRAVEN, G.R. (1976) The function of the N-terminal region of ribosomal protein S4. J. Mol. Biol. 108, 381-401.

CHANGCHIEN, L. and CRAVEN, G.R. (1978) Studies on the role of amino acid residues 31 through 46 of ribosomal protein S4 in the mechanism of 30S ribosome assembly. J. Mol. Biol. 125, 43-56.

CHANGCHIEN, L. and CRAVEN, G.R. (1985) Specific ribosomal RNA recognition by a fragment of E. coli ribosomal protein S4 missing the C-terminal 36 amino acid residues. Nucleic Acids Res. 13, 6343-6360.

CHANGCHIEN, L. and CRAVEN, G.R. (1986) The use of hydroxylamine cleavage to produce a fragment of ribosomal protein S4 which retains the capacity to specifically bind 16S ribosomal RNA. Nucleic Acids Res. 14, 1957-1966.

CHRISTENSEN, T., JOHNSEN, M., FIIL, N.P. and FRIESEN, J.D. (1984) RNA secondary structure and translation inhibition: analysis of mutants in the rplJ leader. EMBO J. 3, 1609-1612.

CHURCH, G.M. and GILBERT, W. (1984) Genomic sequencing. Proc. Natl. Acad. Sci. (USA) 81, 1991-1995.

CLAUDE, A. (1940) Particulate components of normal and tumor cells. Science 91, 77-78.

CLEWELL, D.B. (1972) Nature of Col E_1 plasmid replication in Escherichia coli in the presence of chloramphenicol. J. Bacteriol. 110, 667-676.

COHEN, S.N., CHANG, A.C.Y. and HSU, C.L. (1972) Non-chromosomal antibiotic resistance in bacteria; genetic transformation of Escherichia coli by R factor DNA. Proc. Natl. Acad. Sci. (USA) 69, 2110-2114.

COLE, J.R. and NOMURA, M. (1986) Translational regulation is responsible for growth-rate-dependent and stringent control of the synthesis of ribosomal proteins L11 and L1 in Escherichia coli. Proc. Natl. Acad. Sci. (USA) 83, 4129-4133.

DAVIES, J. and NOMURA, M. (1972) The genetics of bacterial ribosomes. Ann. Rev. Genet. 6, 203-234.

DE BOER, H. and NOMURA, M. (1979) In vivo transcription of rRNA operons in Escherichia coli initiates with purine nucleoside triphosphates at the first promoter and with CTP at the second promoter. J. Biol. Chem. 254, 5609-5612.

DECKMAN, I.C. and DRAPER, D.E. (1985) Specific interaction between ribosomal protein S4 and the α operon messenger RNA. Biochemistry 24, 7860-7865.

DECKMAN, I.C. and DRAPER, D.E. (1987) S4-α mRNA translation regulation complex II. Secondary structures of the RNA regulatory site in the presence and absence of S4. J. Mol. Biol. 196, 323-332.

DECKMAN, I.C., DRAPER, D.E. and THOMAS, M.S. (1987) S4-α mRNA translation regulation complex I. Thermodynamics of formation. J. Mol. Biol. 196, 313-322.

DENNIS, P.P. (1974) In vivo stability, maturation and relative differential synthesis rates of individual ribosomal proteins in Escherichia coli B/r. J. Mol. Biol. 88, 25-41.

DENNIS, P.P. and NOMURA, M. (1975) Regulation of the expression of ribosomal protein genes in Escherichia coli. J. Mol. Biol. 97, 61-76.

DONLY, B.C. and MACKIE, G.A. (1988) Affinities of ribosomal protein S20 and C-terminal deletion mutants for 16S rRNA and S20 mRNA. Nucleic Acids Res. 16, 997-1010.

DRAPER, D.E., DECKMAN, I.C. and VARTIKAR, J.V. (1988) Physical studies of ribosomal protein-RNA interactions. Methods in Enzymol. (in press).

EHRESMANN, B., BACKENDORF, C., EHRESMANN, C. and EBEL, J.P. (1977) Characterization of the regions from E. coli 16 S RNA covalently linked to ribosomal proteins S4 and S20 after ultraviolet irradiation. F.E.B.S. Lett. 78, 261-266.

ELLWOOD, M. and NOMURA, M. (1982) Chromosomal locations of the genes for rRNA in Escherichia coli K-12. J. Bacteriol. 149, 458-468.

FAHNESTOCK, S., ERDMANN, V. and NOMURA, M. (1973) Reconstitution of 50S ribosomal subunits from protein-free ribonucleic acid. Biochem. 12, 220-224.

FELLNER, P. (1969) Nucleotide sequences from specific areas of the 16S and 23S ribosomal RNAs of E. coli. Eur. J. Biochem. 11, 12-27.

FREEDMAN, L.P, ZENGEL, J.M. and LINDAHL, L. (1985) Genetic dissection of stringent control and nutritional shift-up response of the Escherichia coli S10 ribosomal protein operon. J. Mol. Biol. 185, 701-712.

GALLANT, J.A. (1979) Stringent control in E. coli. Ann. Rev. Genet. 13, 393-415.

GARNIER, J., OSGUTHORPE, D.J. and ROBSON, B. (1978) Analysis of the accuracy and implications of simple methods for predicting the secondary structure of globular proteins. J. Mol. Biol. 120, 97-120.

GARRETT, R.A. (1979) The structure, assembly, and funtion of ribosomes. Chemistry of Macromolecules IIB 25, 121-177.

GARRETT, R.A., RAK, K.H., DAYA, L. and STOFFLER, G. (1971) Ribosomal proteins XXIX. Specific protein binding sites on 16S rRNA of Escherichia coli. Mol. Gen. Genet. 114, 112-124.

GARRETT, R.A., VESTER, B., LEFFERS, H., SORENSEN, P.M., KJEMS, S.O., CHRISTENSEN, A., CHRISTIANSEN, J. and DOUTHWAITE S. (1984) Mechanisms of protein-RNA recognition and assembly in ribosomes. In Gene Expression, Alfred Benzon Symposium 19 (eds. Clark, B.F.C. and Petersen, H.U.) Munksgaard, Copenhagen, Denmark. pp. 331-349.

GEYL, D. and BOCK, A. (1977) Synthesis of ribosomal proteins in merodiploid strains and in minicells of Escherichia coli. Molec. Gen. Genet. 154, 327-34.

GIRI, L., HILL, W.E. and WITTMANN, H.G. (1984) Ribosomal proteins: their structure and spatial arrangement in prokaryotic ribosomes. Adv. in Prot. Chem. 36, 1-78.

GLASER, G., SARMIENTOS, P. and CASHEL, M. (1983) Functional interrelationship between two tandem E. coli ribosomal RNA promoters. Nature, 302, 74-76.

GOLD, L., PRIBNOW, D., SCHNEIDER, T., SHINEDLING, S., SINGER, B.S. AND STORMO, G. (1981) Translational initiation in prokaryotes. Ann. Rev. Microbiol. 35, 365-403.

GOLD, L., STORMO, G. and SAUNDERS, R. (1984) Escherichia coli translational initiation factor IF3: A unique case of translational regulation. Proc. Natl. Acad. Sci. (USA) 81, 7061-7065.

GOLDBERG, A.L. and ST. JOHN, A.C. (1976) Intracellular protein degradation in mammalian and bacterial cells: Part 2. Ann. Rev. of Biochem. 45, 747-803.

GOURSE, R.L., SHARROCK, R.A. and NOMURA, M. (1986a) Control of ribosome synthesis in Escherichia coli. In "Structure, function, and genetics of ribosomes" (B. Hardesty, G. Kramer, eds.). Springer-Verlag, New York, USA. pp 766-788.

GOURSE, R.L., DE BOER, H.A. and NOMURA, M. (1986b) DNA determinants of rRNA synthesis in E. coli: growth rate dependent regulation, feedback inhibition, upstream activation, antitermination. Cell, 44, 197-205.

GREGORY, R.J., ZELLER, M.L., THURLOW, D.L., GOURSE, R.L., STARK, M.J.R., DAHLBERG, A.E. and ZIMMERMANN, R.A. (1984) Interaction of ribosomal proteins S6, S8, S15 and S18 with the central domain of the 16S ribosomal RNA from Escherichia coli. J. Mol. Biol. 178, 287-302.

GUERRIER-TAKADA, C., GARDINER, K., MARSH, T., PACE, N. and ALTMAN, S. (1983) The RNA moiety of ribonuclease P is the catalytic subunit of the enzyme. Cell 35, 849-857.

HALL, M.N., GABAY, J., DEBARBQUILLE, M. and SCHWARTZ, M. (1982) A role for mRNA secondary structure in the control of translation initiation. Nature 295, 616-618.

HOCHKEPPEL, H.-K., SPICER, E. and CRAVEN, G.R. (1976) A method of preparing Escherichia coli 16 S RNA possessing previously unobserved 30 S ribosomal protein binding sites. J. Mol. Biol. 101, 155-170.

HOLBEN, W.E.. and MORGAN, E.A. (1984) Antitermination of transcription from an Escherichia coli ribosomal RNA promoter. Proc. Natl. Acad. Sci. (USA) 81, 6789-6793.

HUI, A., HAYFLICK, J., DINKELSPIEL, K. and DE BOER, H.A. (1984) Mutagenesis of the three bases preceding the start codon of β-galactosidase mRNA and its effect on translation in Escherichia coli. EMBO J. 3, 623-629.

JASKUNAS, S.R., LINDAHL, L. and NOMURA, M. (1975) Specialized transducing phages for ribosomal protein genes of Escherichia coli. Proc. Natl. Acad. Sci. (USA) 72, 6-10.

JOHNSEN, M., CHRISTENSEN, T., DENNIS, P.P. and FIIL, N.P. (1982) Autogenous control: ribosomal protein L10-L12 complex binds to the leader sequence of its mRNA. EMBO J. 1, 999-1004.

KALTSCHMIDT, E. (1971) Ribosomal proteins XIV. Isoelectric points of ribosomal proteins of E. coli as determined by two-dimensional polyacrylamide gel electrophoresis. Analytical Biochemistry 43, 25-31.

KALTSCHMIDT, E. and WITTMANN, H.G. (1970) Ribosomal proteins VII. Two-dimensional polyacrylamide gel electrophoresis for finger printing of ribosomal proteins. Anal. Biochem. 36, 401-412.

KASSAVETIS, G.A., BUTLER, E.T., ROULLAND, D. and CHAMBERLIN, M.J. (1982) Bacteriophage SP6-specific RNA polymerase. J. Biol. Chem. 257, 5772-5776.

KRUGER, K., GRABOWSKI, P.J., ZAUG, A.J., SANDS, J., GOTTSCHLING, D.E. AND CECH, T.R. (1982) Self-splicing RNA: autoexcision and autocyclization of the ribosomal RNA intervening sequence of Tetrahymena. Cell 31, 147-157.

KURLAND, C.G. (1960) Molecular characterization of ribonucleic acid from Escherichia coli ribosomes I. Isolation and molecular weights. J. Mol. Biol. 2, 83-91.

LINDAHL, L., ARCHER, R. and ZENGEL, J.M. (1983) Transcription of the S10 ribosomal protein operon is regulated by an attenuator in the leader. Cell 33, 241-248.

LINDAHL, L. and ZENGEL, J.M. (1982) Expression of ribosomal genes in bacteria. Adv. in Genet. 21, 53-121.

LINDAHL, L. and ZENGEL, J.M. (1986) Ribosomal genes in Escherichia coli. Ann. Rev. Genet. 20, 297-326.

LITTLEFIELD, J.W., KELLER, E.B., GROSS, J. and ZAMECNIK, P.C. (1955) Studies on cytoplasmic ribonucleoprotein particles from the liver of the rat. J. Biol. Chem. 217, 111-123.

LURIA, S.E., DELBRUCK, M. and ANDERSON, T.F. (1943) Electron microscope studies of bacterial viruses. J. Bacteriol. 46, 57-77.

MACKIE, G.A. (1977a) Evidence for a precursor-product relationship in the biosynthesis of ribosomal protein S20. Biochem. 16, 1391-1398.

MACKIE, G.A. (1977b) Synthesis in vitro of ribosomal protein S20 and its precursor. Biochem. 16, 4497-4503.

MACKIE, G.A. (1981) Nucleotide sequence of the gene for ribosomal protein S20 and its flanking regions. J. Biol. Chem. 256, 8177-8182.

MACKIE, G.A. (1986) Structure of the DNA distal to the gene for ribosomal protein S20 in Escherichia coli K12: presence of a strong terminator and an IS1 element. Nucleic Acids Res. 14, 6965-6981.

MACKIE, G.A. and PARSONS, G.D. (1983) Tandem promoters in the gene for ribosomal protein S20. J. Biol. Chem. 258, 7840-7846.

MACKIE, G.A. and ZIMMERMANN, R.A. (1978) RNA-protein interactions in the ribosome. IV. Structure and properties of binding sites for proteins S4, S16/S17 and S20 in 16S RNA. J. Mol. Biol. 121, 17-39.

MAGER, W.H. (1988) Control of ribosomal protein gene expression. Biochem. Biophys. Acta 949, 1-15.

MALY, P. and BRIMACOMBE, R. (1983) Refined secondary structure models for the 16S and 23S ribosomal RNA of Escherichia coli. Nucleic Acids Res. 11, 7263-7286.

MANIATIS, T., FRITSCH, E.F. and SAMBROOK, J. (1982) "Molecular cloning: a laboratory manual." Cold Spring Harbor Laboratory, Cold Spring Harbor, N.Y.

MAXAM, A.M. and GILBERT, W. (1980) Sequencing end-labeled DNA with base-specific chemical cleavages. Methods Enzymol. 65, 499-560.

MCALLISTER, W.M., MORRIS, C., ROSENBERG, A.H. and STUDIER, F.W. (1981) Utilization of bacteriophage T7 late promoters in recombinant plasmids during infection. J. Mol. Biol. 153, 527-544.

MELTON, D.A., KRIEG, P.A., REBAGLIATI, M.R., MANIATIS, T., ZINN, K. and GREEN, M.R. (1984) Efficient in vitro synthesis o f biologically active RNA and RNA hybridization probes from plasmids containing a bacteriophage SP6 promotor. Nucleic Acids Res. 12, 7035-7056.

MESSING, J. and VIEIRA, J. (1982) A new pair of M13 vectors for selecting either DNA strand of double-digest restriction fragments. Gene 19, 269-276.

MIZUSHIMA, S. and NORUMA, M. (1970) Assembly mapping of 30S ribosomal proteins from E. coli. Nature 226, 1214-1218.

MOAZED, D., STERN, S. and NOLLER, H.F. (1986) Rapid chemical probing of conformation in 16S ribosomal RNA and 30S ribosomal subunits using primer extension. J. Mol. Biol. 187, 399-416.

MORGAN, E. (1982) Ribosomal RNA genes in Escherichia coli. in "The cell nucleus." (H. Busch and L. Rothblum, eds), Academic Press, New York. pp 1-29.

MOORE, P.B. (1988) The ribosome returns. Nature 331, 223-227.

NEWBERRY, V., BROSIUS, J., and GARRETT, R. (1978) Fragment of protein L18 from the Escherichia coli ribosome that contains the 5S RNA binding site. Nucleic Acids Res. 5, 1753-1766.

NIERHAUS, K.H. (1982) Structure, assembly and function of ribosomes. Curr. Topics Microbiol. Immunol. 97, 82-155.

NOLLER, H.F. (1974) Topography of 16S RNA in 30S ribosomal subunits. Nucleotide sequences and location of sites of reaction with kethoxal. Biochemistry 13, 4694-4703.

NOLLER, H.F. (1984) Structure of ribosomal RNA. Ann. Rev. Biochem. 53, 119-162.

NOLLER, H.F., ASIRE, M., BARTA, A., DOUTHWAITE, S., GOLDSTEIN, T., GUTELL, R.R., MOAZED, D., NORMANLY, J., PRINCE, J.B., STERN, S., TRIMAN, K., TURNER, S., VAN STOLK, B., WHEATON, V., WEISER, B. and WOESE, C.R. (1986) Studies on the structure and function of ribosomal RNA. In "Structure, function, and genetics of ribosomes." (B. Hardesty, G. Kramer, eds.) Springer-Verleg, New York; pp 143-165.

NOMURA, M. (1984) The control of ribosome synthesis. Scientific American, 250, 102-114.

NOMURA, M., YATES, J.L., DEAN, D. and POST, L.E. (1980) Feedback regulation of ribosomal protein gene expression in Escherichia coli : structural homology of ribosomal RNA and ribosomal protein mRNA. Proc. Natl. Acad. Sci. (USA) 77, 7084-7088.

NOMURA, M., GOURSE, R. and BAUGHMAN, G. (1984) Regulation of the synthesis of ribosomes and ribosomal components. Ann. Rev. Biochem. 53, 75-117.

NOMURA, M. and HELD, W.A. (1974) Reconstitution of ribosomes: studies of ribosome structure, function and assembly. In "Ribosomes." (Nomura, M., Tissieres, A. and Lengyel, P. eds.) Cold Spring Harbor Laboratory. Cold Spring Harbor, N.Y. pp 193-223.

NOWOTNY, V., MAY, R.P. and NIERHAUS, K.H. (1986) Neutron scattering analysis of structural and functional aspects of the ribosome: the strategy of the glassy ribosome. In " Structure, function, and genetics of ribosomes." (B. Hardesty, G. Kramer, eds.) Springer-Verleg, New York, pp 101-111.

PARSONS, G.D. and MACKIE, G.A. (1983) Expression of the gene for ribosomal protein S20: effects of gene dosage. J. Bacteriol. 154, 152-160.

PARSONS, G.D., DONLY, B.C. and MACKIE, G.A. (1988) Mutations in the leader sequence and initiation codon of the gene for ribosomal protein S20 (rpsT) affect both translational efficiency and autoregulation. J. Bacteriol. 170, 2485-2492.

PATERAKIS, K. and LITTLECHILD, J. (1982) Structural domains of ribosomal protein S8 and their relationship to ribosomal RNA binding. F.E.B.S. Lett. 149, 328-333.

PATERAKIS, K., LITTLECHILD, J. and WOOLLEY, P. (1983) Structural and functional studies on protein S20 from the 30-S subunit of the Escherichia coli ribosome. Eur. J. Biochem. 129, 543-548.

PEATTIE, D.A. and GILBERT, W. (1980) Chemical probes for higher-order structure in RNA. Proc. Natl. Acad. Sci. 77, 4679-4682.

QUEEN, C. (1983) A vector that uses phage signals for efficient synthesis of proteins in Escherichia coli. J. Mol. Appl. Genet. 2, 1-10.

RABIN, D. and CROTHERS, D.M. (1979) Analysis of RNA secondary structure by photochemical reversal of psoralen crosslinks. Nuc. Acids Res. 7, 689-703.

ROSS, A. and BRIMACOMBE, R. (1979) Experimental determination of interacting sequences in ribosomal RNA. Nature 281, 271-276.

SCHWARZBAUER, J. and CRAVEN, G.R. (1979) The use of membrane filtration to determine apparent association constants for ribosomal protein-RNA complex formation. Methods in Enzymology, 59, 583-591.

SCHWARZBAUER, J. and CRAVEN, G.R. (1981) Apparent association constants for E. coli ribosomal proteins S4, S7, S8, S15, S17 and S20 binding to 16S RNA. Nucleic Acids Res. 9, 2223-2227.

SCHWARZBAUER, J. and CRAVEN, G.R. (1985) Evidence that E. coli ribosomal protein S13 has two separable functional domains involved in 16S RNA recogniton and protein S19 binding. Nucleic Acids Res. 13, 6767-6786.

STEIGE, W., ZWIEB, C. and BRIMACOMBE, R. (1982) Precise localisation of three intra-RNA cross-links in 23S RNA and one in 5S RNA, induced by treatment of Escherichia coli 50S ribosomal subunits with bis-(chloroethyl)-methylamine. Nuc. Acids Res. 10, 7211-7229.

STERN, S., WILSON, R.C. and NOLLER, H.F. (1986) Localization of the binding site for protein S4 on 16S ribosomal RNA by chemical and enzymatic probing and primer extension. J. Mol. Biol. 192, 101-110.

STORMO, G.D., SCHNEIDER, T.D. and L. GOLD. (1982) Characterization of translational initiation sites in E. coli. Nucl. Acids Res. 10, 2971-2996.

SUBRAMANIAN, A.R. (1975) Copies of proteins L7 and L12 and heterogeneity of the large subunit of Escherichia coli ribosome. J. Mol. Biol. 95, 1-8.

SUBRAMANIAN, A.R. (1983) Structure and functions of ribosomal protein S1. Prog. Nucleic Acid Res. Mol. Biol. 28, 101-142.

SUBRAMANIAN, A.R. and MIZUSHIMA, S. (1979) Characterization of a mutant form of ribosomal protein S1 from Escherichia coli. J. Biol. Chem. 254, 4309-4312.

SUBRAMANIAN, A.R., RIENHARDT, P., KIMURA, M. and SURYANARAYANA, T. (1981) Fragments of ribosomal protin S1 and its mutant form ml-S1. Eur. J. Biochem. 119, 245-249.

SURYANARAYANA, T. and SUBRAMANIAN, A.R. (1979) Functional domains of Escherichia coli ribosomal protein S1. J. Mol. Biol. 127, 41-54.

SWANK, R.T. and MUNKRES, K.D. (1971) Molecular weight analysis of oligopeptides by electrophoresis in polyacrylamide gel with sodium dodecyl sulfate. Anal. Biochem. 39, 462-477.

THOMAS, M.S. and NOMURA, M. (1987) Translational regulation of the L11 ribosomal protein operon of Escherichia coli: mutations that define the target site for repression by L1. Nucl. Acids Res. 15, 3085-3096.

THOMPSON, J.F. and HEARST, J.E. (1983) Structure of E. coli 16S RNA elucidated by psoralen crosslinking. Cell 32, 1355-1365.

TRAUB, P. and NOMURA, M. (1968) Structure and function of E. coli ribosomes, V. reconstitution of functionally active 30S ribosomal particles from RNA and proteins. Proc. Natl. Acad. Sci. 59, 777-784.

TRAUB, P. and NOMURA, M. (1969) Structure and function of Escherichia coli ribosomes. J. Mol. Biol. 40, 391-413.

TRAVERS, A.A. (1980) Promoter sequence for stringent control of bacterial ribonucleic acid synthesis. J. Bacteriol. 141, 973-976.

TRAVERS, A.A. (1984) Conserved features of coordinately regulated E. coli promoters. Nucleic Acids Res. 12, 2605-2618.

UNGEWICKELL, E., GARRETT, R., EHRESMANN, C., STIEGLER, P. and FELLNER, P. (1975) An investigation of the 16-S RNA binding sites of ribosomal proteins S4, S8, S15 and S20 from Escherichia coli. Eur. J. Biochem. 51, 165-180.

VASILIEV, V.D., SERDYUK, I.N., GUDKOV, A.T. and SPIRIN, A.S. (1986) Self-organization of ribosomal RNA. In "Structure, function, and genetics of ribosomes" (B. Hardesty, G. Kramer, eds.). Springer-Verlag, New York, USA. pp 128-142.

VIGNE, R., JORDAN, B.R. and MONIER, R. (1973) A common conformational feature in several prokayotic and eukaryotic 5S RNAs: A highly exposed, single-stranded loop around position 40. J. Mol. Biol. 76, 303-311.

VON HIPPEL, P.H. and FAIRFIELD, F.R. (1983) Quantitative approaches to the autogenous regulation of gene expression. In 'Mobility and recognition in cell biology.' (H. Sund and C. Veeger, eds.) Walter de Gruyter & Co., New York. pp. 413-436.

WICKENS, M.P. and DAHLBERG, J.E. (1987) RNA-Protein interactions. Cell 51, 339-342.

WIENER, L., SCHULER, D. and BRIMACOMBE, R. (1988) Protein binding sites on Escherichia coli 16S ribosomal RNA; RNA regions that are protected by proteins S7, S9 and S19, and by proteins S8, S15 and S17. Nucleic Acids Res. 16, 1233-1250.

WIRTH, R. and BOCK, A. (1980) Regulation of synthesis of ribosomal protein S20 in vitro. Molec. Gen. Genet. 178, 479-481.

WIRTH, R., KOHLES, V. and BOCK, A. (1981) Factors modulating transcription and translation in vitro of ribosomal protein S20 and isoleucyl-tRNA synthetase from Escherichia coli. Eur. J. Biochem. 114, 429-437.

WIRTH, R., LITTLECHILD, J. and BOCK, A. (1982) Ribosomal protein S20 purified under mild conditions almost completely inhibits its own translation. Mol. Gen. Genet. 188, 164-166.

WITTMANN, H.G. (1986) Structure of ribosomes. In "Structure, function, and genetics of ribosomes" (B. Hardesty, G. Kramer, eds.). Springer-Verlag, New York, USA. pp 1-27.

WITTMANN, H.G., LITTLECHILD, J.A. and WITTMAN-LIEBOLD, B. (1980) Structure of ribosomal proteins. In "Ribosomes. Structure, function, and genetic." (G. Chambliss et al., eds.) University Park Press, Baltimore. pp 51-88.

WOESE, C.R., MAGRUM, L.J., GUPTA, R., SIEGEL, R.B. and STAHL, D.A. (1980) Secondary structure model for bacterial 16S ribosomal RNA: phylogenetic, enzymatic and chemical evidence. Nuc. Acids Res. 8, 2275-2293.

WOLLENZEIN, P.L. and CANTOR, C.R. (1982) Gel electrophoretic technique for separating crosslinked RNAs: application to improved electron microscopic analysis of psoralen crosslinked 16 S ribosomal RNA. J. Mol. Biol. 159, 151-166.

WOWER, I. and BRIMACOMBE, R. (1983) The localization of multiple sites on 16S RNA which are cross-linked to proteins S7 and S8 in Escherichia coli 30S ribosomal subunits by treatment with 2-iminothiolane. Nuc. Acids Res. 11, 1419-1437.

WU, H.-M. and CROTHERS, D.M. (1984) The locus of sequence directed and protein-induced binding. Nature 308, 509-513.

YATES, J.L., ARFSTEN, A.E. and NOMURA, M. (1980) In vitro expression of Escherichia coli ribosomal protein genes: autogenous inhibition of translation. Proc. Natl. Acad. Sci. (USA) 77, 1837-1841.

ZENGEL, J.M. and LINDAHL, L. (1986) Transcription of ribosomal genes during nutritional shift-up of Escherichia coli. J. Bacteriol. 167, 1095-1097.

ZIMMERMANN, R.A. (1974) RNA-protein interactions in the ribosome. In " Ribosomes." (Nomura, M., Tissieres, A. and Lengyel, P. eds.) Cold Spring Harbor Laboratory. Cold Spring Harbor, N.Y. pp 225-269.

ZIMMERMANN, R.A. (1980) Interactions among protein and RNA components of the ribosome. In " Structure, function, and genetics of ribosomes." (B. Hardesty, G. Kramer, eds.) Springer-Verleg, New York, pp 135-169.

ZIMMERMANN, R.A., MUTO, A., FELLNER, P. and BRANLANT, C. (1972) The interaction of 30S ribosomal proteins with 16S RNA and RNA fragments. FEBS Symposium 23, 53-73.

ZOLLER, M.J. and SMITH, M. (1984) Oligonucleotide-directed mutagenesis: a simple method using two oligonucleotide primers and a single-stranded DNA template. DNA 3, 479-488.

ZUBAY, G. (1977) In vitro synthesis of protein in microbial systems. Ann. Rev. Genet. 7, 267-287.

ZWIEB, C. and BRIMACOMBE, R. (1979) RNA-protein cross-linking in Escherichia coli 30S ribosomal subunits: precise localisation of the nucleotide in 16S RNA which is coupled to protein S7 by ultraviolet irradiation. Nucleic Acids Res. 6, 1775-1790.

ZWIEB, C. and BRIMACOMBE, R. (1980) Localisation of a series of intra-RNA cross-links in 16S RNA, induced by ultraviolet irradiation of Escherichia coli 30S ribosomal subunits. Nucleic Acids Res. 8, 2397-2411.